

Australian Water Recycling  
Centre of Excellence



# Industry Academic Exchange Program Report

## Characterising the Performance and Fouling of Hollow Fibre Membranes

A report of a study funded by the  
Australian Water Recycling Centre of Excellence

Mariam Darestani, May 2014



# Characterising the Performance and Fouling of Hollow Fibre Membranes

## Project Leader

Professor S Vigneswaran  
University of Technology Sydney  
15-77 Broadway St  
PO Box 123  
Broadway NSW 2007 AUSTRALIA

Contact: Prof. Saravanamuth Vigneswaran [Saravanamuth.Vigneswaran@uts.edu.au](mailto:Saravanamuth.Vigneswaran@uts.edu.au)

## Partners

INPHAZE Pty Ltd

## About the Australian Water Recycling Centre of Excellence

The mission of the Australian Water Recycling Centre of Excellence is to enhance management and use of water recycling through industry partnerships, build capacity and capability within the recycled water industry, and promote water recycling as a socially, environmentally and economically sustainable option for future water security.

The Australian Government has provided \$20 million to the Centre through its National Urban Water and Desalination Plan to support applied research and development projects which meet water recycling challenges for Australia's irrigation, urban development, food processing, heavy industry and water utility sectors. This funding has levered an additional \$40 million investment from more than 80 private and public organisations, in Australia and overseas.

**ISBN** 978-1-922202-75-8

### Citation:

Derestani, M. (2014). *Characterising the Performance and Fouling of Hollow Fibre Membranes*, Australian Water Recycling Centre of Excellence, Brisbane, Australia.

### © Australian Water Recycling Centre of Excellence

This work is copyright. Apart from any use permitted under the Copyright Act 1968, no part of it may be reproduced by any purpose without the written permission from the publisher. Requests and inquiries concerning reproduction right should be directed to the publisher.

**Date of publication:** May 2014

### Publisher:

Australian Water Recycling Centre of Excellence  
Level 5, 200 Creek St, Brisbane, Queensland 4000  
[www.australianwaterrecycling.com.au](http://www.australianwaterrecycling.com.au)

This report was funded by the Australian Water Recycling Centre of Excellence through the Australian Government's National Urban Water and Desalination Plan.

### Disclaimer

Use of information contained in this report is at the user's risk. While every effort has been made to ensure the accuracy of that information, the Australian Water Recycling Centre of Excellence does not make any claim, express or implied, regarding it.

# Characterising the Performance and Fouling of Hollow Fibre Membranes

*Final Report  
May 2014*

*Author: Mariam Darestani*

*Supervisor: Prof. S. Vigneswaran (UTS)*

*Advisor: Prof. Hans Coster (USYD / INPHAZE)*

*Collaborators:*



*Financial Support:*



## Table of Contents

1. Introduction.....	1
2. Objectives .....	3
3. Project outcomes .....	5
3.1. Materials .....	5
3.2. Methods.....	8
3.2.1. Membrane module preparation .....	8
3.2.2. Filtration experiments .....	8
3.2.2.1. Electrical impedance spectroscopy .....	12
3.3. Results.....	13
3.3.1. Summary of the first report.....	13
3.3.2. Flat membranes .....	15
3.3.2.1. Summary .....	31
3.3.3. Outside-in hollow fibre membranes.....	32
3.3.3.1. Summary .....	37
3.3.4. Inside-out hollow fibre membranes .....	38
3.3.4.1. Summary .....	44
3.4. Design and manufacturing a prototype module .....	46
3.5. Fouling of outside-in hollow fibre using an industrial feed.....	48
3.5.1. Effect of electrode configuration on detection of fouling.....	48
3.5.2. Effect of electrode configuration on monitoring the backwashing process .....	56
3.5.3. Effect of electrode configuration on characterisation of fouled membranes .....	62
3.5.4. Separation performance of hollow fibre membranes .....	67
3.6. Summary .....	71
4. Conclusions.....	72
5. Future works .....	74
6. Collaborations .....	75
7. Progress and delays.....	76
8. Networking activities .....	77
8.1. Publicity and documents .....	77
9. Signatures.....	78
10. References.....	79

## List of Figures

Figure 1- Structure of outside-in hollow fibre membranes .....	5
Figure 2- structure of inside-out Multibore® hollow fibre membrane.....	5
Figure 3- Microstructure of flat membrane used in the first phase of the project .....	6
Figure 4- Hollow fibre membranes at the beginning of filtration experiment using 10% dunder waste feed in the membrane bioreactor. Aeration is used to preserve the feed and to reduce fouling. ....	7
Figure 5- Schematic diagram of the filtration/EIS experimental setup for characterising outside-in hollow fibre membranes.....	9
Figure 6- Filtration/EIS experimental setup to monitor fouling of outside-in hollow fibre membranes by bio-feed.....	10
Figure 7- Schematic diagram of the filtration/EIS experimental setup for characterising inside-out hollow fibre membranes.....	11
Figure 8- Schematic diagram of the filtration/EIS experimental setup for characterising flat membranes	11
Figure 9- Structure of the 4-terminal chamber used for characterization of flat membranes .....	12
Figure 10- Sinusoidal function of $v$ and $i$ and $v$ with a shift of $\phi/\omega$ . $\omega$ is the angular frequency and $\omega=2\pi/T$ where $T$ is the period and the frequency in cycle per second is $f=1/T$ .....	13
Figure 11- Four prototypes used in monitoring filtration of PEG solution using outside-in hollow fibre membranes. Total percentage changes of capacitance (C) and Conductance (G) during fouling is plotted at frequencies ranging from 1 Hz to 1 MHz. The frequency ranges dominant by impedance properties of the membrane; electrodes and solution are marked in each graph. ....	14
Figure 12- The average capacitance change (%) at $\sim 1$ kHz detected using four prototypes (a) and a typical flux decline pattern during filtration of 1 gr/l PEG solution.....	15
Figure 13- Electrode configuration of 2-terminal experiments on flat membranes using the voltage electrodes fitted adjacent to the membrane on the feed and the permeate sides.....	16
Figure 14- Changes in conductance and capacitance during fouling of flat membrane using 1 gr/l PEG solution at 100 kPa.....	16
Figure 15- Flux change during fouling of flat membrane using 1 gr/l PEG solution at 100 kPa .....	17
Figure 16 - Electrode configuration of 2-terminal EIS experiments on flat membranes using the current electrodes fitted on the feed and the permeate sides .....	18
Figure 17 - Changes in conductance and capacitance during fouling of flat membrane using 1 gr/l PEG solution at 100 kPa. Experiments were performed in 2-terminal mode using current electrodes.....	18
Figure 18 – Conductance and capacitance change as a function of time at (a) low frequency of 10 Hz and (b) high frequency of 10 kHz. Experiments were performed in 2-terminal mode using current electrodes.	19
Figure 19 – Conductance and capacitance change as a function of time at 1 kHz. Experiments were performed in 2-terminal mode using current electrodes.....	20
Figure 20- Relative capacitance (at 1 kHz) and flux decline as a function of time without considering early stages of filtration experiments. EIS measurements were performed in 2-terminal mode using current electrodes.....	21
Figure 21 - Electrode configuration of 3-terminal experiments on flat membranes with 2 electrodes on feed side and 1 electrode on permeate side (3T-P1). ....	22
Figure 22 - Changes in conductance and capacitance during fouling of flat membrane using 1 gr/l PEG solution at 100 kPa. Experiments were performed in 3-terminal mode with 2 electrodes on feed side and 1 electrode on permeate side (3T-P1). ....	22

Figure 23 – Conductance and capacitance change as a function of time at (a) low frequency of 10 Hz and (b) high frequency of 1 MHz. Experiments were performed in 3-terminal mode with 2 electrodes on feed side and 1 electrode on permeate side (3T-P1).....	23
Figure 24 – Conductance and capacitance change as a function of time at 1 kHz. Experiments were performed in 3-terminal mode with 2 electrodes on feed side and 1 electrode on permeate side (3T-P1).	24
Figure 25- Capacitance (at 1 kHz) and relative flux changes as a function of time (a), and without considering the early stage of the filtration (b) experiments. EIS measurements in 3-terminal mode with 2 electrodes on feed side and 1 electrode on permeate side (3T-P1).....	24
Figure 26 - Electrode configuration of 3-terminal experiments on flat membranes with 2 electrodes on permeate side and 1 electrode on feed side (3T-F1).....	25
Figure 27 - Changes in conductance and capacitance during fouling of flat membrane using 1 gr/l PEG solution at 100 kPa. Experiments were performed in 3-terminal mode with 1 electrode on feed side and 2 electrodes on permeate side (3T-F1).....	25
Figure 28 – Conductance and capacitance change as a function of time at (a) low frequency of 10 Hz and (b) high frequency of 100 kHz. Experiments were performed in 3-terminal mode with 1 electrode on feed side and 2 electrodes on permeate side (3T-F1). ....	26
Figure 29 – Conductance and capacitance change as a function of time at 1 kHz. Experiments were performed in 3-terminal mode with 1 electrode on feed side and 2 electrodes on permeate side (3T-F1).	27
Figure 30- Capacitance (at 1 kHz) and relative flux changes as a function of time without considering the early stage ( i.e. first 17 minutes ) of the filtration experiments. EIS measurements were performed in 3-terminal mode with 1 electrode on feed side and 2 electrodes on permeate side (3T-F1).....	27
Figure 31 - Electrode configuration of 4-terminal experiments on flat membranes with 2 electrodes on permeate side and 2 electrodes on feed side.....	28
Figure 32 - Changes in conductance and capacitance during fouling of flat membrane using 1 gr/l PEG solution at 100 kPa. Experiments were performed in 4-terminal mode. ....	29
Figure 33 – Conductance and capacitance change as a function of time at (a) low frequency of 10 Hz and (b) high frequency of 100 kHz. Experiments were performed in 4-terminal mode. ....	29
Figure 34 – Conductance and capacitance change as a function of time at 1 kHz. Experiments were performed in 4-terminal mode. ....	30
Figure 35- Capacitance (at 1 kHz) and relative flux changes as a function of time without considering the early stage ( i.e. first 17 minutes ) of the filtration experiments. EIS measurements were performed in 4-terminal mode .....	30
Figure 36- 2-terminal electrode configuration used for EIS characterisation of outside-in hollow fibre membranes .....	32
Figure 37- Total percentage changes of capacitance (C) and conductance (G) during fouling measured using configurations 1 and 2. ....	33
Figure 38- Total percentage changes of capacitance (C) and conductance (G) during filtration of 5 gr/l PEG solution. EIS experiments were performed using configurations 2, 3 and 4. ....	34
Figure 39- Capacitance (C) at 10 kHz as a function of time during filtration of 5 gr/l PEG solution. EIS experiments were performed using configurations 2, 3 and 4. ....	36
Figure 40- Four prototypes used in monitoring filtration of PEG solution using inside-out hollow fibre membranes. Total percentage changes of capacitance (C) and Conductance (G) during fouling is plotted at frequencies ranging from 1 Hz to 1 MHz. ....	40
Figure 41- Percentage changes of capacitance (C) at 1 kHz compared to relative flux decline for (a): prototypes 3 (i.e. with wire electrode fitted inside hollow fibre), and (b): prototype 4 (i.e. with no wire inside hollow fibre membrane).....	41

Figure 42- Total percentage changes of capacitance (C) and conductance (G) during fouling and backwashing of inside-out hollow fibre membrane: a) using prototype 3 (one wire inside fibres and a long electrode outside the membrane) , and b) using prototype 4 (no wire inside fibres and a long electrode outside the membrane).....	42
Figure 43- Capacitance at 1 kHz during backwashing of inside-out hollow fibre membrane: a) using prototype 3 (one wire inside fibres and a long electrode outside the membrane), and b) using prototype 4 (no wire inside fibres and a long electrode outside the membrane). ....	43
Figure 44- Effect of inserting a wire inside one of the fibres of inside-out hollow fibre membrane. ....	44
Figure 45- Effect of electrode position on performance of EIS in detection of fouling using outside-in and inside-out hollow fibre membranes .....	45
Figure 46- The structure of the prototype module designed for characterisation of hollow fibre membranes using EIS.....	46
Figure 47- Typical capacitance and conductance change at a) low frequency (1 Hz) and b) high frequency (1 MHz) during filtration of 1% dunder feed using outside-in hollow fibre membranes. The module was fitted with one common electrode on the permeate side. ....	49
Figure 48- Relative capacitance change at 1 kHz during filtration without considering the early stage of fouling experiment using 1% dunder. The module was fitted with one common electrode on the permeate side .....	49
Figure 49- Capacitance and conductance change (percentage) during filtration without considering the early stage of fouling experiment 1% dunder feed using outside-in hollow fibre membranes. The module was fitted with one common electrode on the permeate side.....	50
Figure 50- Typical capacitance and conductance change at a) low frequency (1 Hz) and b) high frequency (1 MHz) during filtration of 10% dunder feed using outside-in hollow fibre membranes. The module was fitted with one common electrode on the permeate side. ....	51
Figure 51- Capacitance at 10 kHz during filtration without considering the early stage of fouling experiment using 10% dunder feed. The module was fitted with one common electrode on the permeate side .....	51
Figure 52- Capacitance and conductance change (percentage) during filtration without considering the early stage of fouling experiment 10% dunder feed using outside-in hollow fibre membranes. The module was fitted with one common electrode on the permeate side.....	52
Figure 53- Typical capacitance and conductance change at a) low frequency (1 Hz) and b) high frequency (1 MHz) during filtration of 1% dunder feed using outside-in hollow fibre membranes. One of the fibres was fitted with a wire electrode. ....	53
Figure 54- Capacitance and conductance change at 1 kHz during filtration of 1% dunder feed using outside-in hollow fibre membranes. One of the fibres was fitted with a wire electrode.....	53
Figure 55- Capacitance and conductance change (percentage) during filtration of 1% dunder feed using outside-in hollow fibre membranes. One of the fibres was fitted with a wire electrode.....	54
Figure 56- Typical capacitance and conductance change at: a) low frequency (1 Hz) and b) high frequency (1 MHz) during filtration of 10% dunder feed using outside-in hollow fibre membranes. One of the fibres was fitted with a wire electrode. ....	54
Figure 57- Capacitance and conductance change at 1 kHz during filtration of 10% dunder feed using outside-in hollow fibre membranes. One of the fibres was fitted with a wire electrode.....	55
Figure 58- Capacitance and conductance change (percentage) during filtration of 1% dunder feed using outside-in hollow fibre membranes. One of the fibres was fitted with a wire electrode.....	55
Figure 59- Percentage of decline during fouling in flux and capacitance at 1 kHz using modules with different electrode configurations. * Capacitance at 10 kHz. ....	56

Figure 60- Capacitance and conductance at 1 kHz during backwashing of hollow fibre membrane fouled with : (a) 1% and (b) 10% dunder feed. The module was fitted with one common electrode on the permeate side. ....	57
Figure 61- Total percentage change of capacitance, conductance during backwashing of hollow fibre membrane fouled : (a) 1% and (b) 10% dunder feed. The module was fitted with one common electrode on the permeate side.....	58
Figure 62- Capacitance, conductance change during the first stage of backwashing of hollow fibre membrane fouled with 10% dunder feed. The module was fitted with one common electrode on the permeate side. ....	59
Figure 63- Capacitance and conductance at 1 kHz during backwashing of hollow fibre membrane fouled with : (a) 1% and (b) 10% dunder feed. One of the fibres was fitted with a wire electrode.....	60
Figure 64- Total percentage change of capacitance, conductance during backwashing of hollow fibre membrane fouled with 10% dunder feed. One of the fibres was fitted with a wire electrode. ....	61
Figure 65- Capacitance change during backwashing recorded using modules with different electrode configurations.* Capacitance increase recorded at early stage of backwashing is considered for the configuration with no wire inside the fibres.** In comparison with the values for 1 wire module , this value is an over estimation. ....	61
Figure 66- Impedance of clean, fouled, backwashed and chemically cleaned hollow fibre membrane measured using the module with one common electrode on the permeate side (i.e. no wire): a) membrane fouled using 1% dunder feed, and b)membrane fouled using 10% dunder feed.....	63
Figure 67- Impedance of clean, fouled, backwashed and chemically cleaned hollow fibre membrane measured using the module with one wire electrode fitted in one of the fibres (i.e. one wire): a) membrane fouled using 1% dunder feed, and b) membrane fouled using 10% dunder feed. ....	64
Figure 68- Typical water flux data at different stages of fouling and cleaning process .....	66
Figure 69- Impedance decline relative to clean membrane measured using modules with different electrode configurations: after fouling, backwashing and cleaning processes. ....	66
Figure 70- Accumulated weight of the filtrate during filtration of 1% dunder feed at 100 kPa using flat PES microfiltration membranes with average pore size of 3, 0.8, 0.22 and 0.1 $\mu\text{m}$ . ....	67
Figure 71- Flux decline as a function of time (a) and initial , average and final flux of permeate (b) during filtration of 1% dunder feed at 100 kPa using flat PES microfiltration membranes with average pore size of 0.8, 0.22 and 0.1 $\mu\text{m}$ . ....	68
Figure 72- Solid content of 1% dunder feed compared with the solid content of the permeate s of flat microfiltration and hollow fibre membranes. ....	68
Figure 73- Flux decline during filtration of the permeate of hollow fibre membrane using ultrafiltration membrane with 20kDa molecular weight cut off.....	70
Figure 74- Solid content of the feed , permeate hollow of fibre and ultrafiltration membranes: a) 1% and b) 10% dunder feed. The permeate of hollow fibre membrane was used as feed for ultrafiltration membranes. ....	70

## List of Tables

Table 1 - Characterisation of dunder waste.....	7
Table 2 -Characterisation of feed and permeate of hollow fibre membranes.....	69
Table 3 -Timetable of the project .....	76

## 1. Introduction

Hollow fibre membranes and membrane bioreactors (MBRs) have been actively used for municipal and industrial wastewater treatments [1]. The two main issues hindering wider applications of this technology are the high cost of membrane materials and membrane fouling [2-4]. On the latter case, the efforts of research institutes and the industry sector are focused on understanding the mechanism of fouling, the nature of foulant, visualising and direct monitoring of fouling [2, 5]. Usually, fouling and its dependencies are characterised from filtration data [6]. In situ methods are preferred because they do not involve potential changes of feed or permeate properties by sampling or storage [2]. The basic of most in situ methods developed for detection of fouling in MBRs is measuring filtration parameters such as flux and trans-membrane pressure. In the present study, we examined the feasibility of using electrical measurements for monitoring of fouling in MBRs.

For this, we used an electrical impedance spectrometer (EIS). EIS measures the electrical impedance (i.e. the complex electrical resistance) by injecting a small signal to the sample and measuring the ratio of an alternating voltage to its corresponding current and the phase difference between them [7, 8]. Therefore, EIS can potentially be used as a simple non-destructive method to monitor the filtration process in MBRs [9].

There are two different types of hollow fibre membranes depending on the direction of permeate flow. For membranes with rejection (or skin layer) facing outside, the feed moves from outside and permeate is extracted from inside of the membrane. These membranes are called outside-in and are more common than the inside-out type. The hollow fibre membranes used in the first phase of this project were an outside-in type. In the case of the inside-out membrane, the flow is in the opposite direction, the feed is inside the membrane and permeate flows through the sides of hollow fibre [10-12].

The biggest advantage of an outside-in system is the possibility of filtering feeds with high suspended solids content. Most of the commercially available hollow fibre modules for MBR operate in outside-in mode. On the other hand, using inside-out type hollow fibre membranes it is possible to maintain uniform hydrodynamics in the lumen. However, it is not practical to generate the turbulence that is crucial to mitigate fouling [11].

Our preliminary experiments showed that EIS can be used to monitor the fouling of outside-in hollow fibre membranes. In this report, we present the results obtained using inside-out hollow fibre membranes in addition to outside-in membranes and flat membranes.

The performance of EIS for detection of fouling is also examined using an industrial bio-feed. The by-product of yeast, called “dunder” was used as the model wastewater. For instance, Appleton produces about 78 million litres of dunder waste as the by-product of six million litres of rum <sup>1</sup>. Dunder water has created serious health and environmental problems in the past. One problem is that decomposition of dunder generates hydrogen sulphide gas which is flammable and poisonous. This has created severe health problems for people living close to yeast manufacturing companies.

Dunder happens to be rich in nutrients such as potassium, nitrogen and phosphorous [13]. This suggests that this waste material can be used as fertilizer [14, 15]. For example, Appleton is using dunder in about 500 hectares its 2,270 hectares of sugar cane and has predicted to save about \$50,000 in fertilizer cost while solving the waste issue. However, some studies have shown that using dunder can result in sodium toxicity when the soil or irrigation water has inherently high sodium levels [15]. Therefore, separating organic matters and cations (such as potassium) of dunder has been the focus of the research at AB Mauri to reuse dunder waste. Filtration using flat membranes has been proven to be ineffective due to fouling nature of the feed. In the present study, the performance of hollow outside-in fibre membranes in this separation process is examined. The

---

<sup>1</sup> <http://www.ipsnews.net/1999/12/jamaica-company-finds-silver-lining-in-noxious-cane-waste/>

filtration process is monitored using EIS and the capability of this technique in detection of fouling is investigated.

## 2. Objectives

“Membrane fouling” is one of the biggest problems of operating membrane-based water treatment plants. Regular backwashing and cleaning are examples of the methods used to tackle this problem. If detected early, the flux reduction (or pressure increase) due to fouling can be prevented by simple backwash or cleaning. However, progressed fouling can only be reversed, partially, using strong cleaning chemicals that can damage the membranes. Eventually, the membrane modules need to be replaced. Therefore, finding new techniques to detect fouling can help to reduce the cost of operation in water treatment plants.

This research aimed to:

- Develop an experimental measuring cell, fitted with suitable electrodes for simultaneous electrical impedance spectroscopy (EIS) measurements and filtration experiments.
- Characterise using EIS the structure of various hollow fibre membranes and their fouling.
- Comparative studies of the EIS characterisations of flat sheet and hollow fibre membranes.
- Design a special sample chamber for hollow fibres.

Electrical impedance spectroscopy has been proven to be effective for in-situ monitoring of fouling in *flat* membranes [16-29] but to the best of our knowledge, there is no report on the application of this method to hollow fibre membranes. This could be partially due to the spatial limitations in hollow fibre membranes. In most of the EIS methods used for characterisation of flat membranes, a 4-terminal electrode configuration has been used. In this method, the current and voltage electrodes are separated. Two current electrodes are fitted in feed and permeate sides, and two voltage sensing electrodes are fitted very close to the membrane on each side. In the case of hollow fibre

membranes, there is not much limitation on size, number and location of electrodes outside the membrane. However, it is not possible to fit two electrodes inside the membrane fibres. The best case scenario is that one thin wire can be fitted inside each fibre if the internal diameter of the fibre is significantly greater than that of the wire. If the fibre is very thin, fitting a wire inside it is not possible and fitting a common electrode, possibly a porous disc, at the cross section of the fibres bundle is the only practical option.

In the first phase of this project, we showed that in principal EIS can detect changes in electrical properties due to membrane fouling. We also examined the effect of electrode configuration on accuracy of these measurements relative to the extent of fouling. It was concluded that fitting electrodes inside each membrane fibre is not necessary for detection of fouling; however, can slightly improve the sensitivity of the method.

In this final report, we investigate this further and also compare the results with those obtained for flat membranes and hollow fibre membrane with inside-out filtration design. This is to explain the outcome of the experiments on normal outside-in hollow fibres and to design a prototype. The system is then used to characterise the fouling behaviour of an industrial feed.

### 3. Project outcomes

#### 3.1. Materials

**Outside-in hollow fibres:** The hollow fibre membranes used in the present study were Ultraflo membranes (ULTRA-FLO, Singapore), with an internal diameter of 0.5 mm. Figure 1 shows the microstructure of these hollow fibre membranes.

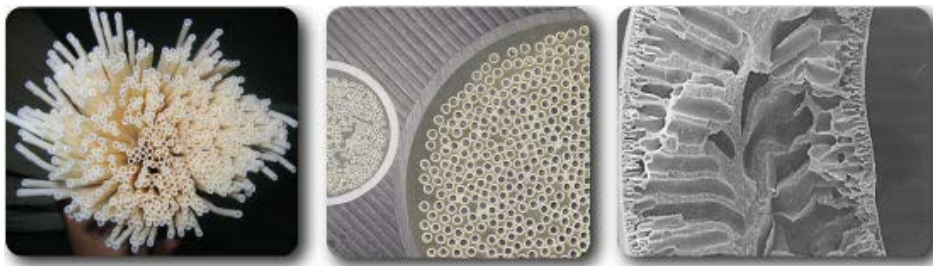


Figure 1 - Structure of outside-in hollow fibre membranes.

**Inside- out hollow fibres:** The Multibore® Inge membranes from BASF Germany were used as model inside-out hollow fibre membranes. As shown in Figure 2, each Multibore® hollow fibre is comprised of seven individual capillaries in a single fibre. These innovative membranes have higher mechanical strength. It is claimed that these membranes are of ultrafiltration type and also capable of removing viruses from water [30-33].



Figure 2- Structure of inside-out Multibore® hollow fibre membrane.

**Flat membranes:** The flat membranes used in the present study were PVDF microfiltration membranes (Pall Fluoro Tran® W) supplied by PALL Life Sciences (Australia). The thickness and the nominal pore size of the membranes were 123 and 0.22  $\mu\text{m}$ , respectively. Typical SEM image of the PVDF microfiltration membranes is shown in Figure 3.

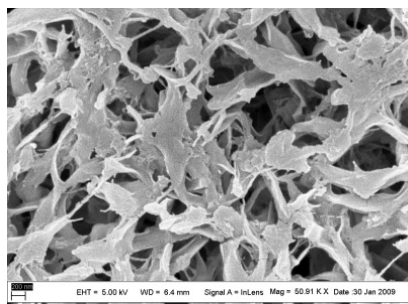


Figure 3 - Microstructure of flat membrane used in the first phase of the project.

**Laboratory model feed:** Polyethylene glycol (PEG) was chosen as the model foulant for filtration tests because the fouling behaviour of PEG is very similar to proteins and other organic materials found in waste water. PEG is a synthetic material and can be readily obtained with reproducible average molecular weight and molecular weight distribution. More importantly, it is rather difficult to control consistency of electrical properties of model biological feeds. PEG with average nominal molecular weight of 100,000 Dalton (i.e., 100 kDa), was purchased from Sigma Aldrich and was used in filtration experiments.

**Industrial model feed:** Dunder waste, a by-product of yeast production, was supplied by AB Mauri<sup>2</sup>. The waste was centrifuged to remove the large solid particles. The liquid phase of the processed waste was characterised and used in the filtration experiments. Table 1 shows the characteristic properties of this wastewater.

The chemical oxygen demand<sup>3</sup> (COD) of this feed (after centrifuge) is about 300,000 mg/L. This value is significantly higher than COD of municipal wastewater and even some heavy industrial wastewaters. The COD of high strength industrial waste water treated using specially designed MBRs range from 700-67,000 mg/L[34]. A typical COD value for municipal waste water is usually

<sup>2</sup> AB Mauri is a division of Associated British Foods plc (ABF) that produces yeast and bakery ingredients. This company is one of the largest yeast manufacturers in the world.

<sup>3</sup> COD - chemical oxygen demand. The COD test is commonly used to indirectly measure the amount of organic compounds in water. The COD is often measured using a strong oxidant (e.g. potassium dichromate) under acidic conditions. A known excess amount of the oxidant is added to the sample by titration and using an indicator solution. The amount of oxidant for complete oxidation of 1 litre feed is reported.

500 to 700 mg/l [35]. Therefore, solutions containing 1% and 10% of this waste were used for filtration experiments.

Table 1 - Characterisation of dunder waste.

pH	4.5
Conductivity (mS/cm <sup>2</sup> )	131-141
Colour (Pt/Co Units)	207,000-211,000
Osmolality (Osm/kg)	2,970
COD (mg/L), UV/TiO <sub>2</sub> method (Aquadiagnostic)	345,000- 415,000
Solid content (%)	34-40
Chloride (mg/L), Merck Spectroquant	17,500
Ammonium (mg/L), Merck Spectroquant	50
Ammonium (mg/L), Ion Specific Electrode (Hanna)	66

Strong brown colour and smell of molasses are other properties of the dunder waste. It is rather difficult to measure and present the latter, but the brown colour of the 10% feed (or sludge) in contrast with white hollow fibres is depicted in Figure 4.

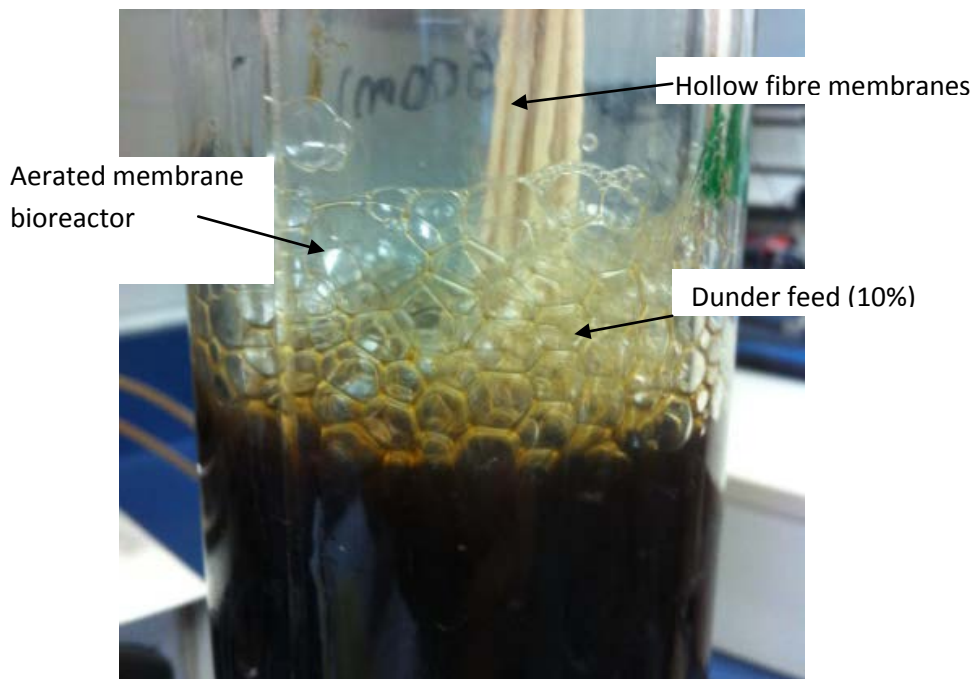


Figure 4 - Hollow fibre membranes at the beginning of filtration experiment using 10% dunder waste feed in the membrane bioreactor. Aeration is used to preserve the feed and to reduce fouling.

## 3.2. Methods

### 3.2.1. Membrane module preparation

**Outside-in hollow fibre membranes:** For experiments using the model feed (i.e. PEG solution), the modules were made of three membrane fibres of about 150 mm length which were fitted in 10 mm tube on one side. The free side of the tube was filled with epoxy resin. The other end of the fibres was sealed in the same way but using a 250 mm tube. The epoxy resin was left to set thoroughly at least for 24 hours. Then, 50 mm of the longer side of the tube (250 mm) was cut using a sharp cutter to expose the cross section of the membranes. This side of the membrane bundle was then fitted inside the plastic fittings required for connecting the module to a vacuum pump. For experiments using biological waste solution, the same bundling method was used to assemble 10 hollow fibres of about 240-300 mm length.

**Inside-out hollow fibre membranes:** single Multibore hollow fibre tube of about 250 mm was used in each experiment. The membrane was fitted in a ¼” Swagelok fitting on one side, and the free side was sealed using epoxy resin.

The membrane modules were pre-wetted for 12 hr in ethanol/water mixture [36] followed 3 hr in distilled water. The water was changed a few times, and the membranes were washed repeatedly with water to ensure the complete removal of ethanol. When using PEG as feed, removing the ethanol was important because PEG is insoluble in ethanol [37]. Residual ethanol could result in precipitation of PEG in the membrane and could lead to premature blocking.

### 3.2.2. Filtration experiments

**Outside-in hollow fibre membranes:** Figure 5 schematically shows the experimental set up used for testing the filtration performance and electrical properties of hollow fibre membranes. The membrane module was connected to a vacuum pump generating -0.5 bar (-50 kPa) suction force. A

trap was installed between the membrane module and the pump to collect the filtrate and also to protect the pump. The membrane was immersed in a container filled with the feed solution. The level of the feed was kept constant by fitting an outlet for overflow. The feed was pumped in a constant rate of 5 ml/min from the feed reservoir to the membrane container, and the excess was returned to the reservoir via the overflow outlet. The reservoir was placed on a digital balance, and its weight reduction was monitored by time to estimate the permeate flux. Electrodes were fitted on permeate and feed sides and were connected to an electrical impedance spectrometer for monitoring the electrical properties of the system during filtration. The water flux generated using this set up was about 4.4 L/hr/m<sup>2</sup>. The flux change during fouling was recorded by time and was normalized to the initial flux of PEG solution to indicate the level of fouling. Higher vacuum levels could result in higher flux and hence accelerated the fouling. However, -50 kPa was the maximum suction force that this pump was able to maintain for a long time. This was not of great concern in the present study because the main purpose of these experiments was to find out if there is a relationship between EIS data and flux decline.

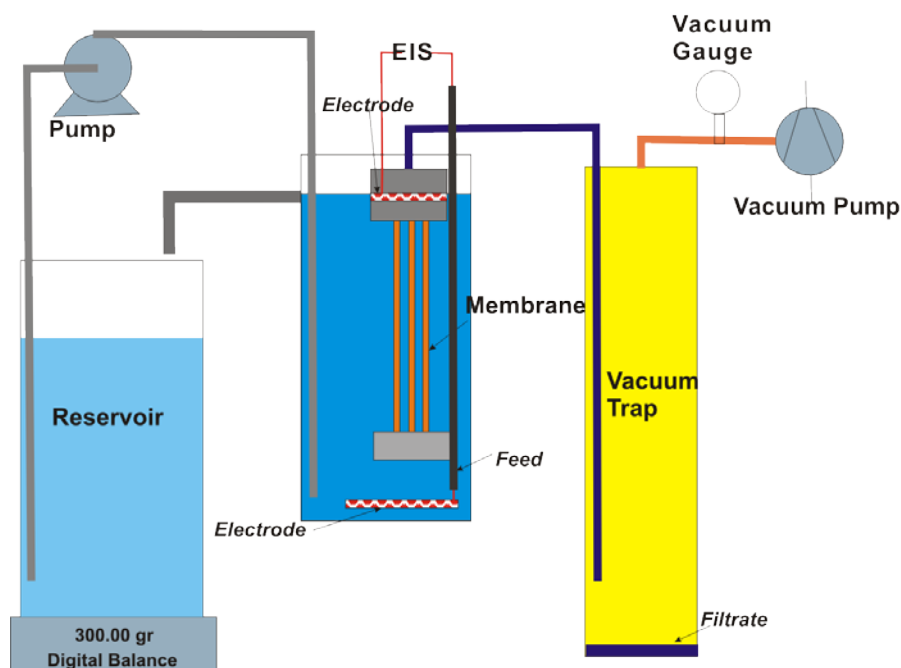


Figure 5 - Schematic diagram of the filtration/EIS experimental setup for characterising outside-in hollow fibre membranes.

**Bio-feed filtration** using inside in hollow fibre membranes were performed using a setup similar to the rig shown in Figure 5. However, because the surface area of the membrane was larger, the flux was generated using a normal pump instead of the vacuum pump. The permeate was collected, and its weight was monitored to detect fouling. Similar to the experiments performed on PEG solution, the experiments were conducted at constant vacuum of  $-95\pm 2$  kPa. For this, the setting on the pump head was adjusted for a thicker tube than the diameter of the tube fitted in the pump. The vacuum level was monitored, and its deviation was recorded.

A constant flow of air was injected to the membrane bioreactor to aerate the feed. The feed was circulated from a well-mixed reservoir to MBR via an overflow outlet to keep the feed level constant. This experiment setup is shown in Figure 6.

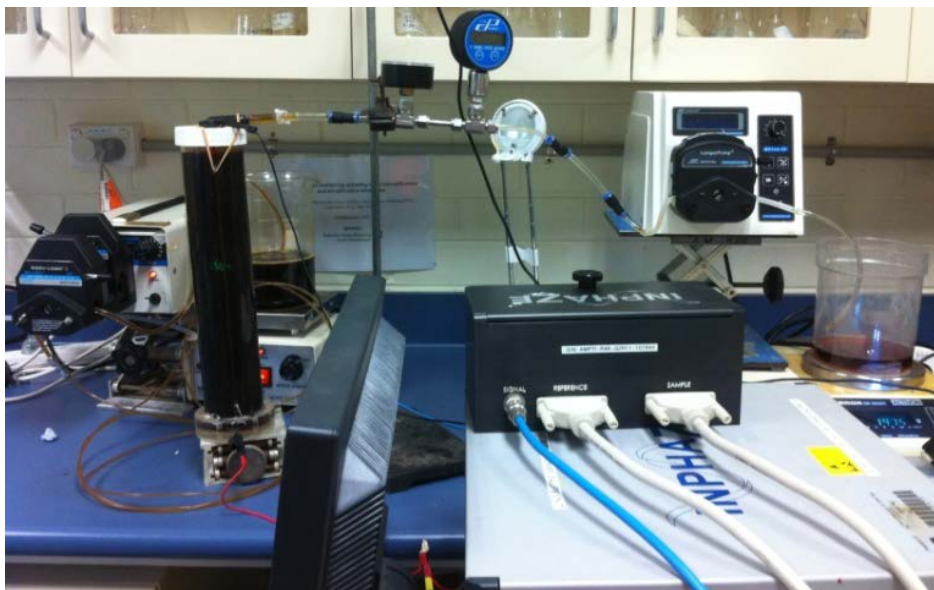


Figure 6 - Filtration/EIS experimental setup to monitor fouling of outside-in hollow fibre membranes by bio-feed.

**Inside-out hollow fibre membranes:** the setup used for testing these membranes (shown in Figure 7) was slightly different. The filtration experiments were performed in dead-end mode. The feed was stored in a reservoir and was injected to the membrane module at constant pressure of 100 kPa pressure generated using compressed air. The feed level was kept constant by fitting an overflow outlet. The permeate was collected in a reservoir, and its mass was measured using a digital balance.

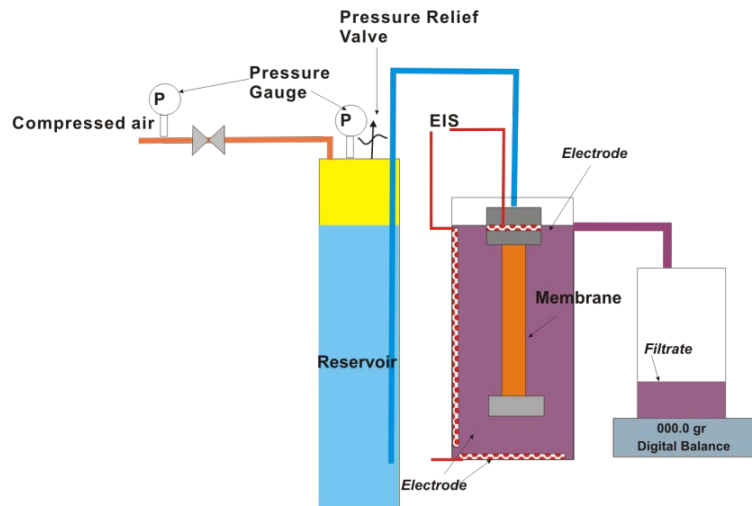


Figure 7 - Schematic diagram of the filtration/EIS experimental setup for characterising inside-out hollow fibre membranes.

**Flat membranes:** Figure 8 schematically shows the filtration setup used for online monitoring of flat microfiltration membranes fouling. The dead end filtration experiments were performed at constant pressure of 100 kPa. The feed was stored in a 1500 ml reservoir installed between the pressure source and the filtration cell. Pressure was obtained by compressed air and was maintained at a constant value using a pressure regulator. The permeate was collected in a reservoir placed on an electronic balance. The permeate flux was calculated from recordings of the mass as a function of time.

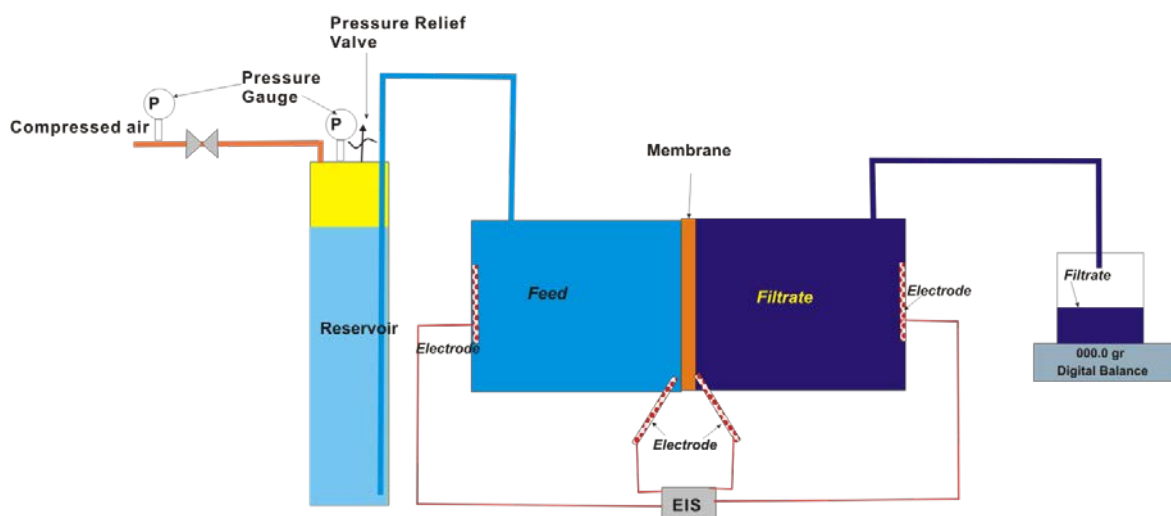


Figure 8 - Schematic diagram of the filtration/EIS experimental setup for characterising flat membranes.

Figure 9 shows the structure of the membrane chamber used in these experiments. Two silver discs coated with Silver Chloride (Ag/ AgCl) were fitted in each compartment that are usually used for injecting the current. One voltage sensing electrodes fitted on each side close to the membranes are usually used for sensing the voltage. 2-terminal, 3-terminal and 4-terminal measurements were performed to monitor the fouling of flat membranes.

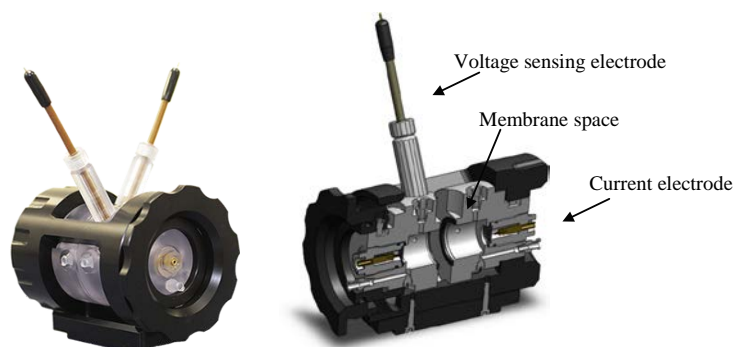


Figure 9 - Structure of the 4-terminal chamber used for characterization of flat membranes.

### 3.2.2.1. Electrical impedance spectroscopy

Electrical impedance spectroscopy (EIS) measures the electrical potential ( $v_0$ ) and the phase shift ( $\phi$ ) of a sample in response to an alternating current of small amplitude ( $i_0$ ) and known angular frequency  $\omega$  [9, 38]. The voltage across the sample is  $v$  and has the same frequency as the current ( $i$ ). However, they are out of phase by  $\phi$  as illustrated in Figure 10.

The impedance ( $Z$ ) is defined by its magnitude ( $|Z| = v_0 / i_0$ ) and its phase angle ( $\phi$ ) which is the phase angle between the AC voltage and the AC current. The impedance that is generally frequency-dependent can be expressed in terms of conductance ( $G$ ) and capacitance ( $C$ ) as shown below:

$$G(\omega) = 1/|Z| \cos(\phi) \quad (1)$$

$$C(\omega) = -1/(\omega|Z|) \sin(\phi) \quad (2)$$

More information about the impedance spectroscopy and its application can be found elsewhere [7, 9].

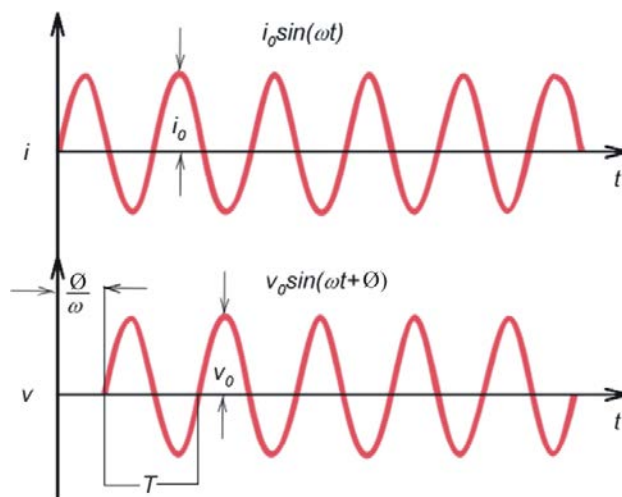


Figure 10 - Sinusoidal function of  $v$  and  $i$  and  $v$  with a shift of  $\phi/\omega$ .  $\omega$  is the angular frequency and  $\omega=2\pi/T$  where  $T$  is the period and the frequency in cycle per second is  $f=1/T$ .

In the present study an INPHAZE<sup>TM</sup> high resolution impedance spectrometer (developed by INPHAZE Co., Australia) was used to measure the impedance of the system. In the spectrometer, the unknown impedance element (i.e. the membrane) is in series with a standard (known) impedance. The latter can be adjusted to increase the accuracy of the measurements.

### 3.3. Results

#### 3.3.1. Summary of the first report

In the first phase of this research, four prototypes were prepared with different electrode configurations to detect fouling of hollow fibre membranes using EIS. As shown in Figure 11, in prototype 1 there is a wire electrode in only one of the fibres and outside electrode is a wire close to the membranes. In prototype 2 the outer electrode was changed to a disc further away from the membranes. In prototype 3, a wire electrode was inserted in each wire. However, a porous disc was used as a common electrode in prototype 4, and no wire was inserted inside the wires. The results of experiments using 1 gr/l Peg showed that fitting electrodes inside each membrane fibre is not necessary for detection of fouling; however, can slightly improve the sensitivity of EIS data to membrane fouling.

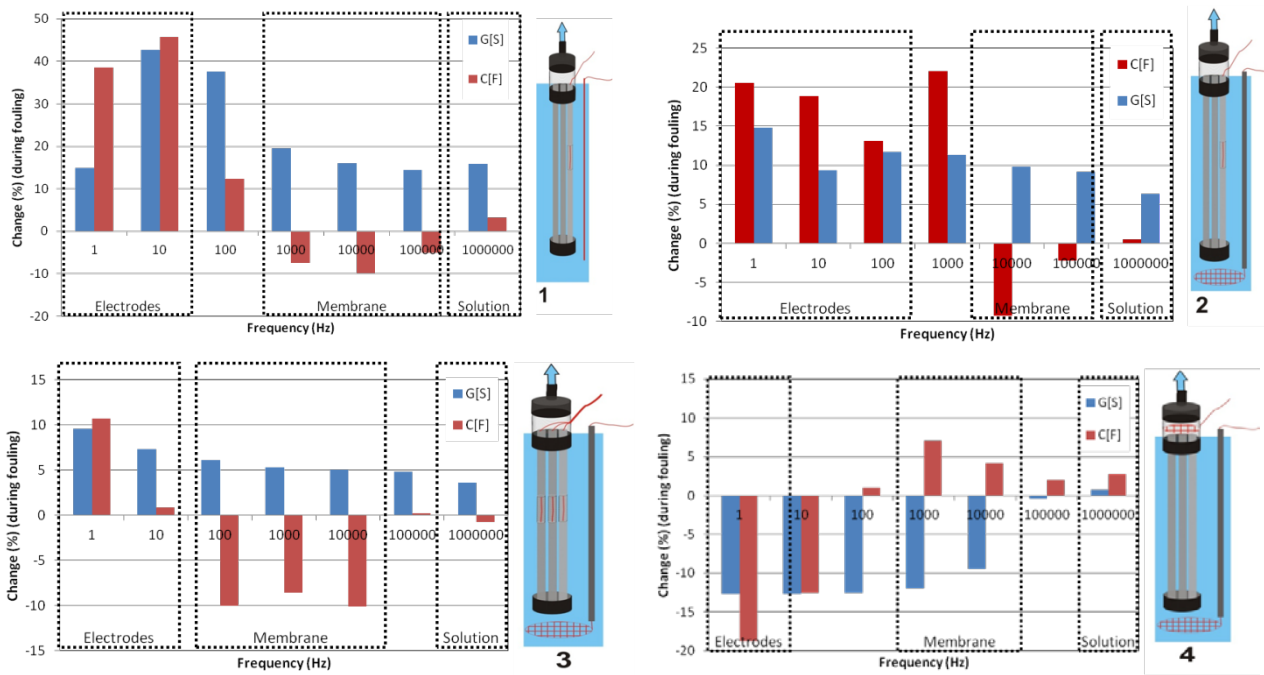


Figure 11 - Four prototypes used in monitoring filtration of PEG solution using outside-in hollow fibre membranes. Total percentage changes of capacitance (C) and Conductance (G) during fouling is plotted at frequencies ranging from 1 Hz to 1 MHz. The frequency ranges dominant by impedance properties of the membrane; electrodes and solution are marked in each graph.

Analysing the changes in electrical properties at different frequencies showed that the electrical properties at mid-frequency range (~ 1000 Hz) were dominated by impedance of the membrane. This suggested mid-frequency range is the most appropriate range for sensing the changes in membrane during the filtration process (see Figure 11). However, it was also found that exact range of the frequency was affected by position of the electrodes and hence needs to be identified for different electrode configurations.

In general, the relative changes in electrical properties detected using EIS was similar to the relative flux decline during the filtration process as shown in Figure 12 . Therefore, it was concluded that electrical impedance spectroscopy (EIS) can be used for online monitoring of fouling in hollow fibre membranes.

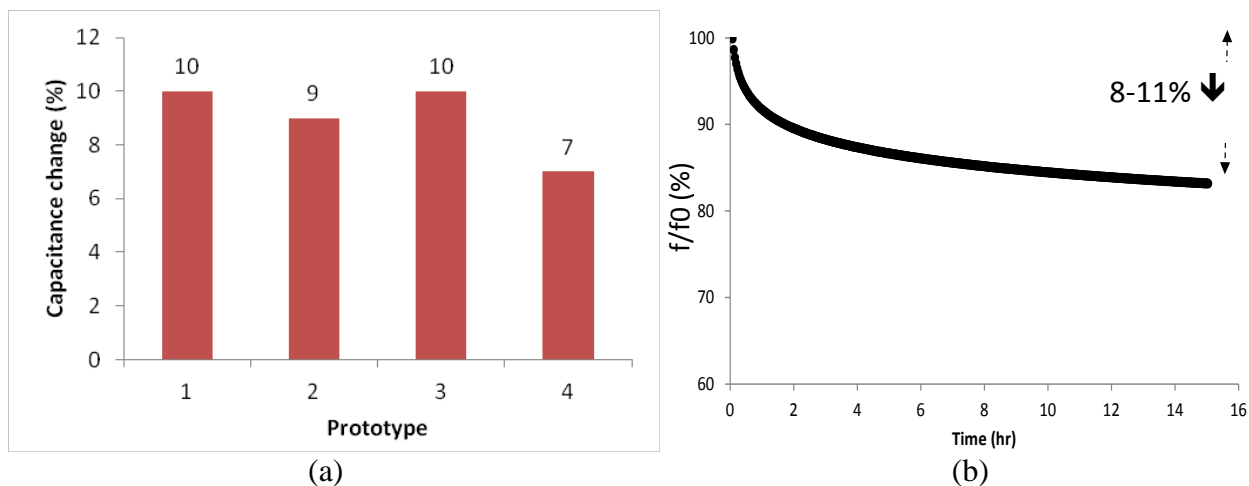


Figure 12 - The average capacitance change (%) at ~ 1 kHz detected using four prototypes (a) and a typical flux decline pattern during filtration of 1 gr/l PEG solution.

Comparing EIS spectra of clean and fouled membranes, it was shown that fouling changes the electrical properties of membranes noticeably. This suggested that EIS has the potential of being used as a non-destructive technique for autopsy characterisation of hollow fibre membranes.

Similar experiments were performed on flat membranes to understand the effect of electrode configuration on accuracy of EIS in detection of membrane fouling. This is because most of the earlier works on fouling detecting using EIS have been performed on flat membranes [9, 39-47]. The preliminary experiments performed in the first phase showed that an electrode configuration can affect the accuracy of EIS measurement for detection of membrane fouling. These experiments were continued in the second phase of this research.

### 3.3.2. Flat membranes

The membrane chamber used for testing the flat membranes had four electrodes: one electrode at each compartment commonly used for injecting the electric current and two electrodes adjacent to the membrane surface usually used for sensing the voltage. This electrode configuration has been used for characterising clean and fouled reverse osmosis (RO), and nanofiltration membranes [44].

In the present study, experiments using different electrode configurations were performed in order to understand the effect of electrode configuration on ability of EIS for detection of fouling in flat

membranes. The preliminary experiments presented in the first report were obtained in 2-terminal mode using the voltage electrodes fitted adjacent to the membrane on the feed and the permeate sides (shown in Figure 13).

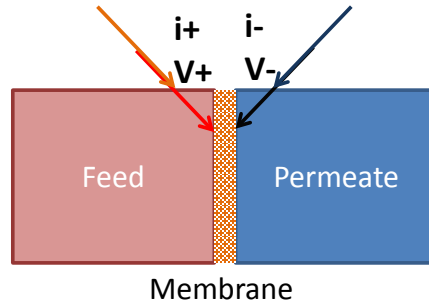


Figure 13 - Electrode configuration of 2-terminal experiments on flat membranes using the voltage electrodes fitted adjacent to the membrane on the feed and the permeate sides.

In preliminary experiments, 1 and 2 gr/l PEG solutions were filtered using PVDF microfiltration membranes and the fouling was monitored using electrical impedance spectroscopy. Figure 14 showed the changes in capacitance and conductance of the system after about 4.5 hours filtration using 1 gr/l PEG solution at 100 kPa.

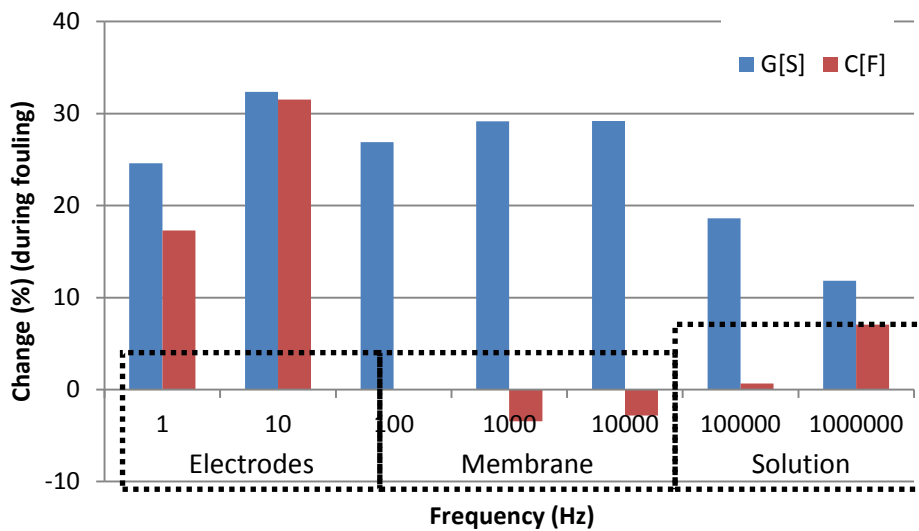


Figure 14 - Changes in conductance and capacitance during fouling of flat membrane using 1 gr/l PEG solution at 100 kPa

The sensitivity of EIS for detection of fouling was compared with flux changes. Figure 15 shows the flux data collected during the filtration of 1 gr/l PEG at constant pressure of 100 kPa.

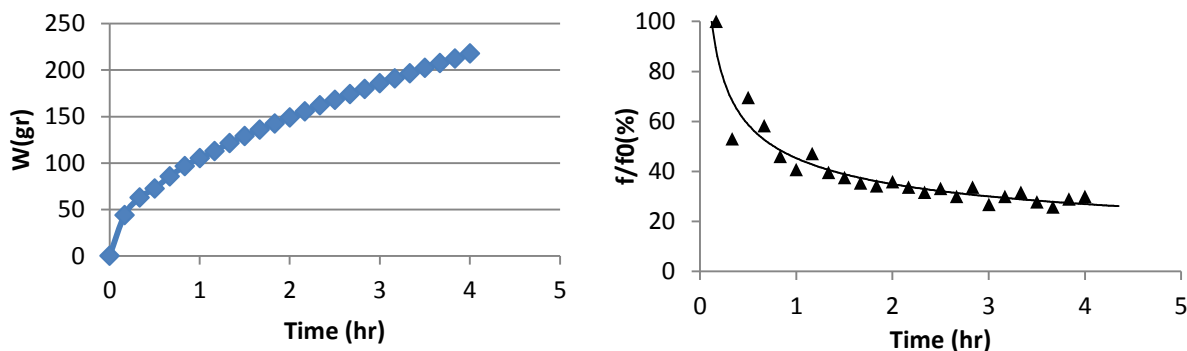


Figure 15 - Flux change during fouling of flat membrane using 1 gr/l PEG solution at 100 kPa.

These results showed that the flux declined about 70% during about 4.5 hour filtration. However, the capacitance and conductance changes recorded by EIS were below 40%. The decline in capacitance at 1 kHz-10 kHz range was correlated to fouling. This change was below 10% that is significantly lower than the fouling estimated by flux decline.

These results showed that 2-terminal measurements using Ag/AgCl electrodes fitted close to the membrane is not a proper design for online detection of fouling in flat microfiltration membranes. This should be pointed out that the voltage electrode had very small surface area and hence were only able to probe a very small area of the membrane. The efficiency of 2-terminal measurements could be improved using larger electrodes. However, fitting larger electrodes close to the membrane, even if made porous, can affect the flow pattern and fouling.

To examine the effect of electrode size, two large electrodes fitted at feed and permeate compartments, but not adjacent to the membrane, were used in the next step. These electrodes are usually used as current electrodes. This 2-terminal configuration is schematically depicted in Figure 16.

The percentage changes in conductance and capacitance during fouling are presented in Figure 17. Both conductance and capacitance increased during fouling at all frequencies. However, at mid-frequency range (i.e. about 1 kHz); the conductance rise was greater than that of capacitance. This could be an indication that impedance of membrane itself was dominant at this frequency range. Capacitance and conductance values as a function of time at typical low and high frequencies (e.g.

10 Hz and 10 kHz) are shown in Figure 18. These results confirm overall changes values at low and high frequencies (Figure 17). However, the trend of changes at mid-frequency range (100 Hz to 1 kHz) was different.

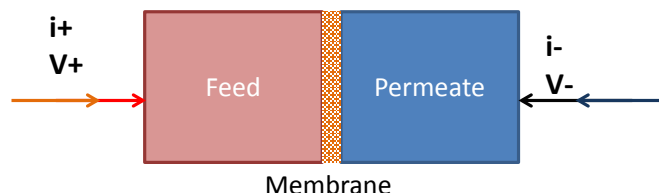


Figure 16 - Electrode configuration of 2-terminal EIS experiments on flat membranes using the current electrodes fitted on the feed and the permeate sides.

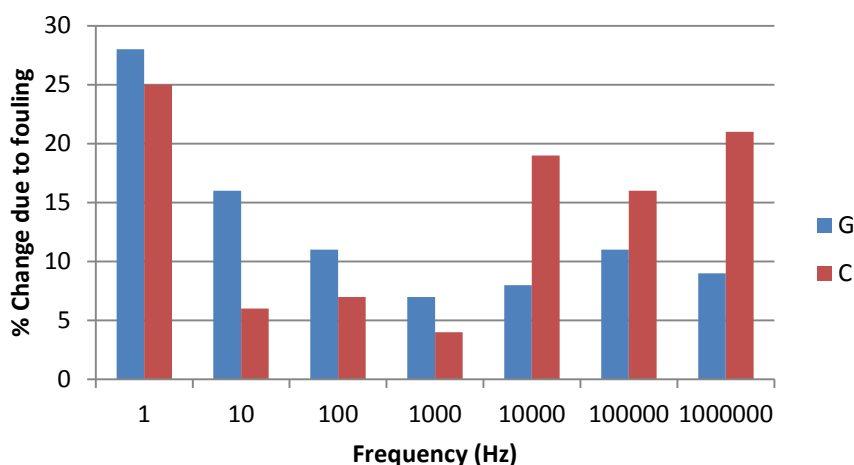


Figure 17 - Changes in conductance and capacitance during fouling of flat membrane using 1 gr/l PEG solution at 100 kPa. Experiments were performed in 2-terminal mode using current electrodes.

Capacitance and conductance value at 1 kHz as a function of fouling time are depicted in Figure 19. These graphs revealed that capacitance increased at early stages of fouling but then declined later. Conductance increases could be explained by increasing concentration of feed in electrolyte and the wet membrane. The higher concentration of feed also results in stronger ionic double layer<sup>4</sup> which translates to higher capacitance. The ionic double layer is usually the dominant part of overall impedance at low frequencies due to its high capacitive nature [48-50]. However, its effect can be extended to higher frequencies if the voltage is measured using the same electrode used for

<sup>4</sup> The water molecules and the anions are oriented on the surface of electrodes, satisfying the requirement of neutrality. The layer of two ions (i.e. ionic double layer) has a high capacitance due to its low thickness. More information was provided in the first report of the project.

injecting the current, that is 2-terminal measurements. The concentration of feed can also affect the range of frequencies dominated by the effect of ionic double layer. It was shown that a higher concentration of electrolyte extends the effect of ionic double layer to higher frequencies [51]. It seems one of the important factors on efficiency of electrode configuration design is finding a frequency range that the overall impedance is not dominated by the effect of ionic double layer.

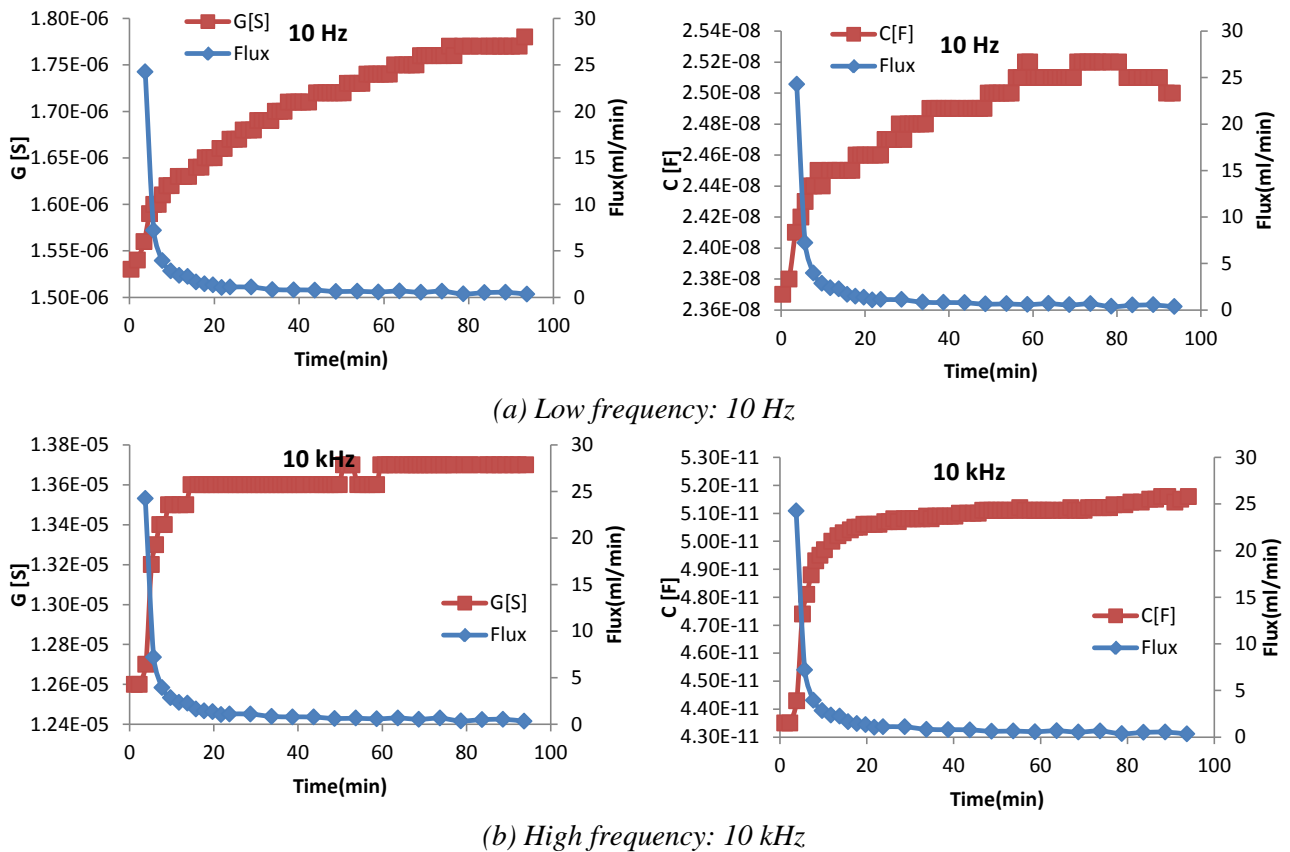


Figure 18 - Conductance and capacitance change as a function of time at (a) low frequency of 10 Hz and (b) high frequency of 10 kHz. Experiments were performed in 2-terminal mode using current electrodes.

At 1 kHz, after about 17 min after starting the filtration experiments, the capacitance declined in spite of conductance increase. This could be due to thickness growth as a result of foulant deposition on the surface of membrane. Moreover, this is an indication that the effect of ionic double layer was not extended to mid-frequency range.

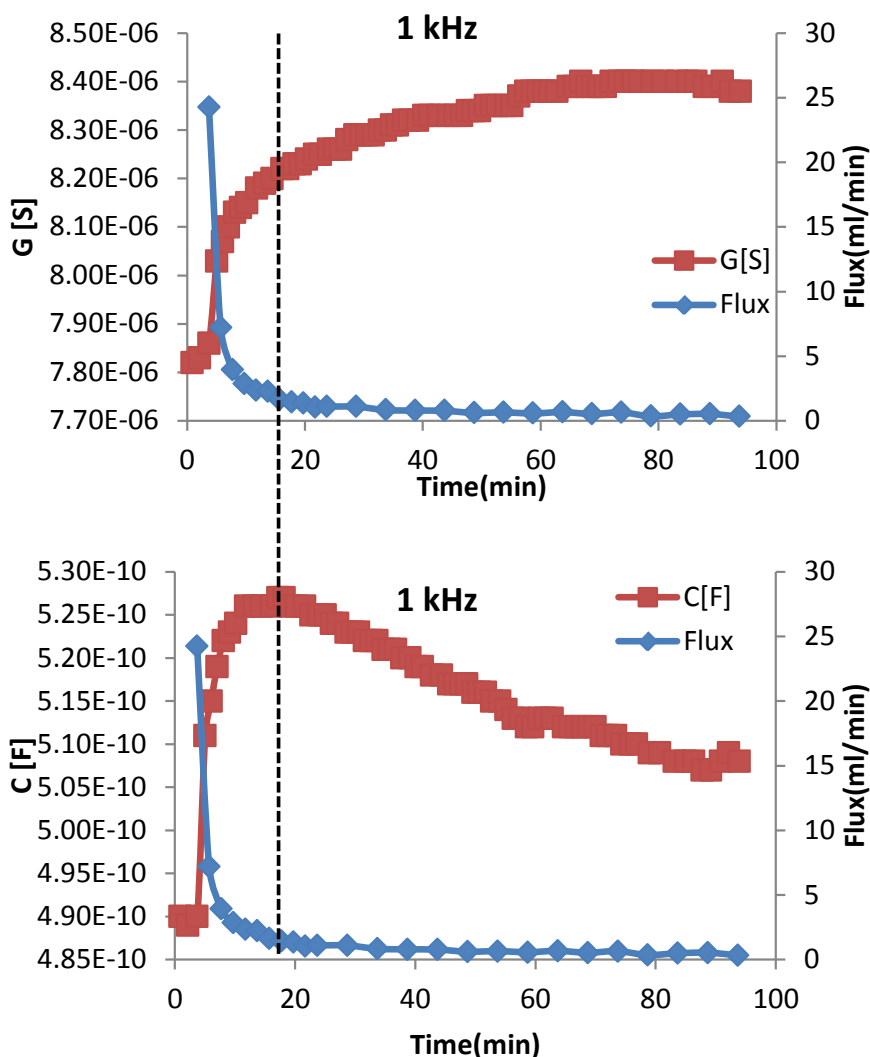


Figure 19 - Conductance and capacitance change as a function of time at 1 kHz. Experiments were performed in 2-terminal mode using current electrodes.

The trend of capacitance change can also be related to fouling phenomena. One theory is that the capacitance increase at early stages of fouling is due to the membrane compaction. Assuming that membrane is the dominant factor in total impedance of the system, which is in agreement with earlier reports [17, 19, 52] [24] compaction reduces the thickness of the membrane and hence could potentially increase the capacitance. Another theory is that capacitance trend can be affected by fouling mechanism. Our previous study showed that fouling of these PVDF microfiltration membranes using 100 kDa PEG begins with pore blocking because of smaller size molecules filling the membrane pores. Later, an organic film is formed on the surface of membrane. From the electrical point of view deposition of foulant particle can increase dielectric constant of the

membrane and the capacitance. This could be another reason for capacitance at early stages of fouling. We examined these theories by changing electrode configuration.

The flux decline relative to initial flux was modified to only cover the flux data obtained in the second stage of filtration, i.e. after 17 minutes. Comparing the relative capacitance decline at 1 kHz and relative flux decline (shown in Figure 20) it can be said that the trend of changes in two parameters is similar.

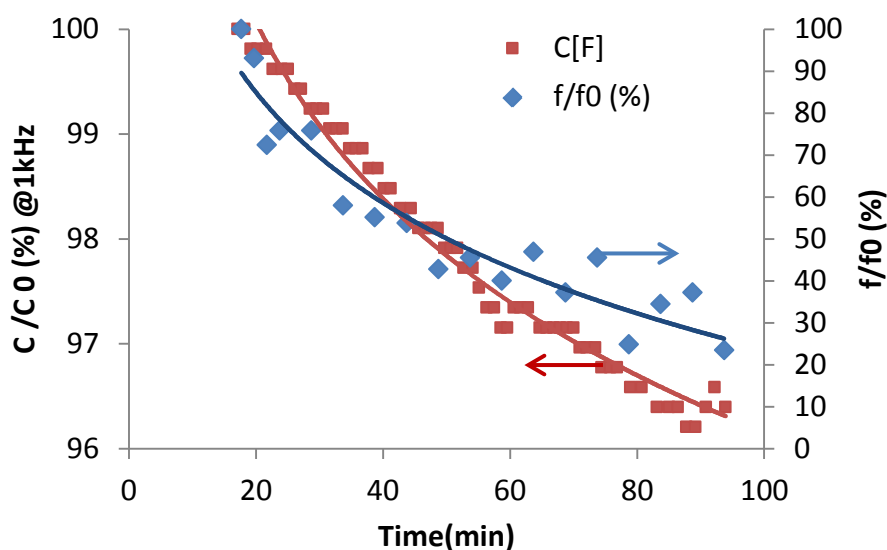


Figure 20 - Relative capacitance (at 1 kHz) and flux decline as a function of time without considering early stages of filtration experiments. EIS measurements were performed in 2-terminal mode using current electrodes.

This suggests that using this 2-terminal configuration, EIS data can be used to monitor fouling of microfiltration membranes. However, the flux decline was about 70% while capacitance declined only about 4%. This could be a limiting factor on using EIS to monitor fouling. Changing electrode configuration could provide a solution for increasing sensitivity of capacitance to membrane fouling. The next configuration examined was 3-terminal configuration with separate current and voltage electrodes on the feed side. The configuration is schematically shown in Figure 21 , and Figure 22 shows the total changes in conductance and capacitance during fouling. The filtration experiment parameters were similar to the experiment performed at 2-terminal mode.

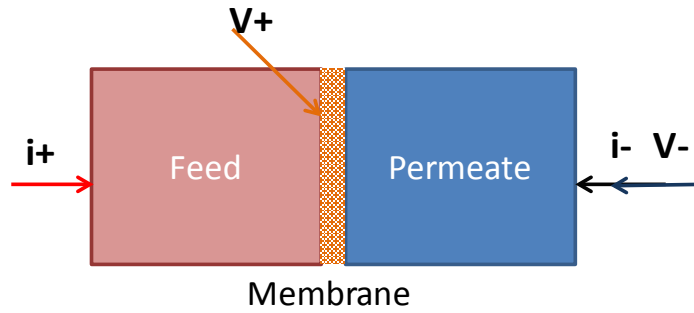


Figure 21 - Electrode configuration of 3-terminal experiments on flat membranes with 2 electrodes on feed side and 1 electrode on permeate side (3T-P1).

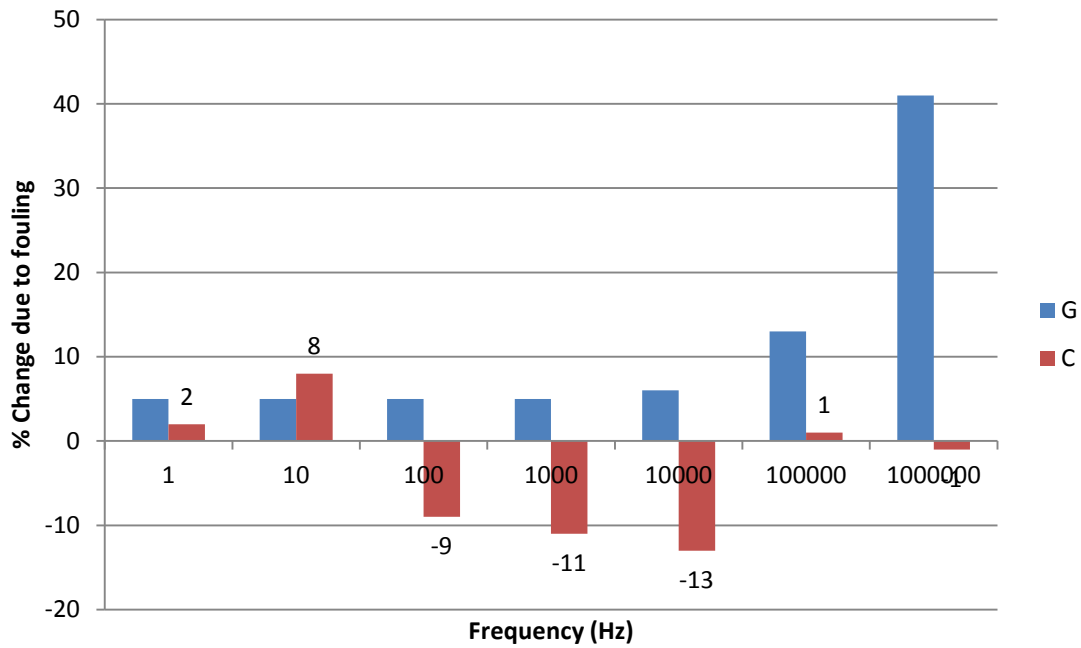


Figure 22 - Changes in conductance and capacitance during fouling of flat membrane using 1 gr/l PEG solution at 100 kPa. Experiments were performed in 3-terminal mode with 2 electrodes on feed side and 1 electrode on permeate side (3T-P1).

The results obtained using this electrode configuration significantly differed from those obtained using 2-terminal configuration. Conductance increased at most frequencies while changes in capacitance varied over the frequency spectrum. Capacitance increased at low and high frequencies while an overall decline was recorded at mid-frequency range of 100 Hz to 100 kHz. Example of changes in conductance and capacitance at low and high frequencies are shown in Figure 23.

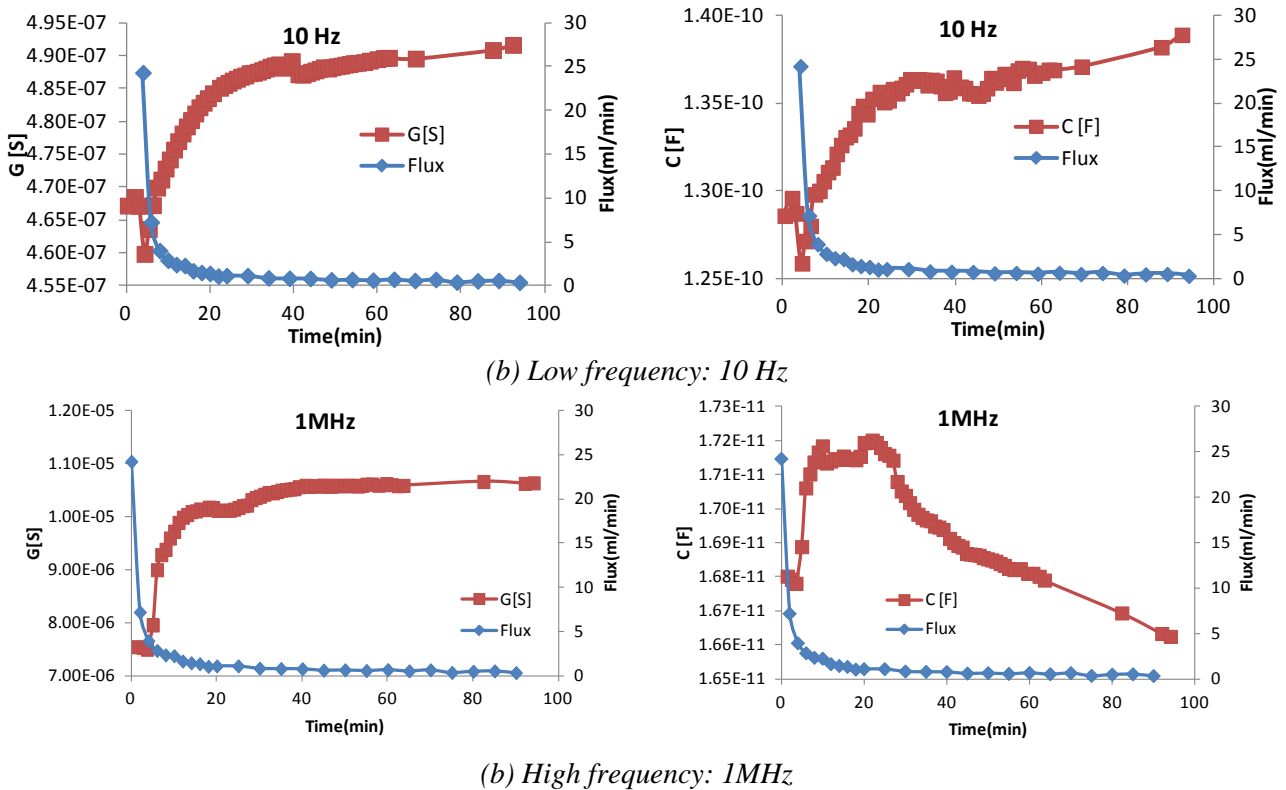


Figure 23 - Conductance and capacitance change as a function of time at (a) low frequency of 10 Hz and (b) high frequency of 1 MHz. Experiments were performed in 3-terminal mode with 2 electrodes on feed side and 1 electrode on permeate side (3T-P1).

The highest capacitance decline was recorded at 10 kHz. But, in order to compare the results with those of previous 2-terminal configuration, the EIS data at 1 kHz were compared with flux decline pattern. These data are shown in Figure 24. The conductance increased with time while the capacitance declined from beginning the filtration experiments. This is in clear contrast with the data obtained using 2-terminal configuration.

Capacitance decline detected from the beginning of the filtration suggested that initial capacitance increase detected in 2-terminal experiments cannot be due to pore-blocking fouling or membrane compaction. The capacitance decline at 1 kHz could predict the fouling; however, the rate of changes was slower than the decline in flux (see Figure 25-a). Total capacitance decline recorded at 1 kHz was about 11% that is significantly lower than >90% decline in flux, as shown in Figure 25-a. The trend of changes in capacitance and relative flux seems to be closer during the second stage of filtration, i.e. after 17 minutes (see Figure 25-b). The total capacitance decline and relative flux

decline during this stage were  $\sim 7\%$  and  $\sim 70\%$ , respectively. This outcome was slightly better than the outcome of 2-terminal measurements.

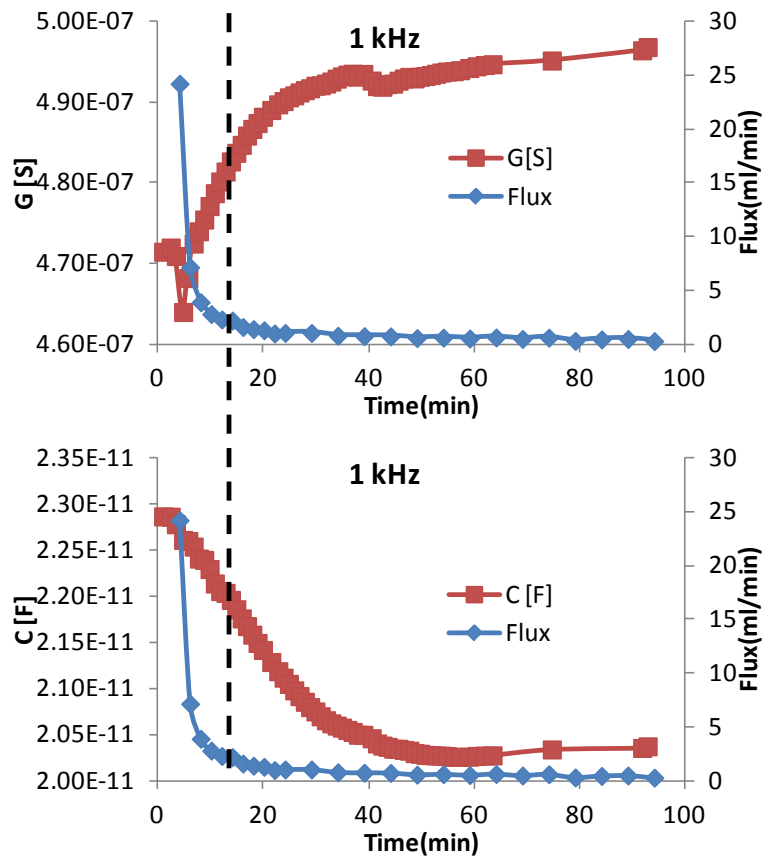


Figure 24 - Conductance and capacitance change as a function of time at 1 kHz. Experiments were performed in 3-terminal mode with 2 electrodes on feed side and 1 electrode on permeate side (3T-P1).

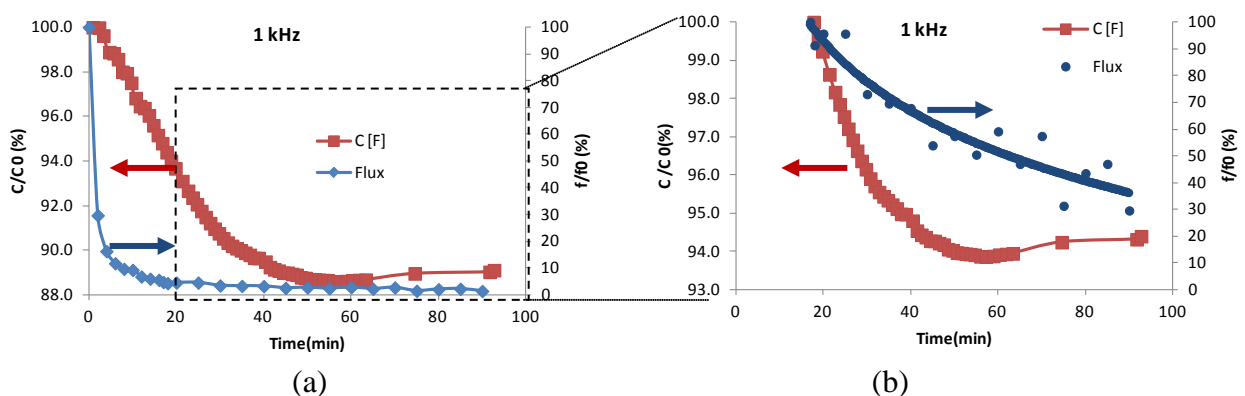


Figure 25 - Capacitance (at 1 kHz) and relative flux changes as a function of time (a), and without considering the early stage of the filtration (b) experiments. EIS measurements in 3-terminal mode with 2 electrodes on feed side and 1 electrode on permeate side (3T-P1).

Capacitance decline detected using this configuration suggested that the effect of ionic double layer was reduced. This could be due to moving the voltage electrode closer to the surface of membrane,

and hence reducing the effect of feed on overall electrical impedance. This is assuming higher concentration of ions on the feed side compared to the permeate side.

To examine this, the next series of experiments were performed in 3-terminal mode with one electrode on the feed side but two electrodes on the permeate side. This electrode configuration is schematically shown in Figure 26. The total changes in capacitance and conductance are shown in Figure 27.

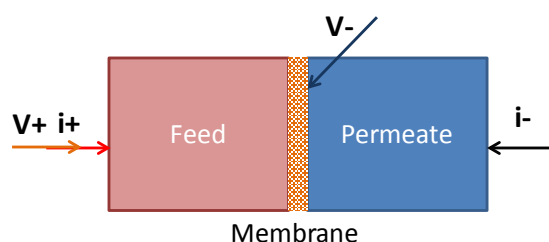


Figure 26 - Electrode configuration of 3-terminal experiments on flat membranes with 2 electrodes on permeate side and 1 electrode on feed side (3T-F1).

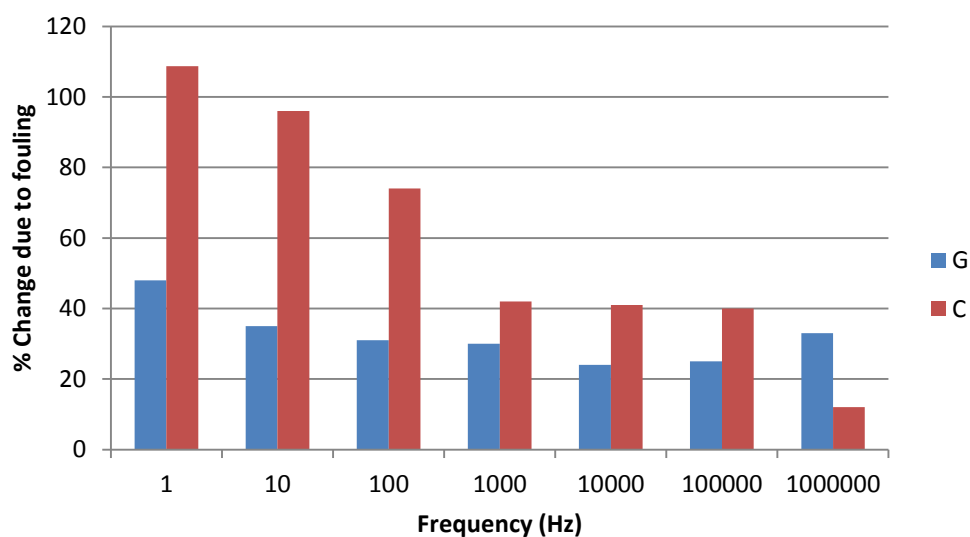


Figure 27 - Changes in conductance and capacitance during fouling of flat membrane using 1 gr/l PEG solution at 100 kPa. Experiments were performed in 3-terminal mode with 1 electrode on feed side and 2 electrodes on permeate side (3T-F1).

Interestingly, the results are similar to those of 2-terminal configurations (see Figure 17). Both conductance and capacitance increased over a wide range of frequencies. Typical data obtained at low and high frequencies are shown in Figure 28. These results show that at high and low frequencies, no capacitance decline was recorded during fouling experiments. However, as shown

in Figure 29, at mid-frequency range, a slight decline of capacitance was measured in second phase of filtration. This is similar to the trend observed when using a 2-terminal configuration was used.

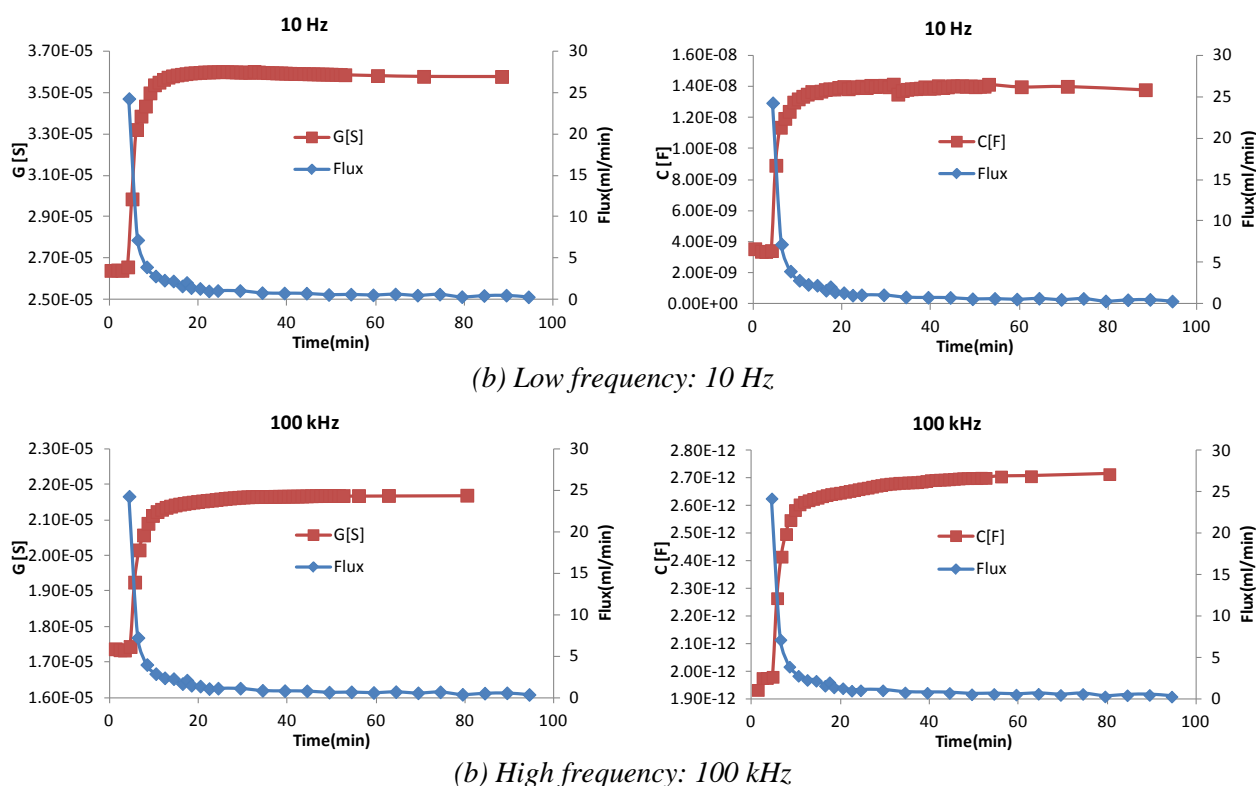


Figure 28 - Conductance and capacitance change as a function of time at (a) low frequency of 10 Hz and (b) high frequency of 100 kHz. Experiments were performed in 3-terminal mode with 1 electrode on feed side and 2 electrodes on permeate side (3T-F1).

Relative capacitance decline during the second stage of filtration (i.e. after 17 min) were compared with relative flux decline. The results are presented in Figure 30. The capacitance decline was about 6% while flux declined about 70%. The capacitance decline recorded using 2-terminal mode was about 4%. It seems, although the general trend of capacitance and conductance was similar for 2-terminal electrode configurations, this 3-terminal configuration has yielded a slightly better fouling detection.

The results obtained using this electrode configuration were different from those obtained using the 3-terminal configuration with one electrode on permeate side. This suggests that the effect of feed on ionic double layer is greater than the effect of permeate. Because, separating voltage and current sensing electrodes on feed side reduced the dominance of ionic double layer, while separating voltage and current electrode on the permeate side had little effect if any.

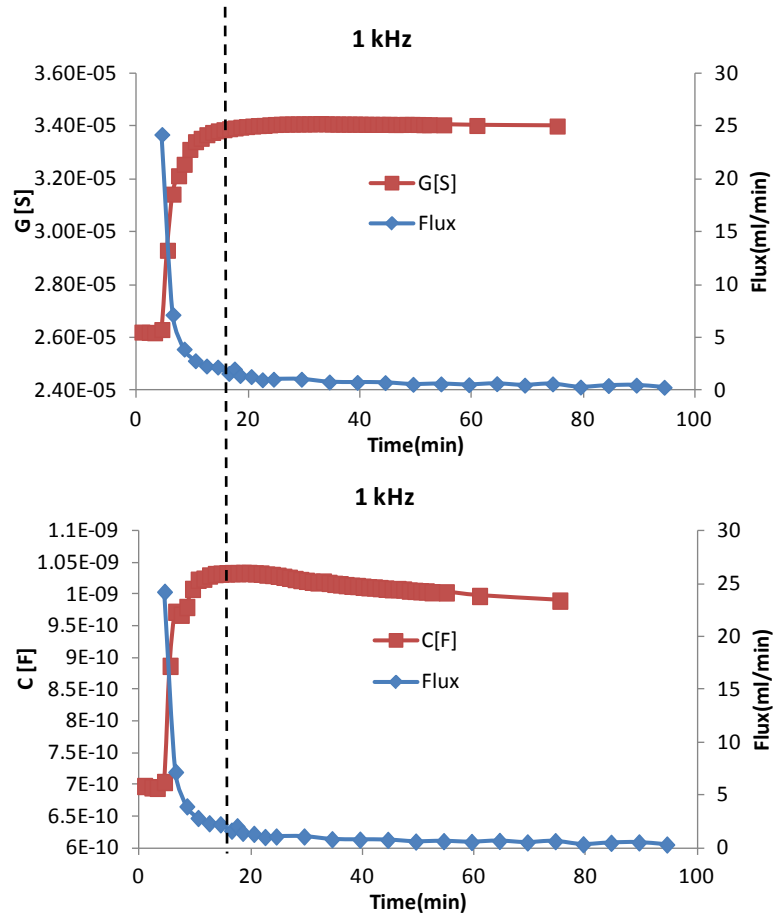


Figure 29 - Conductance and capacitance change as a function of time at 1 kHz. Experiments were performed in 3-terminal mode with 1 electrode on feed side and 2 electrodes on permeate side (3T-F1).

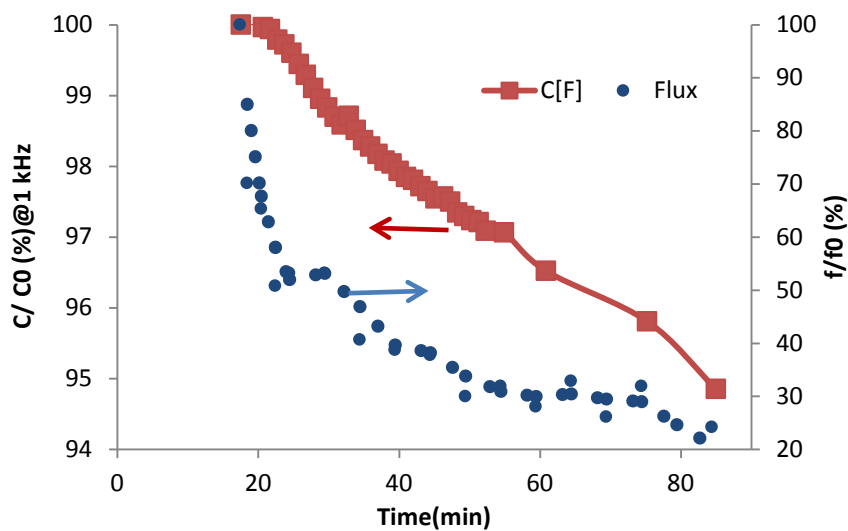


Figure 30 - Capacitance (at 1 kHz) and relative flux changes as a function of time without considering the early stage (i.e. first 17 minutes) of the filtration experiments. EIS measurements were performed in 3-terminal mode with 1 electrode on feed side and 2 electrodes on permeate side (3T-F1).

An important factor on ionic double layer is the surface area of electrode. In the chamber design, we used for EIS measurements in the present study the voltage sensing electrodes had significantly smaller surface area compared to current electrodes. In first 3-terminal configuration, the large electrode used for current and voltage detection was on the permeate side that has lower foulant concentration. While, in the second design this large electrode was on the feed side that has a high concentration of fouling material. This could be a reason for stronger ionic double layer in second 3-terminal configuration. To examine this theory, the experiments were repeated using a 4-terminal electrode configuration with two small voltage sensing electrodes close to the surface of membrane on each side and two larger current electrodes fitted on the permeate and feed compartments. The 4-terminal configuration is schematically shown in Figure 31.

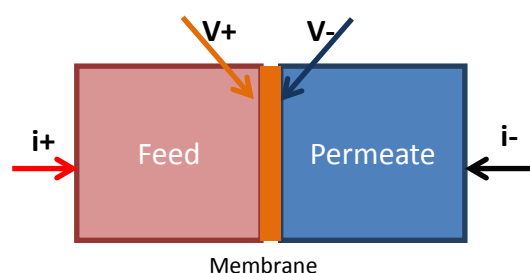


Figure 31 - Electrode configuration of 4-terminal experiments on flat membranes with 2 electrodes on permeate side and 2 electrodes on feed side.

The total changes in conductance and capacitance are shown in Figure 32 and typical trends at high and low frequencies are presented in Figure 33. Similar to the results of 2-terminal measurements, both capacitance and conductance increased at all frequencies. The capacitance change was greater at low frequencies but at mid-frequencies conductance changes were more significant.

At 10 Hz -10 kHz, the increasing trend of capacitance changed during fouling and a declining trend was recorded during the second stage of the filtration. In order to compare these results with those of other electrode configurations, the trend of capacitance and conductance at 1 kHz are presented in Figure 34. The capacitance decline percentage at 1 kHz is compared with relative flux decline during the second stage of the filtration, i.e. after 17 minutes, in Figure 35.

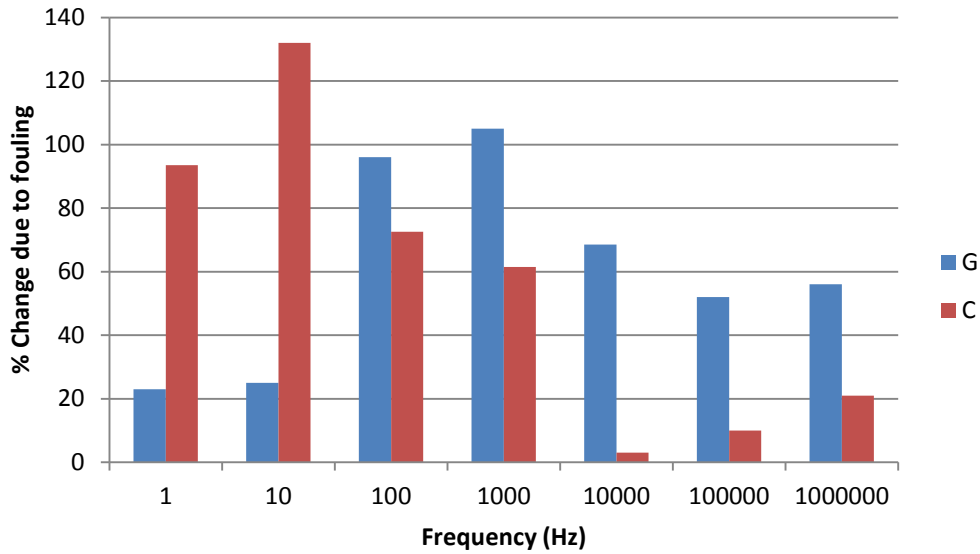


Figure 32 - Changes in conductance and capacitance during fouling of flat membrane using 1 gr/l PEG solution at 100 kPa. Experiments were performed in 4-terminal mode.

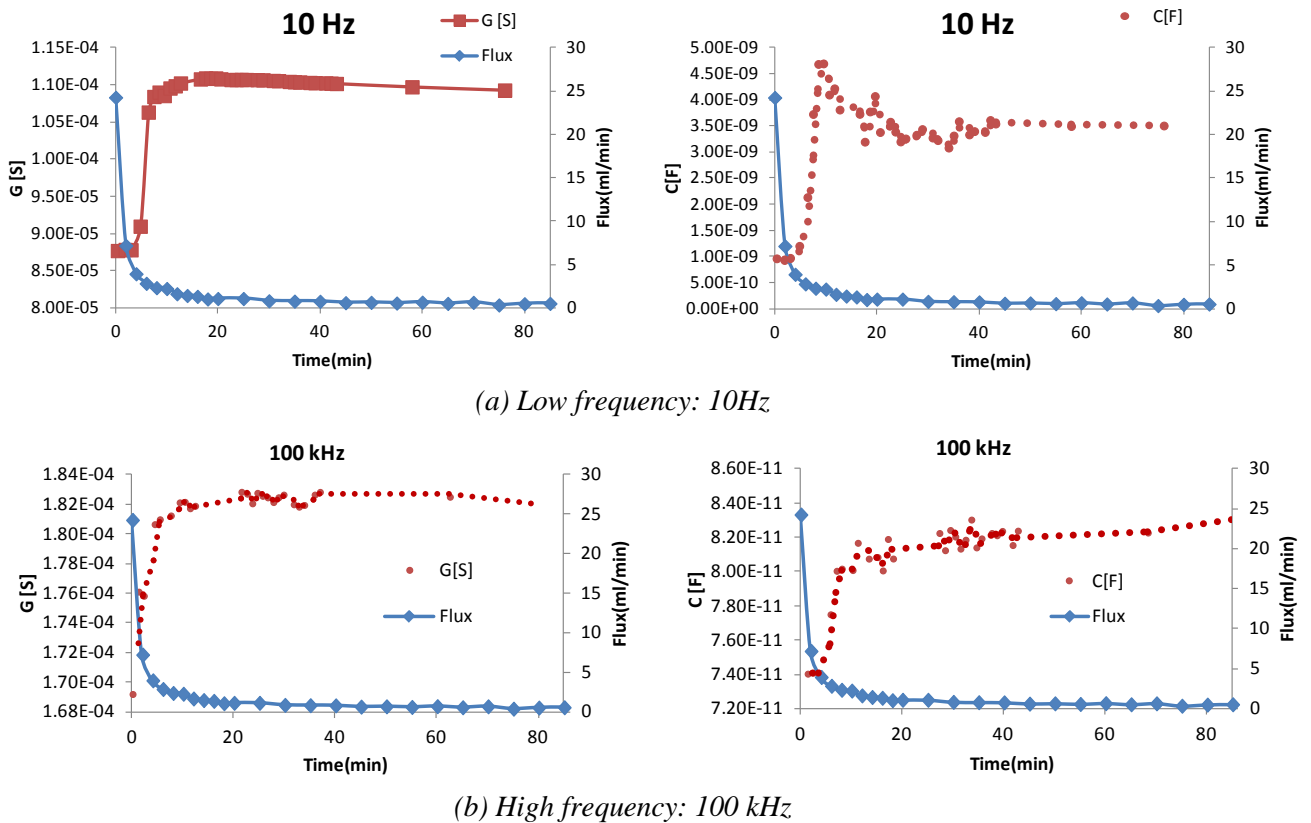


Figure 33 - Conductance and capacitance change as a function of time at (a) low frequency of 10 Hz and (b) high frequency of 100 kHz. Experiments were performed in 4-terminal mode.

The trend of capacitance decline in Figure 35 is very similar to the trend of flux decline. However, the flux declined about 70% while capacitance decreased only about 9%. Although this is not very significant compared to flux decline, this value is more than double of the change detected using 2-terminal configuration (4%) and greater than the changes detected using 3-terminal configurations.

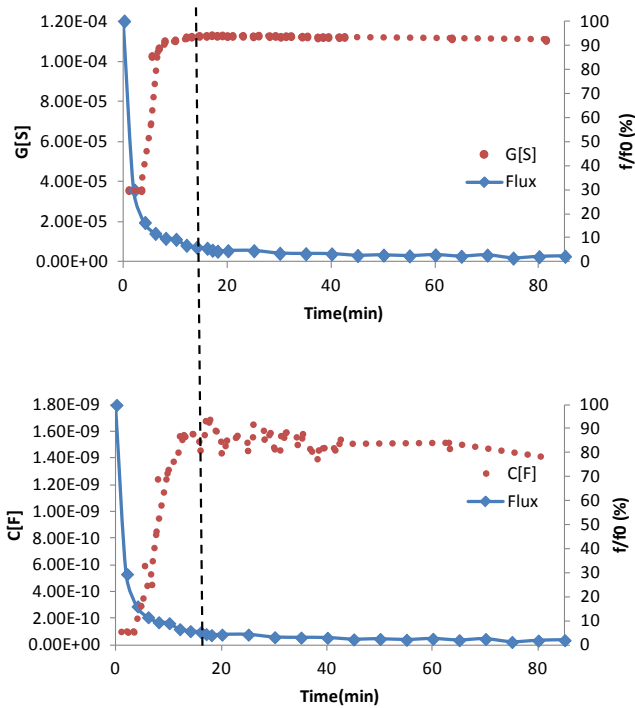


Figure 34 - Conductance and capacitance change as a function of time at 1 kHz. Experiments were performed in 4-terminal mode.

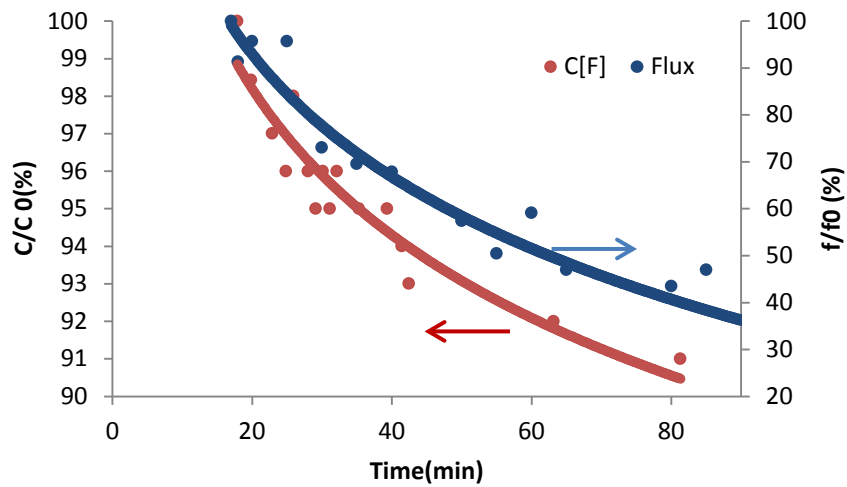


Figure 35 - Capacitance (at 1 kHz) and relative flux changes as a function of time without considering the early stage (i.e. first 17 minutes) of the filtration experiments. EIS measurements were performed in 4-terminal mode.

These results suggested that using 4-terminal measurements reduced the effect of ionic double layer. The overall rising trend of capacitance suggested that the increasing concentration of solute was still the dominant factor at 1 kHz when 4-terminal electrode configuration was used. This was eliminated when 3-terminal configuration with one electrode on the permeate side was used. This could be explained by size of the electrodes. In this 3-terminal configuration voltage sensing electrodes on each side had different sizes while in 4-terminal measurements the size of electrodes was proportionate.

### 3.3.2.1. Summary

Deposition of foulant inside or on the surface of membrane changes its electrical properties during microfiltration. Concentrations of solute in feed and permeate also change. Therefore, electrical properties of the system are a function of various factors including the membrane. These experiments showed that the impedance of membrane itself was more dominant in mid-frequency range of about 1 kHz.

These results suggested that ionic double layer on the surface of electrode was the most important issue limiting EIS capability in detection of fouling. These experiments showed that the effect of ionic double layer can be limited using 4-terminal and 3-terminal configurations. Separating the current and voltage electrode on the feed side was more effective than using separate electrodes on the permeate side. 4-terminal configuration was the most effective method when the capacitance decline at a similar frequency (1 kHz) and same timeframe was used as an indication for fouling. Using 3-terminal measurements with 1 electrode on the permeate side also resulted in a capacitive decline pattern at 1 kHz from the beginning of the filtration. Using different electrode configurations, a 4-13% decline in capacitance was detected at this frequency range that was not proportionate to at least 70% flux decline.

### 3.3.3. Outside-in hollow fibre membranes

In the case of hollow fibre membranes, 4-terminal electrode configuration is not practical because accommodating two electrodes inside the fibres is impossible. 3-terminal configuration with 2 electrodes on the feed side is doable. However, fitting two electrodes in membrane bio-reactor has its difficulties considering its highly fouling environment. Therefore, this research was focused on finding the optimum 2-terminal configuration. The configurations are schematically shown in Figure 36. Two possible configurations were examined for the electrode in the bioreactor: a long electrode probing the total length of the membranes (i.e. configuration 1 in Figure 36), and a disc electrode at the bottom of the reactor (i.e. configuration 2 in Figure 36).

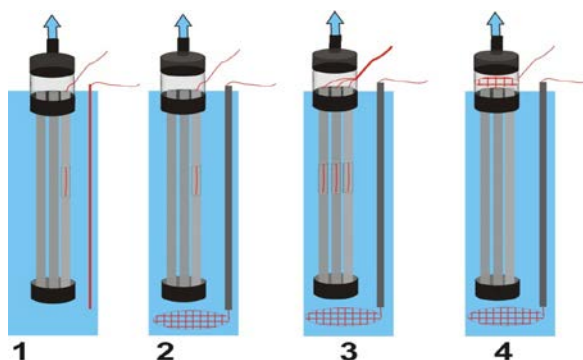


Figure 36 - 2-terminal electrode configuration used for EIS characterisation of outside-in hollow fibre membranes.

The preliminary experiments using 1 gr/l PEG solution showed that the capacitance change at mid-frequency range, which was shown to be electrically dominated by membrane, was not affected by the position of electrode on the permeate side. As shown in Figure 37, capacitance decline at mid-frequency range was about 10% for both configurations. However, capacitance raise at low frequencies was affected by configuration of the electrode on the feed side. These capacitance raise at low frequencies is due to ionic double layer and is affected by solute concentration. The capacitance raise at low frequencies was about two times greater using configuration 1 compared to that of configuration 2.

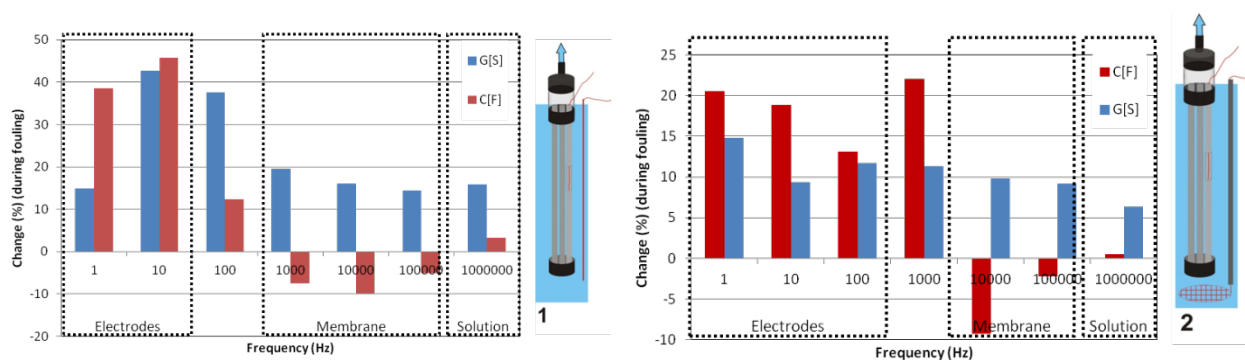


Figure 37 - Total percentage changes of capacitance (C) and conductance (G) during fouling measured using configurations 1 and 2.

The measurements on flat membranes showed that minimising the effect of ionic double layer is required to improve the capability of EIS in detection of fouling. Therefore, configuration 2 was chosen for the electrode outside the membrane, i.e. the feed side.

For the electrode inside the membrane (i.e. permeate side), there are three options: a wire fitted inside only one of the hollow fibres (i.e. configuration 2), a wire electrode inside each membrane fibre (i.e. configuration 3), and a porous disc as common electrode but no electrode inside the fibres (i.e. configuration 4). The preliminary experiments using 1 gr/ PEG solution showed that configurations 2 and 3 yielded slightly better results. It was concluded that although the fouling can be detected without fitting electrode inside the fibres, inserting at least an electrode inside one of the fibres can improve the performance of EIS.

In the next step, the experiments were repeated using 5 gr/l PEG solutions. Configurations 2 (with only one electrode fitted only in one of the fibres), 3 (with electrode inside all fibres), and 4 (with no electrodes inside the fibres) were examined. Figure 38 shows capacitance and conductance change at different frequencies and compares them with relative flux decline.

At low frequency of 1 Hz, a conductance decline was recorded using configurations 2 and 3, but conductance changes were in the positive direction at higher frequencies. With the exception of 1 Hz, independent from electrode configuration, a conductance raise up to 20% was recorded over the frequency spectrum, but capacitance change was affected by electrode configuration.

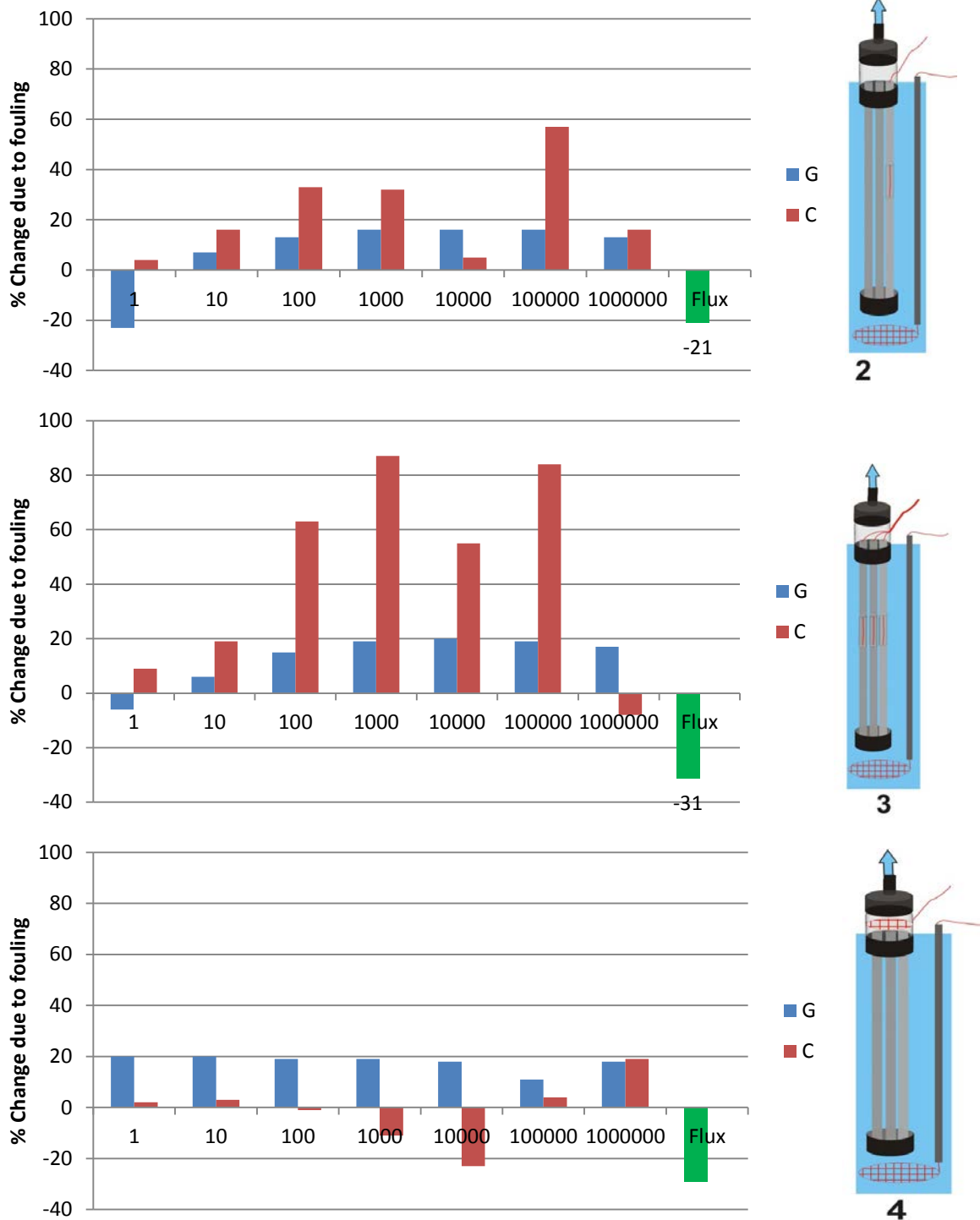


Figure 38 - Total percentage changes of capacitance (C) and conductance (G) during filtration of 5 gr/l PEG solution. EIS experiments were performed using configurations 2, 3 and 4.

In configurations 2 and 3, a capacitance raise was recorded at all frequencies. The capacitance changes were greater when wire electrodes were fitted inside all fibres (i.e. configuration 3). Using both configurations, the minimum capacitance growth was detected at 10 kHz. The capacitance change at 10 kHz was in average ~30% less than its change at 1 kHz and 100 kHz when wire

electrodes were fitted in all fibres. This difference was about 40% when only one fibre was fitted with a wire electrode.

Using configuration 4 with no wire inside the fibres, the direction of capacitance change was a function of frequency. Capacitance increased at low and high frequencies in the same direction with conductance. However, a capacitance decline was detected at 100 Hz to 10 kHz. The maximum capacitance decline of 23% was detected at 10 kHz. This was lower than the flux decline of 30% during filtration.

Comparing the results of these experiments with the results obtained using 1 gr/l PEG, it can be said that the frequency range affected by membranes was shifted from 1 Hz to 10 kHz. This is due to the fact that by increasing the concentration (and hence conductivity) of solute the frequency range dominated by ionic double layer extends to higher frequency range.

At frequency range dominated by electrical impedance of membrane, deposition of foulant on the membrane is expected to reduce the capacitance. While, increase in solute concentration results in stronger ionic double layer and hence higher capacitance. The overall capacitance change is affected by the balance of these two effects. Assuming that 10 kHz was the frequency range most affected by impedance of the membranes, the capacitance change at this frequency was compared for these three configurations (Figure 39). It seems that the ionic double layer was the dominant factor throughout the fouling when wire electrodes were fitted in all fibres (i.e. configuration 3) and therefore a capacitance increase was recorded. However, this increase was significantly lower than the values recorded at other frequencies at which the effect of membrane was less significant (see Figure 38).

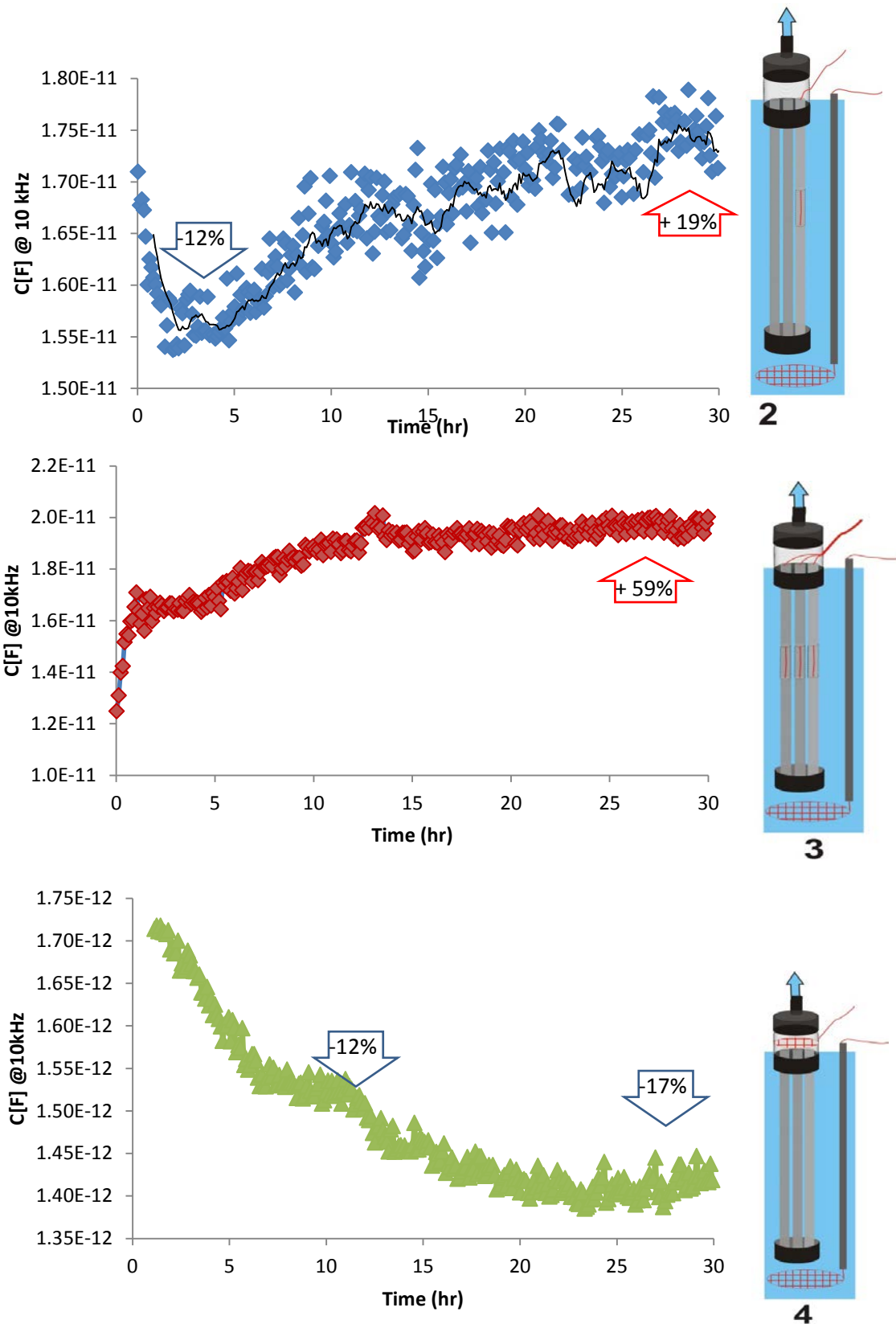


Figure 39 - Capacitance (C) at 10 kHz as a function of time during filtration of 5 gr/l PEG solution. EIS experiments were performed using configurations 2, 3 and 4.

By fitting one of the fibres with a wire electrode, a different trend in capacitance was recorded. At early stages, capacitance declined but this was followed by an almost linear increase during the rest of filtration experiment. In configuration 4, with no electrode inside the fibres, the capacitance declined from beginning of filtration.

Without considering the direction of change, fitting electrodes in all fibres seemed to increase the sensitivity of EIS to fouling. However, the side effect of inserting electrodes inside all fibres is the higher surface of exposed to the solute and the effect of ionic double layer. Using configuration 3, the capacitance decline due to fouling was discounted by increasing capacitance of ionic double layer due to a higher concentration of solute. If the concentration of foulant is kept constant this configuration could be the most appropriate.

Using a common porous disc electrode on the permeate side, instead of probing inside the fibres, (i.e. configuration 4) reduced the surface area of electrode and hence the effect of ionic double layer. Capacitance decline was detected from the beginning of the fouling experiment. However, the sensitivity was reduced as the percentage of capacitance decline was lower than the percentage of flux decline.

Inserting a wire electrode inside one of the fibres (i.e. configuration 2), a capacitance decline of about 12% was recorded during first 3 hours of fouling. The same level of change was recorded after 10 hr when configuration 4 was used. This showed that fitting one off the fibres with a wire electrode can increase the sensitivity of EIS measurements to fouling. This is in agreements with the results of the experiments using low concentration feed of 1 gr/l PEG.

### **3.3.3.1. Summary**

The effect of ionic double layer seems to be the main factor limiting the capability in using EIS for detection of membrane fouling. In the case of flat membranes, the effect of ionic double layer can be reduced using 3 and 4-terminal electrode configurations. However, usually 2-terminal configuration is the only option in the case of hollow fibre membrane. This research showed that

the location of size of the electrodes can affect the results of EIS. Preliminary experiments showed that probing the surface of membrane on the feed side (i.e. in membrane bioreactor) was not necessary.

The results of experiments using higher concentration feed showed that EIS measurements were heavily affected by concentration of the feed. If the concentration of the feed in membrane bioreactor is kept constant, fitting wire electrodes inside each fibre can increase the sensitivity of EIS to fouling. However, in industrial scale this is not a trivial task. Moreover, inserting electrodes inside each fibre is time consuming and expensive, and hence not practical in large scale membrane production.

Using a porous disc electrode on the permeate side without inserting a wire inside any of the fibres was also examined. Capacitance decline at mid-frequency range was found to be an indication of membrane fouling. Independent from solute concentration the flux decline was greater than the decline in capacitance. This showed that EIS was less sensitive to fouling when this electrode configuration was used. This configuration can be easily adopted for different hollow fibre membranes and is the only option when the internal diameter of the fibre is very small. Inserting a wire inside only one of the fibres was shown to be effective in increasing the sensitivity of the EIS while reducing the effect of ionic double layer.

#### **3.3.4. Inside-out hollow fibre membranes**

The results of the experiments on outside-in hollow fibre membranes showed that electrode configuration affect the sensitivity of EIS to fouling. Here, we examine this on inside-out hollow fibre membranes.

Each INGE inside-out hollow fibre, used in the present study, contains 7 individual fibres. The internal diameter of each fibre is smaller than 1 mm and hence it is not easy to fit a wire inside each

fibre. Therefore, it was necessary to investigate if inserting an electrode inside the fibres was necessary to monitor membrane fouling using EIS.

Four configurations were examined, and electrical impedance properties were measured during filtration. For the permeate side (i.e. membrane bioreactor) two options were investigated: a wire electrode probing the length of membrane, and a disc electrode at the bottom of membrane bioreactor. Two options were also examined for the feed side: a wire electrode inside one of the fibres and no wires inside the fibres but a common electrode at the cross section of fibres.

The total percentage change in capacitance and conductance using these 4 configurations is shown in Figure 40. Using a wire inside the fibre and disc electrode outside, a significant increase in conductance was measured at low frequencies, while capacitance and conductance change in mid-frequency range was less than 10%.

By using a common electrode on the feed side instead of fitting a wire, the conductance changes recorded at various frequencies were in general greater in comparison with the data obtained using configuration 1. However, the capacitance change at mid-frequency range was less than 10% and more importantly on the positive direction that is an indication that ionic double layer was more dominant factor in comparison with the capacitance decline due to deposition of material on the membrane surface.

A significant decline in capacitance at mid-frequency range was recorded when a long electrode was used on the permeate side instead of a disc (i.e. configuration 3). Using a wire electrode inside fibres, capacitance and conductance changed in the same direction and almost at same level at mid-frequency range. When a disc was used on the feed side (i.e. configuration 4), a conductance increased about 20% at mid-frequency range while capacitance declined about 50% at 1 kHz.

Based on these results, using a long electrode probing the surface of membrane on the permeate side was necessary to detect a considerable capacitance decline at mid-frequency range. The next step is to find out if it is necessary to fit a wire electrode inside the fibres.

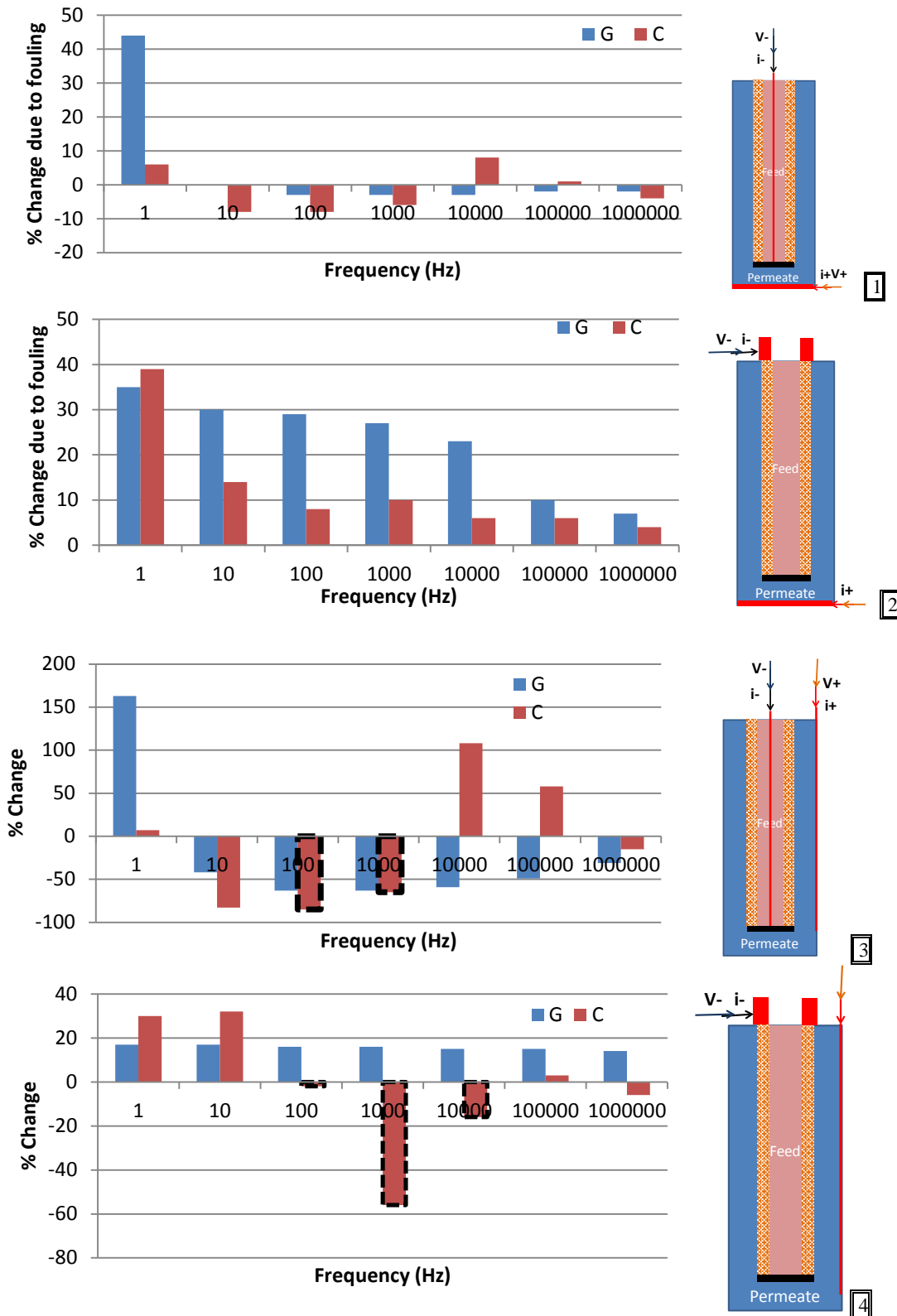


Figure 40 - Four prototypes used in monitoring filtration of PEG solution using inside-out hollow fibre membranes. Total percentage changes of capacitance (C) and Conductance (G) during fouling is plotted at frequencies ranging from 1 Hz to 1 MHz.

The percentage of capacitance change at 1 kHz was compared with the relative flux decline for prototypes 3 and 4. The results are presented in Figure 41. The capacitive decline pattern obtained using a common electrode on the permeate side was closer to the flux decline pattern.

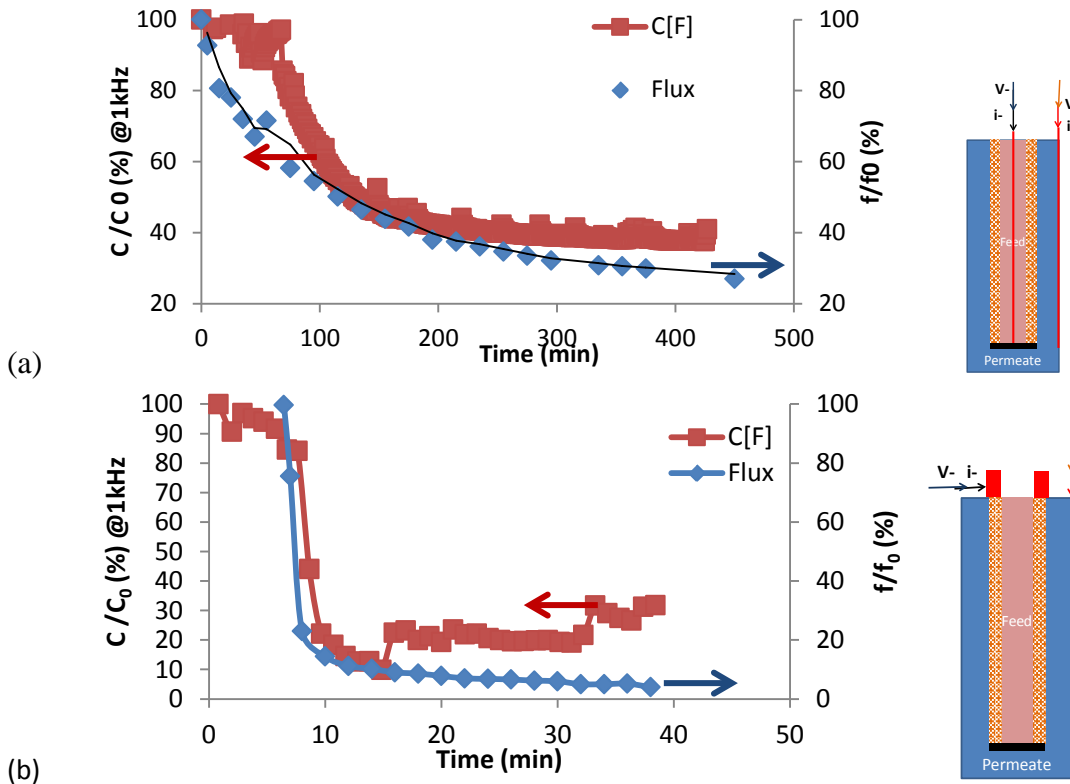


Figure 41 - Percentage changes of capacitance (C) at 1 kHz compared to relative flux decline for (a): prototypes 3 (i.e. with wire electrode fitted inside hollow fibre), and (b): prototype 4 (i.e. with no wire inside hollow fibre membrane).

The performance of two configurations was also compared by monitoring the backwashing process. The fouled membrane was immersed in water, and a pump was used to drive a constant flux of water through the membrane in the outside-in direction. Capacitance and conductance changes during fouling and backwashing processes are compared in Figure 42 for configurations 3 and 4. The conductance over the wide range of frequency remained almost constant during backwashing. Moreover, backwashing did not result in a noticeable change in capacitance at low frequencies. This is due to the fact that the concentration of solute did not change during backwashing. These results show that the ionic double layer was not a factor affecting the electrical impedance change during backwashing.

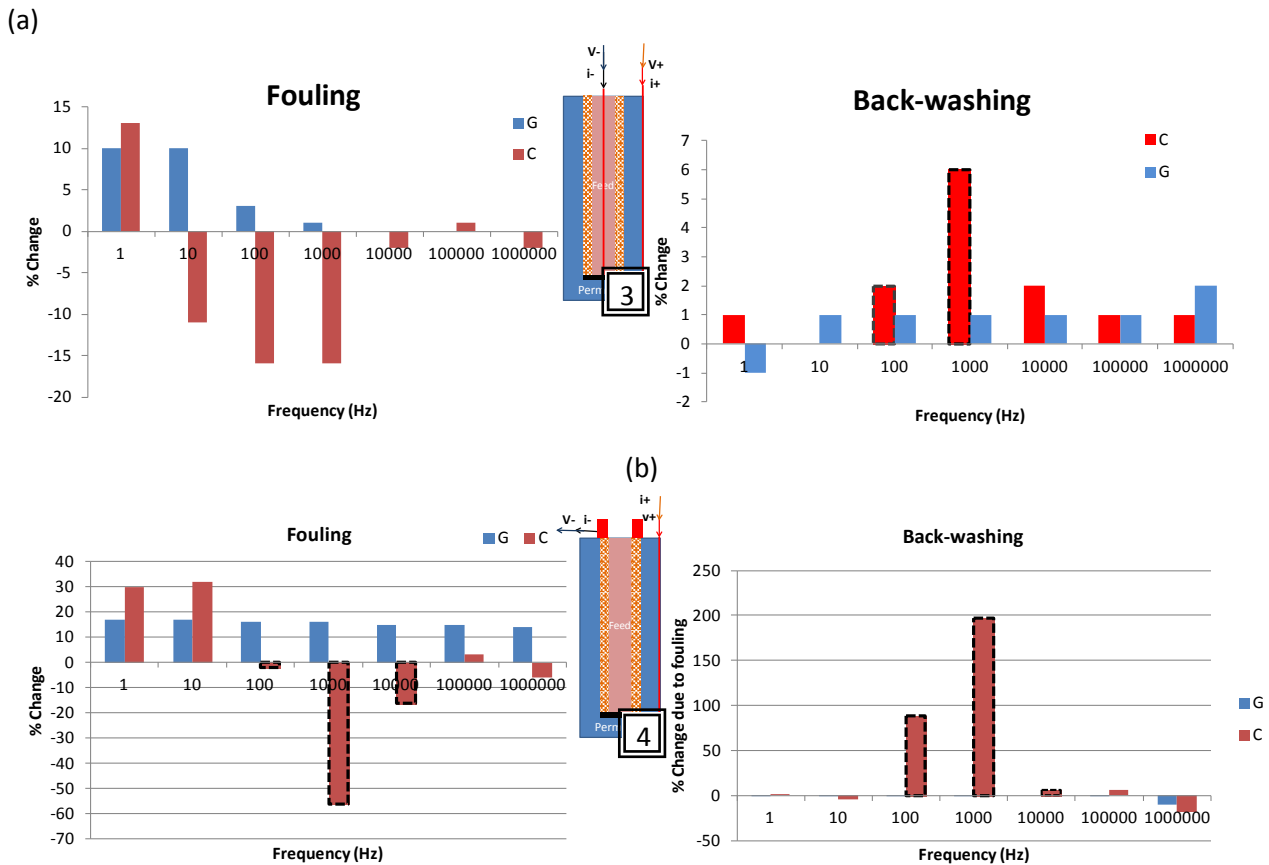


Figure 42 - Total percentage changes of capacitance (C) and conductance (G) during fouling and backwashing of inside-out hollow fibre membrane: a) using prototype 3 (one wire inside fibres and a long electrode outside the membrane) , and b) using prototype 4 (no wire inside fibres and a long electrode outside the membrane).

The capacitance change at mid-frequency range was the most significant change detected during backwashing. The direction of change was on the opposite direction of the change measured during fouling. Using both configurations, membrane fouling and backwashing were best detected at 1 kHz. The capacitance change at 1 kHz during backwashing is compared in Figure 43. Using configuration 3 the capacitance decline of ~16% during fouling was reversed by ~6% capacitance increase during backwashing. Using configuration 4, at 1 kHz, the capacitance decline was about 55% during fouling while a capacitance rise of ~200% was recorded during backwashing.

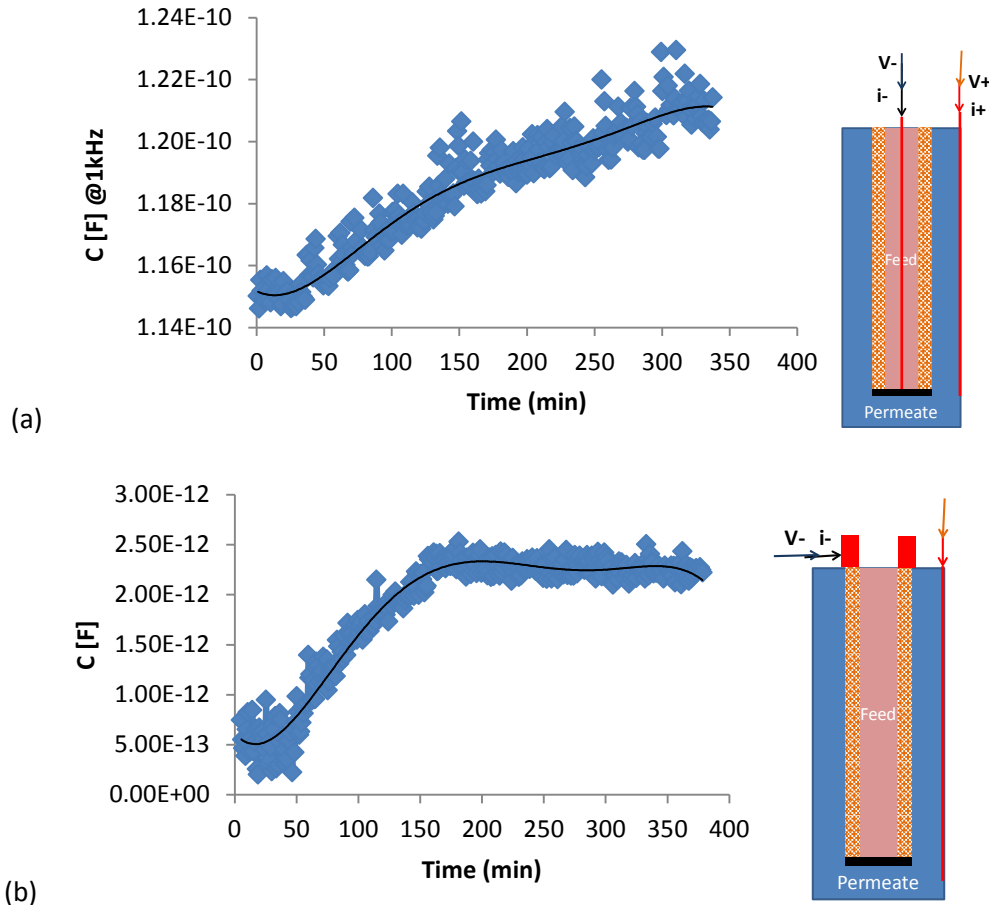


Figure 43 - Capacitance at 1 kHz during backwashing of inside-out hollow fibre membrane: a) using prototype 3 (one wire inside fibres and a long electrode outside the membrane), and b) using prototype 4 (no wire inside fibres and a long electrode outside the membrane).

Although these results were not conclusive for choosing one of these configurations, these results show that fitting a wire electrode is not necessary for detection of fouling using EIS. This is a significant outcome considering difficulties of inserting a wire inside the fibres.

Another important issue is the effect of wire on flux. The effect of inserting a wire inside one of the fibres on flux is shown in Figure 44 . The flux of the membrane with a wire was significantly lower than that of the configuration 4, with no wire inside the membranes.

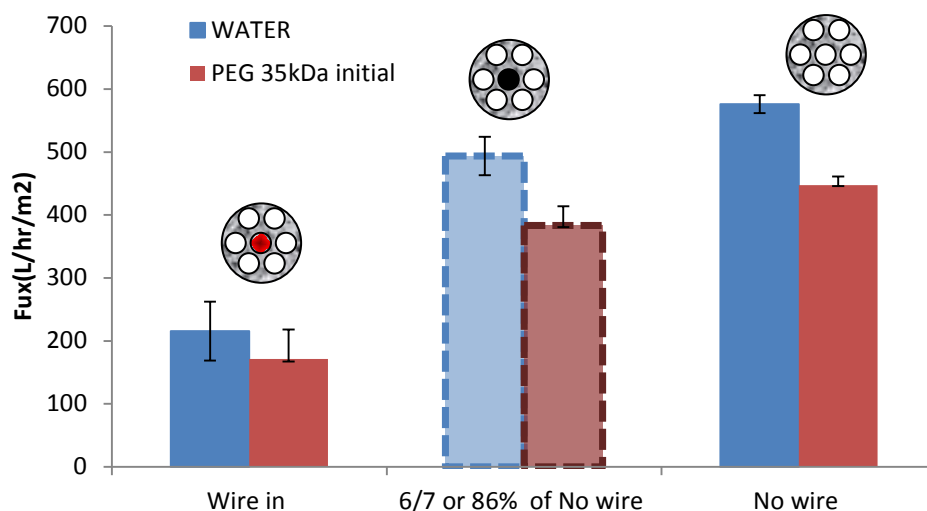


Figure 44 - Effect of inserting a wire inside one of the fibres of inside-out hollow fibre membrane.

The puzzling issue was that the flux was even lower than the theoretical value of 6/7 of the membrane with no wire. This theoretical value was estimated assuming that one of the fibres was completely blocked by the wire, and this blocking did not affect the flux through other 6 fibres. These results suggest that the latter assumption was not correct. More experiments are required to investigate the flow pattern of these membranes that are out of the scope of this research. Independent from the reason behind this excessive flux decline, these results are an indication that fitting a wire electrode inside the fibre affects the flow pattern of these inside-out hollow fibre membranes and thus should be avoided if possible.

### 3.3.4.1. Summary

The results of experiments on inside-out hollow fibre membranes showed that inserting a wire inside the electrode did not improve the sensitivity of EIS to membrane fouling. While, the electrode on the permeate side was an important factor, and using a long electrode to probe the surface of membrane on the permeate side improved the performance of EIS.

As depicted schematically in Figure 45, on the surface, this was in contrast with the results of the experiments on outside-in hollow fibre membranes. However, interestingly experiments on these two different hollow fibre membranes showed that the size and position of the electrode on the feed

side were not an important factor. Using an electrode with large surface area on the permeate side, and a small electrode on the feed side seemed to yield the best results in terms of detection of fouling using EIS. This is in agreement with the results of the experiments on flat membranes.

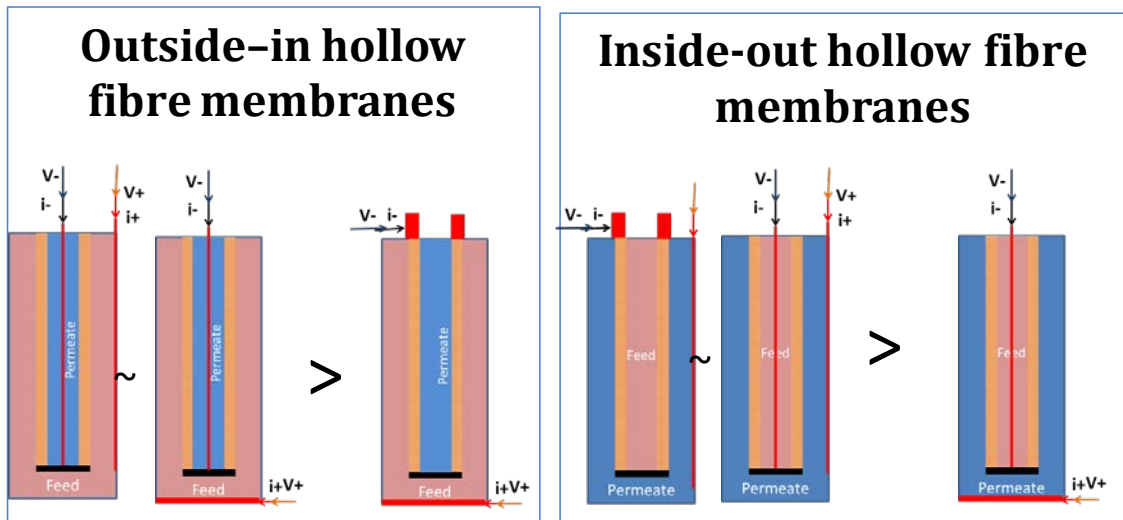


Figure 45 - Effect of electrode position on performance of EIS in detection of fouling using outside-in and inside-out hollow fibre membranes.

From a practical point of view, detection of fouling without the need for fitting a wire inside the membrane is the most desirable outcome. These results showed that fitting a wire inside the membrane was not required for inside-out membranes. For more common outside-in hollow fibre membranes, EIS measurements without wire inside the fibres provided some indication of the level of fouling. However, the accuracy of EIS was improved significantly when at least one of the fibres were fitted with a wire electrode. Inserting the wire did not affect the flux noticeably when the inner diameter of the fibres was significantly greater than the diameter of the wire. While, these experiments showed that for very fine fibres, inserting a wire with comparable diameter can affect flux and possibly EIS data.

### 3.3.5. Design and manufacturing a prototype module

Based on the outcome of the experiments a prototype module was designed and manufactured for characterisation of hollow fibre membranes. The basic design is shown in Figure 46. The module was fitted with two electrodes in the chamber: a disc at the bottom of the chamber, and a long stainless electrode on the side.

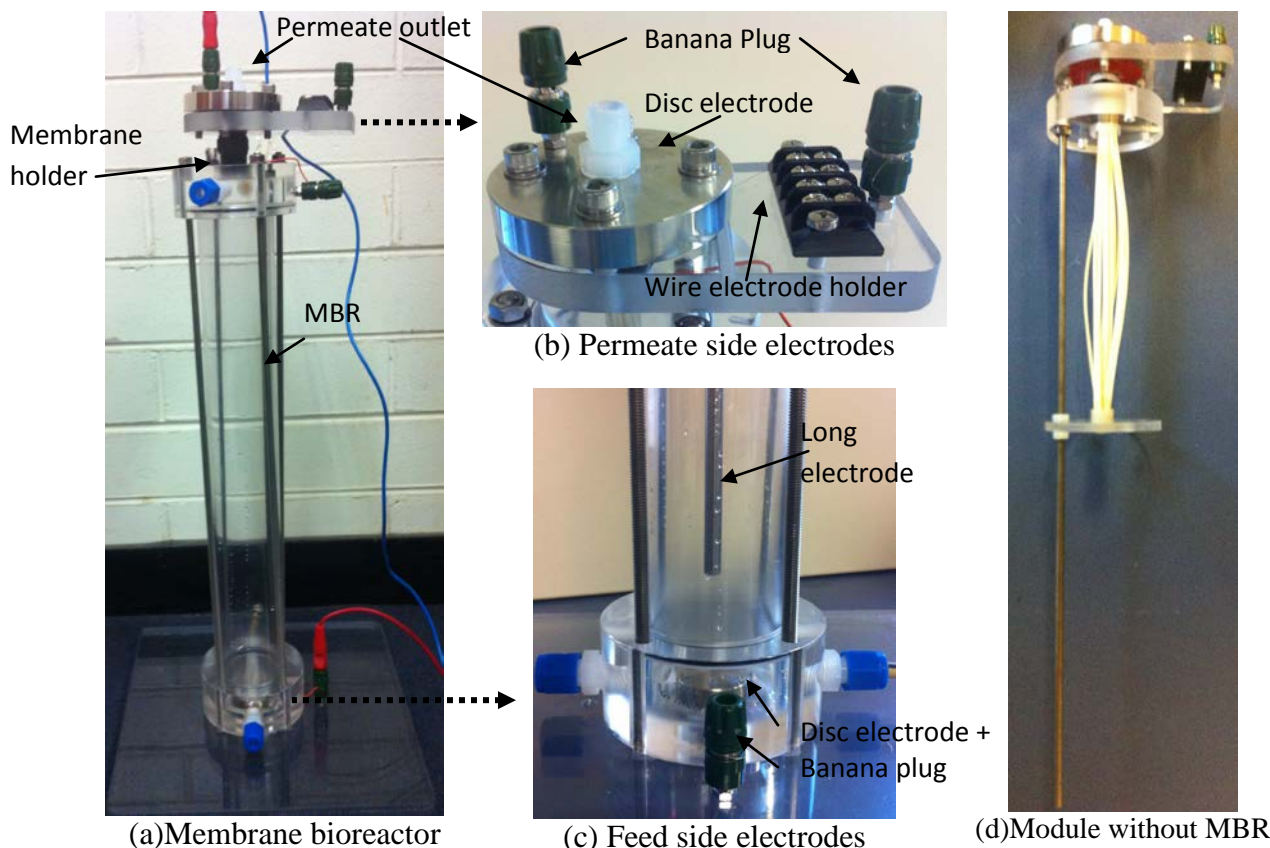


Figure 46 - The structure of the prototype module designed for characterisation of hollow fibre membranes using EIS. Note: for inside-out hollow fibre membrane the top electrode (b) is the feed side and the permeate is on the MBR side (c).

The chamber design is modulated and the cylinder part can be removed from the membrane holder. Therefore, the module can be used for two different purposes. As shown Figure 46-a, the module is a laboratory scale membrane bioreactor (MBR) when the cylinder chamber is used. Figure 46-d shows the other version of the module. The cylinder can be removed, and the membrane holder connected to the side and disc electrode can be immersed in a larger membrane bioreactor. The latter system is designed to be used as canary module for monitoring a large membrane bioreactor.

The version with cylinder (Figure 46-a) is fitted with inlets and outlets for circulating the feed, and an inlet for aeration. The ports are designed to accommodate standard ¼” plastic Swagelok fittings. The membrane holder is designed to accommodate standard and readily available plastic fittings. The fittings are designed to fit and assemble the membrane fibres on one side and can be screwed to the top electrode holder on the other side. The membrane bioreactor side is fitted with two electrodes: a disc at the bottom of MBR, and a long electrode (see Figure 46-c). This provides two options for probing the feed side.

The electrode holder on the permeate side, for outside-in hollow fibre membranes, (see Figure 46-b) provides two options for connection: a stainless steel ring electrode to be used as the common electrode, and a set of connections that can accommodate wires inserted inside the fibres. This electrode has several ports to accommodate wires inserted inside the fibres. These two electrodes are electrically insulated. Banana plugs are connected to the electrodes on the MBR sides and also the top electrode for easy connection of the system to EIS. This module can be used for characterisation of both inside-out and outside-in hollow fibre membranes.

## 3.4. Fouling of outside-in hollow fibre using an industrial feed

### 3.4.1. Effect of electrode configuration on detection of fouling

The results of the fouling experiments using model foulant showed that fouling can be detected without fitting an electrode inside the fibres; however, fitting at least one of the fibres with a wire electrode can improve the performance of EIS in detection of fouling. Solute concentration was shown to have a significant effect on performance of EIS. Here, we examined this further by using a real feed at two different concentrations.

#### *a) Using a module with no wire fitted inside the fibre membranes*

The first series of experiments were performed on a 1% dunder feed (COD ~3000 mg/L) using a membrane module with no wire fitted inside the fibres. The typical conductance and capacitance data at low and high frequencies are shown in Figure 47.

A very sharp increase in both capacitance and conductance was recorded at early stages of fouling. This could be due to replacement of water with permeate inside the hollow fibre membranes. During the rest of the fouling process, very noisy trend was recorded in both capacitance and conductance. The regular shape of variation suggested that these variations were due to changes in water level in the membrane bioreactor. The level of feed in MBR was kept constant using an outlet fitted in the MBR. The surface tension of water created a delay in overflow of the water to the reservoir. These frequent noises indicated that using this electrode configuration, EIS data were very sensitive to the changes in the feed side and possibly not the changes in the membrane itself. This was further examined by ignoring the initial increase in conductance and capacitance and analysing the data. Using this method, a slight capacitance decline was recorded at mid-frequency range. Figure 48 compares relative capacitance decline at 1 kHz with relative flux decline.

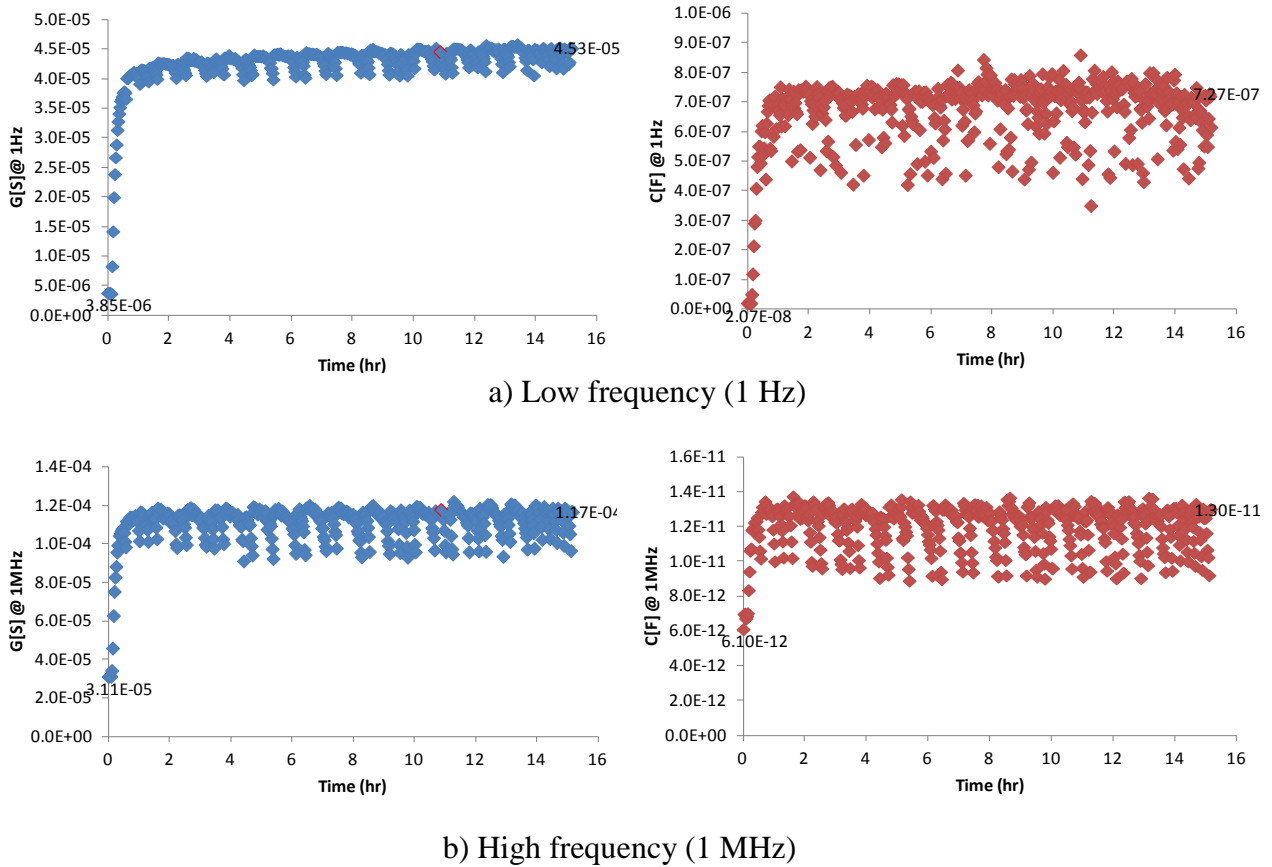


Figure 47 - Typical capacitance and conductance change at a) low frequency (1 Hz) and b) high frequency (1 MHz) during filtration of 1% dunder feed using outside-in hollow fibre membranes. The module was fitted with one common electrode on the permeate side.

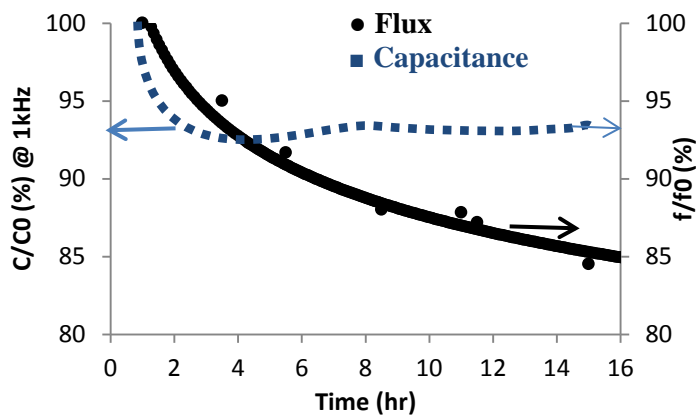


Figure 48 - Relative capacitance change at 1 kHz during filtration without considering the early stage of fouling experiment using 1% dunder. The module was fitted with one common electrode on the permeate side.

The relative capacitance decline of ~ 5% was significantly lower than the flux decline of ~15% recorded at the same time frame. The data at other frequencies were also analysed. Figure 49 shows

the results of this analysis. Conductance increased up to 60% and its rise was lowered by frequency increase.

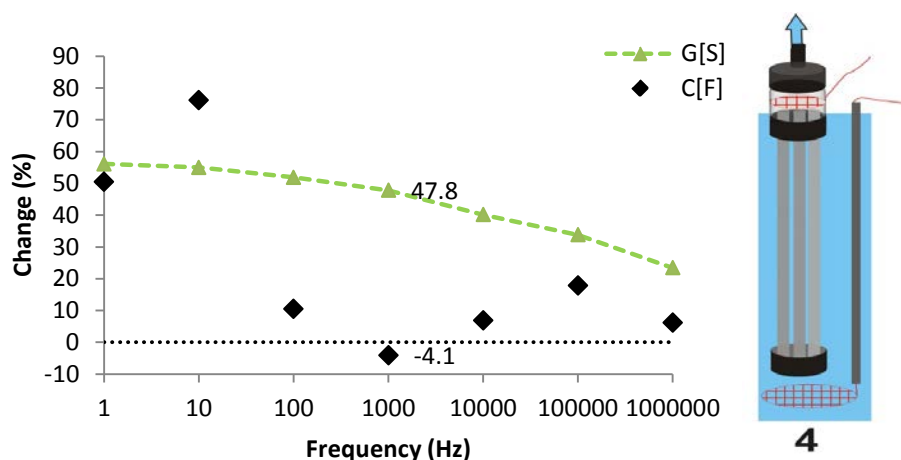


Figure 49 - Capacitance and conductance change (percentage) during filtration without considering the early stage of fouling experiment 1% dunder feed using outside-in hollow fibre membranes. The module was fitted with one common electrode on the permeate side.

At low and high frequencies, capacitance and conductance raises were proportional. However, in mid-frequency range of 100 Hz to 10 kHz, capacitance raise was significantly less than that of conductance and an average capacitance decline of ~4% was recorded at 1 kHz. These results suggested that ionic double layer and changes in concentration were the dominant factors affecting electrical impedance of the system. However, the effect of fouling was detected at mid-frequency range.

The trend of capacitance and conductance was similar when the experiments were performed using 10% (COD ~ 30,000 mg/L) dunder feed. Figure 50 shows the typical EIS data at low and high frequencies. Similar to the experiments performed using 1% feed, a sharp increase in capacitance and conductance was detected at all frequencies. However, at 10 kHz an early sharp increase in capacitance was followed by a decline. Figure 51 compares the relative capacitance decline at 10 kHz with relative flux decline. Although the trend is slightly different, the level of changes is comparable. The flux decline is about 50%, and capacitance declines about 60% in first 4 hours of filtration, and then gradually increases to about 70% of its initial value.

Percentage changes in capacitance and conductance at different frequencies were calculated without considering the sharp growth at the beginning of fouling. The results are presented in Figure 52.

The maximum conductance raise was  $\sim 100\%$  and greater than the value obtained using 1% feed.

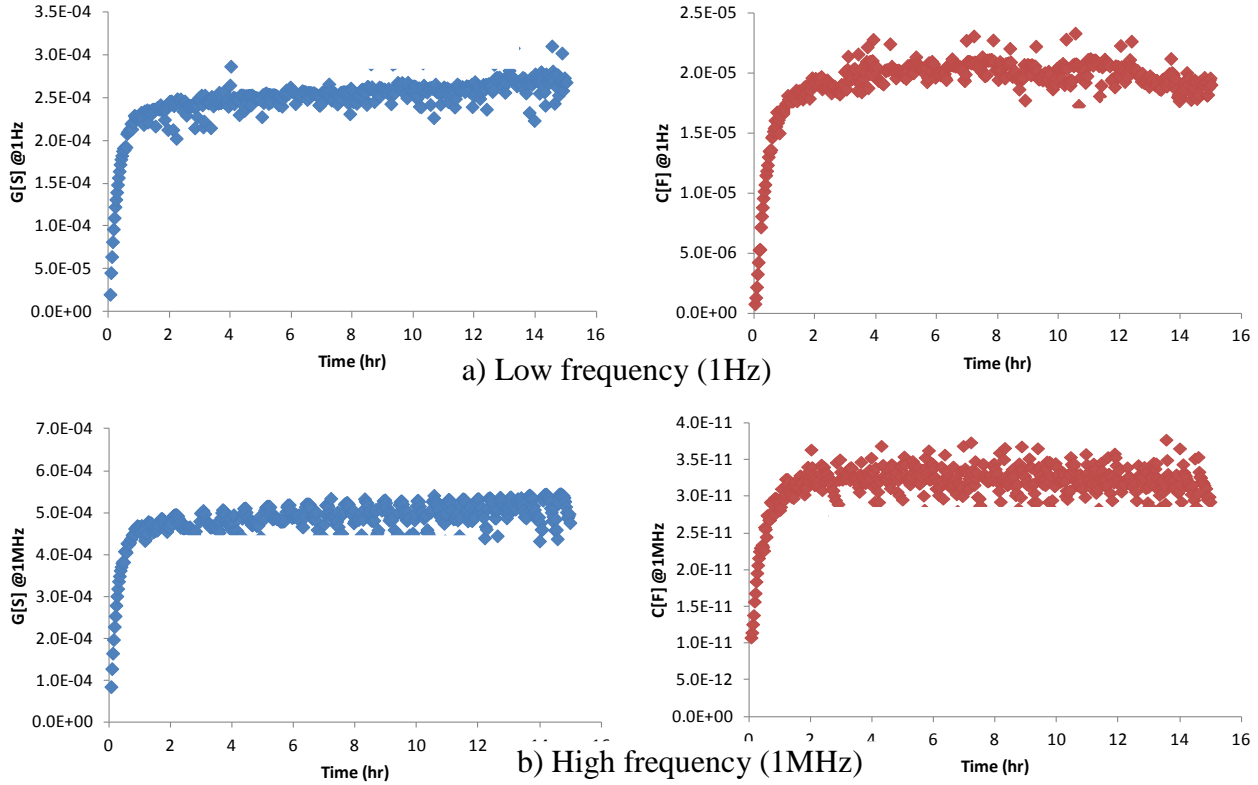


Figure 50 - Typical capacitance and conductance change at a) low frequency (1 Hz) and b) high frequency (1 MHz) during filtration of 10% dunder feed using outside-in hollow fibre membranes. The module was fitted with one common electrode on the permeate side.

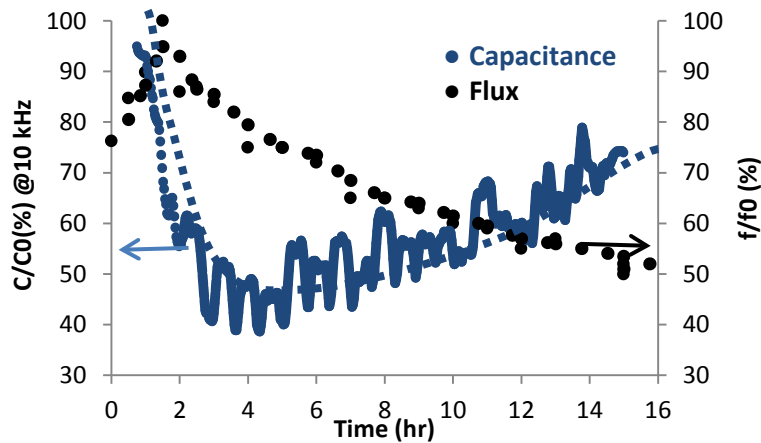


Figure 51 - Capacitance at 10 kHz during filtration without considering the early stage of fouling experiment using 10% dunder feed. The module was fitted with one common electrode on the permeate side.

At low and high frequencies the changes in conductance and capacitance were comparable. While capacitance raise was less than that of conductance at 100 Hz and a capacitance decline was detected at 10 kHz to 100 kHz.

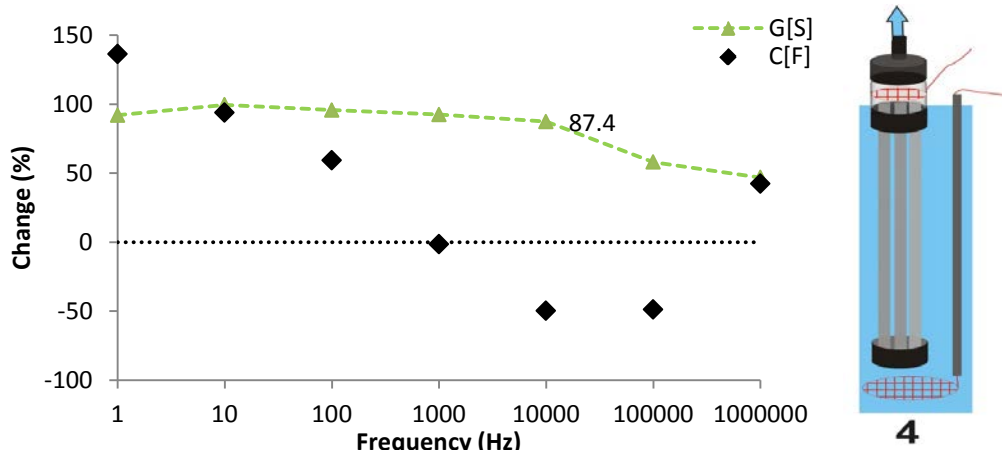


Figure 52 - Capacitance and conductance change (percentage) during filtration without considering the early stage of fouling experiment 10% dunder feed using outside-in hollow fibre membranes. The module was fitted with one common electrode on the permeate side.

These results were similar to the outcome of the experiments using 1% feed. The differences were the higher level of conductance and capacitance change and detecting the highest capacitance decline at higher frequencies. Higher concentration of feed can explain higher conductance and heavier fouling resulted in greater capacitance decline. The shift to high frequencies can be explained by extension of ionic double layer extends to higher frequencies when the concentration of solute increases.

***b) Using a module with a wire electrode fitted inside one of the fibre membranes***

The experiments were repeated using a module fitted with a wire electrode inside one fibre (out of 10 fibres). Figure 53 shows the typical EIS data at low and high frequencies collected using this electrode configuration during fouling experiments using 1% dunder feed. At low frequencies, both conductance and capacitance increased during fouling. The capacitance did not change noticeably at high frequency while a slight conductance raise was recorded.

At mid-frequency range, the trend of EIS data was different. For instance, Figure 54 shows that conductance and capacitance data at 1 kHz. Unlike the data collected using the module with no wire inside the electrodes, capacitance decline was detected from onset of filtration experiment.

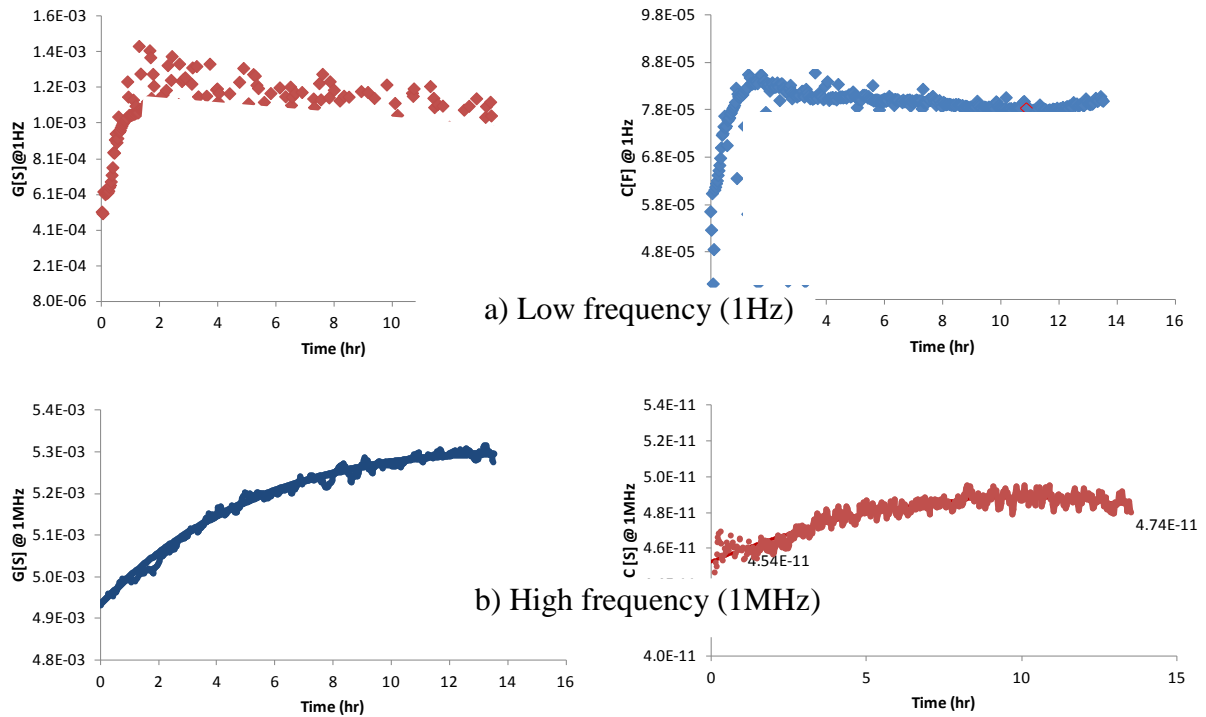


Figure 53 - Typical capacitance and conductance change at a) low frequency (1 Hz) and b) high frequency (1 MHz) during filtration of 1% dunder feed using outside-in hollow fibre membranes. One of the fibres was fitted with a wire electrode.

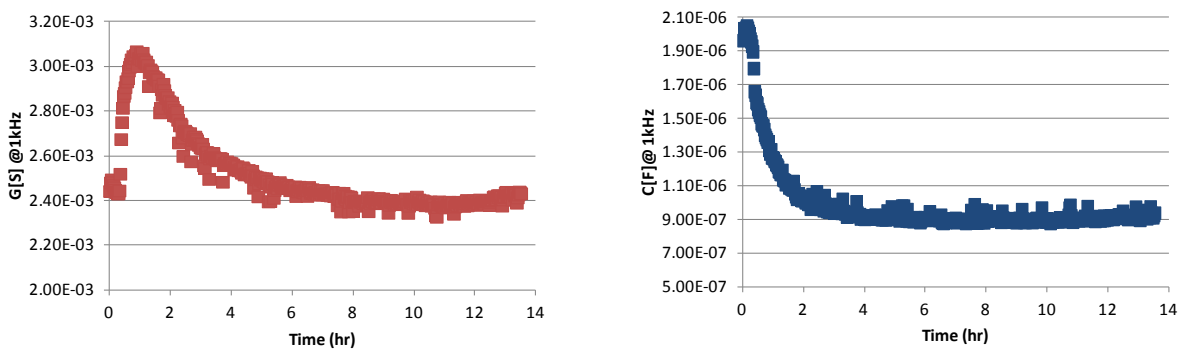


Figure 54 - Capacitance and conductance change at 1 kHz during filtration of 1% dunder feed using outside-in hollow fibre membranes. One of the fibres was fitted with a wire electrode.

Percentage of changes in capacitance and conductance during filtration at different frequencies are plotted in Figure 55. Both capacitance and conductance increased at low and high frequencies. However, the raise at low frequencies was at least ten times greater than the changes at high frequencies. At mid-frequencies, slight conductance decline was detected while capacitance decline

was more significant. Capacitance decline of about 60% was recorded at 100 Hz and 1 kHz. This is significantly higher than the flux decline of ~20% detected during the filtration.

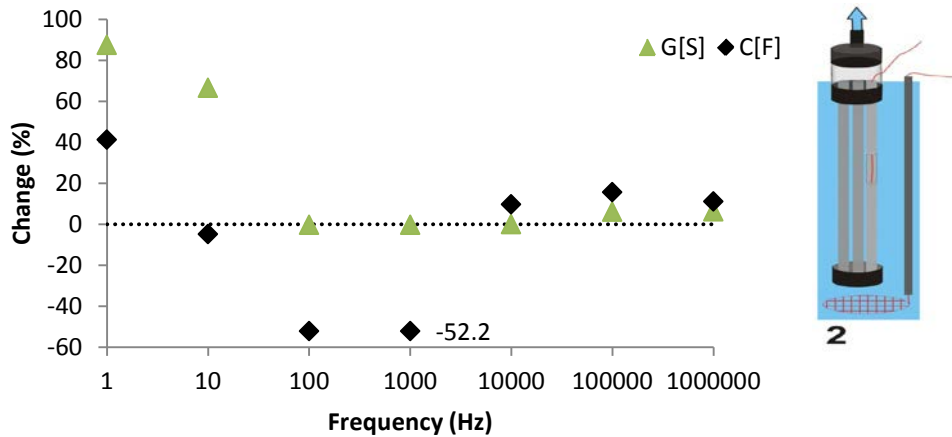


Figure 55 - Capacitance and conductance change (percentage) during filtration of 1% dunder feed using outside-in hollow fibre membranes. One of the fibres was fitted with a wire electrode.

The experiments were repeated using a feed with ten time higher foulant concentration. Figure 56 shows the typical capacitance and conductance values at low and high frequencies. The trends are very similar to those recorded using 1% feed.

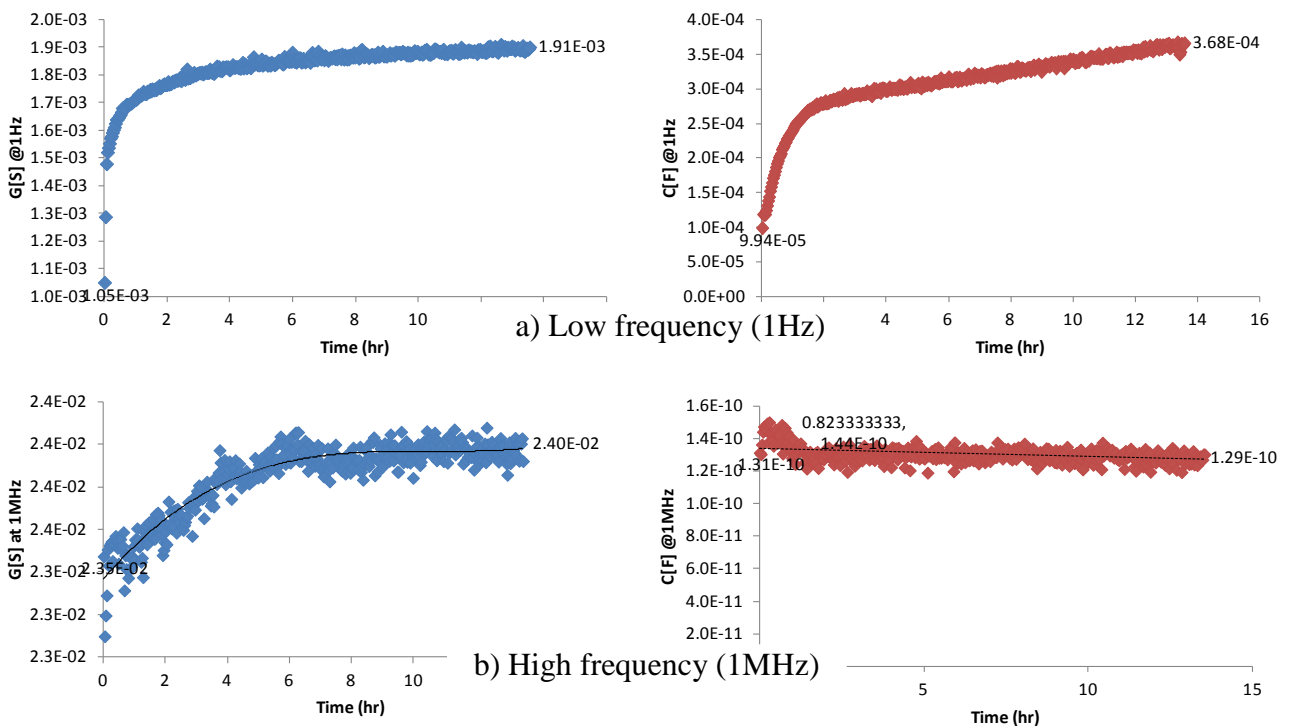


Figure 56 - Typical capacitance and conductance change at: a) low frequency (1 Hz) and b) high frequency (1 MHz) during filtration of 10% dunder feed using outside-in hollow fibre membranes. One of the fibres was fitted with a wire electrode.

A declining pattern in capacitance was detected at 1 kHz as shown in Figure 57. Total percentage change in capacitance and conductance at different frequencies are shown in Figure 58. The maximum conductance change was about 200%, significantly higher than the values measured for 1% feed. Capacitance decline was only recorded at 1 kHz which a narrower range compared to the results obtained using 1% feed. This shift to higher frequencies is in agreement with the results obtained using the electrode configuration with no wire inside the membrane fibres.

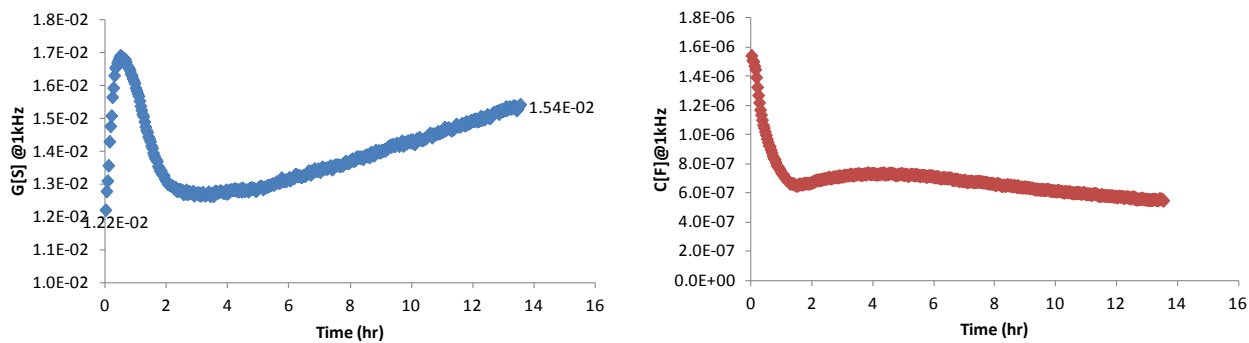


Figure 57 - Capacitance and conductance change at 1 kHz during filtration of 10% dunder feed using outside-in hollow fibre membranes. One of the fibres was fitted with a wire electrode.

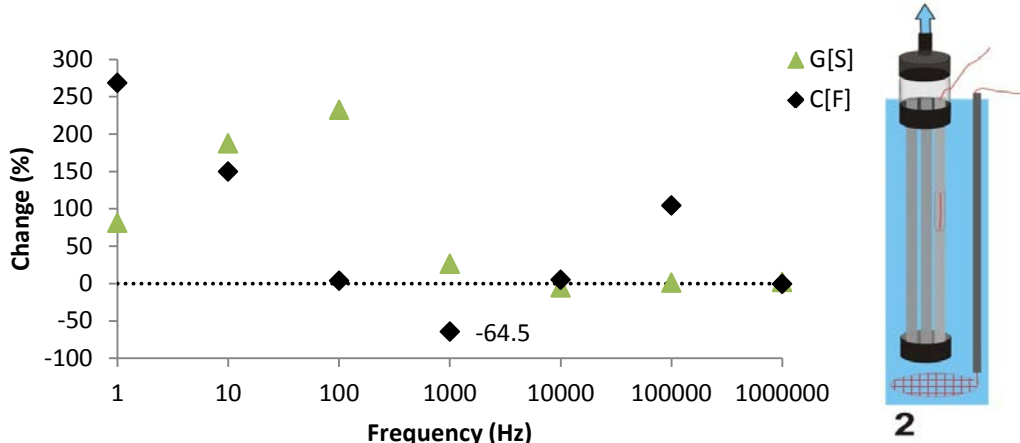


Figure 58 - Capacitance and conductance change (percentage) during filtration of 1% dunder feed using outside-in hollow fibre membranes. One of the fibres was fitted with a wire electrode.

The level of relative capacitance decline at mid-frequency range ( $\sim 1$  kHz) measured using two configurations is compared with the relative flux decline in Figure 59. It should be mentioned that the data presented for the configuration with no wire inside the fibres were analysed differently. The early sharp increase of capacitance at the beginning of the filtration was not considered in the analysis.

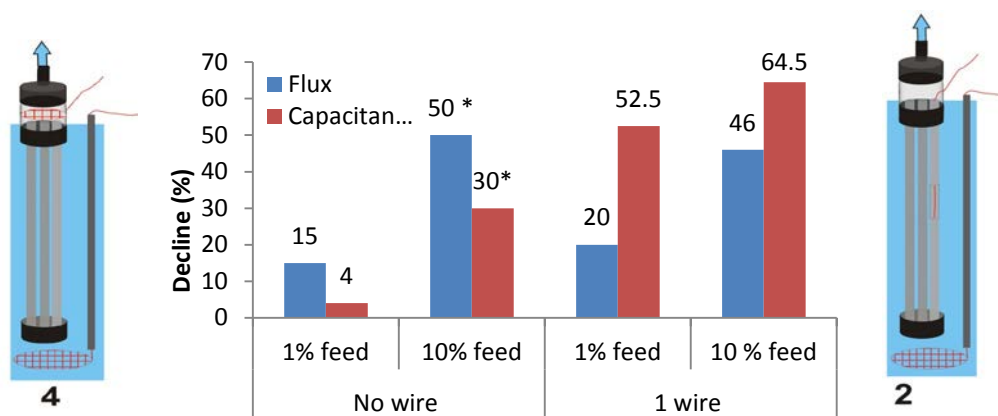


Figure 59- Percentage of decline during fouling in flux and capacitance at 1 kHz using modules with different electrode configurations. \* Capacitance at 10 kHz.

Using the configuration with no wire fitted inside the fibres, flux decline was higher than the capacitance decline. While, by inserting a wire inside one of the fibres, the capacitance decline recorded by EIS was greater than the flux decline recorded by measuring the permeate flow. These results show that EIS can be used for online monitoring of fouling. Comparing the two electrode configurations, it can be concluded that fitting a wire electrode in one of the membrane fibres is necessary for achieving high sensitivity of EIS to membrane fouling. For very fine outside-in membrane (i.e. small inner diameter) inserting a wire inside the fibres is not practical. These results show that EIS data can provide some information on the level of fouling for these membranes. However, filtration parameters (such as flux and trans-membrane pressure) are possibly more sensitive to fouling compared to EIS data.

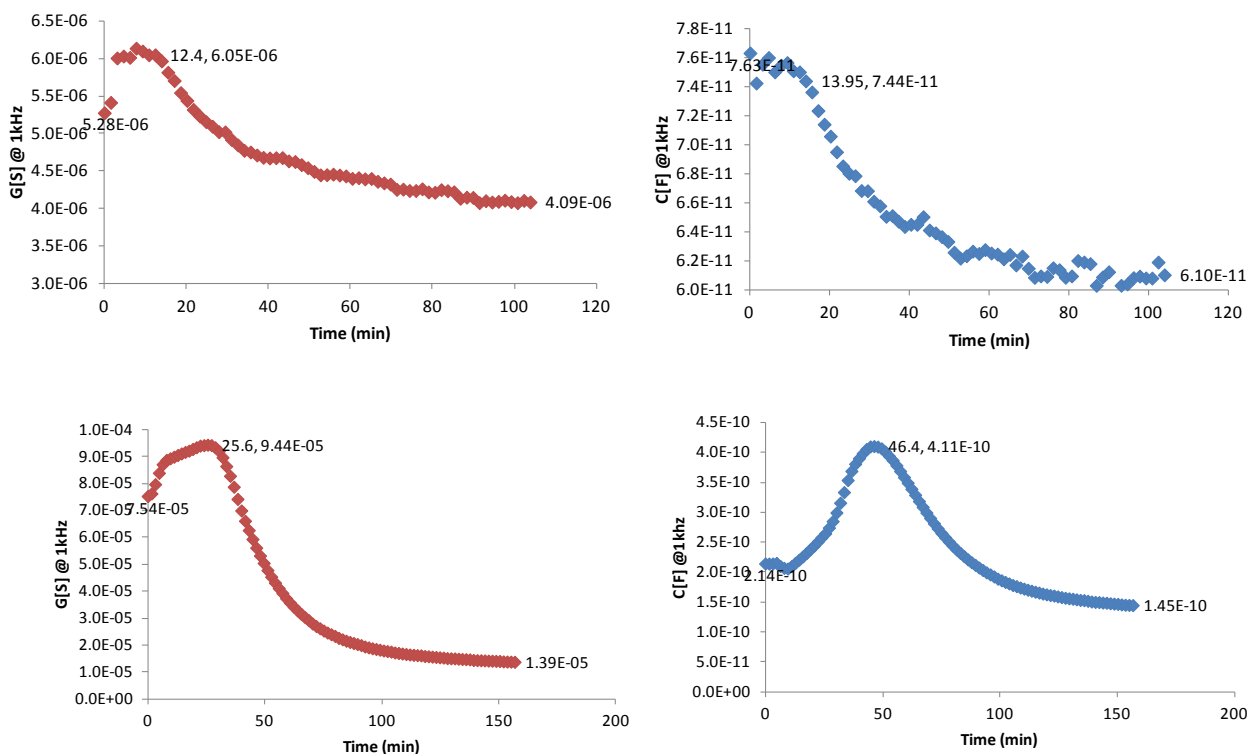
### 3.4.2. Effect of electrode configuration on monitoring the backwashing process

Performance of two electrode configurations was also compared for monitoring the membrane cleaning process. Backwashing is a common process for frequent cleaning of hollow fibre membranes. With backwashing, it is expected to push the foulants from the surface or inside the membrane pores to the membrane bioreactor. This could affect the conductance of the system. However, the capacitance change due to removal of foulant at the frequency range assumed to be dominant with impedance of membrane is more important. In theory, it is expected to record

capacitance change in the opposite direction of the changes recorded during fouling. This is examined by monitoring the cleaning process using EIS. Figure 60 shows the capacitance and conductance change at 1 kHz during backwashing of two membranes fouled with 1% (Figure 60-a) and 10% (Figure 60-b) feed, respectively.

The experiments were performed using the membrane module with a common electrode on the permeate side, but no wire fitted inside the fibres. The slight increase in conductance could be due to release of residue solute inside the membrane or the foulant on the surface of membrane to the membrane bioreactor. The capacitance and conductance decline following the raise at the beginning of backwashing can possibly be explained by decline of solute concentration in the MBR.

(a)



(b)

Figure 60 - Capacitance and conductance at 1 kHz during backwashing of hollow fibre membrane fouled with: (a) 1% and (b) 10% dunder feed. The module was fitted with one common electrode on the permeate side.

The capacitance increase at the beginning of backwashing process could be due to removal of foulant from the surface of membrane and hence decline in the thickness of fouled membrane. In case of the membrane fouled using 1% feed, it is difficult to confirm that the foulant removal was

the source of capacitance raise, because both conductance and capacitance increased over the same period of time. However, in case of the membrane fouled with 10% feed the capacitance increase was more significant, and the increasing trend continued till 50 minutes after beginning of backwashing while conductance increase was stopped after about 30 minutes. Total percentage of change in capacitance and conductance during backwashing of membrane fouled with 1% and 10% feed is shown in Figure 61.

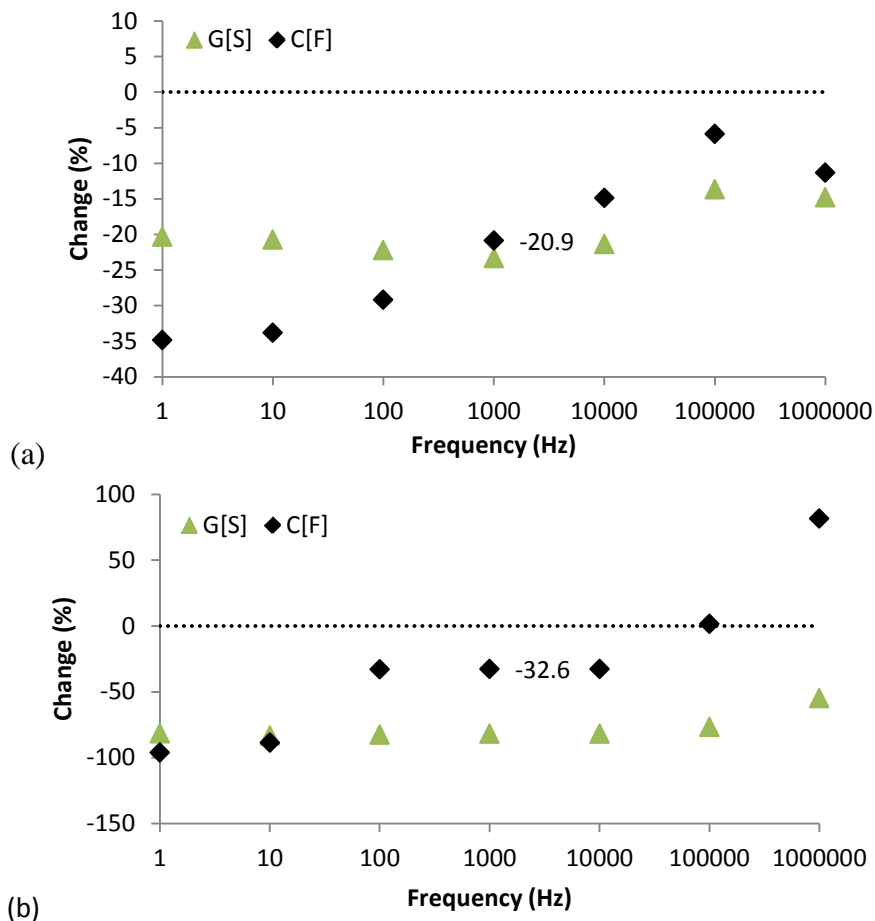


Figure 61 - Total percentage change of capacitance, conductance during backwashing of hollow fibre membrane fouled: (a) 1% and (b) 10% dunder feed. The module was fitted with one common electrode on the permeate side.

Conductance decline of maximum 20% and 100% was detected during backwashing of membrane fouled with 1% and 10% feed, respectively. Conductance decline was at its maximum at low frequency and became less significant by increasing frequency. The capacitance change was greater than, or comparable to, capacitance decline at low and high frequencies. However, at mid-frequency range, the conductance decline was greater than the change in capacitance.

At least in the case of the membrane fouled with 10% feed, capacitance increase at the beginning of backwashing could be the source of lower capacitance decline. In order to examine this theory, conductance and capacitance changes during first 50 minutes of backwashing the membrane fouled with 10% feed were calculated. The results are shown in Figure 62. At mid-frequency range of 1-10 kHz, conductance declined while capacitance increased. This could be an indication of the foulant removal from the surface of fouled membrane.

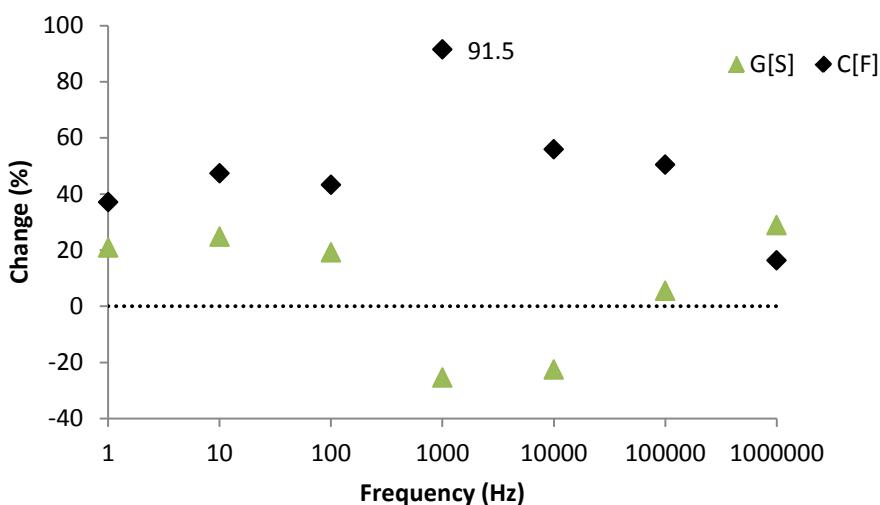


Figure 62 - Capacitance, conductance change during the first stage of backwashing of hollow fibre membrane fouled with 10% dunder feed. The module was fitted with one common electrode on the permeate side.

Similar experiments were performed using the module fitted with a wire electrode inside one of the membrane fibres. The capacitance and conductance at 1 kHz for membrane fouled with 1% and 10% feed are shown in Figure 63.

A conductance increase followed by a slow decline was recorded for both membranes. Although the shape of the graphs is different, the overall trend of conductance was similar to those measured using the module with no wire fitted inside the fibres. However, the capacitance trend was completely different. Using this configuration, capacitance decreased from the beginning of backwashing process.

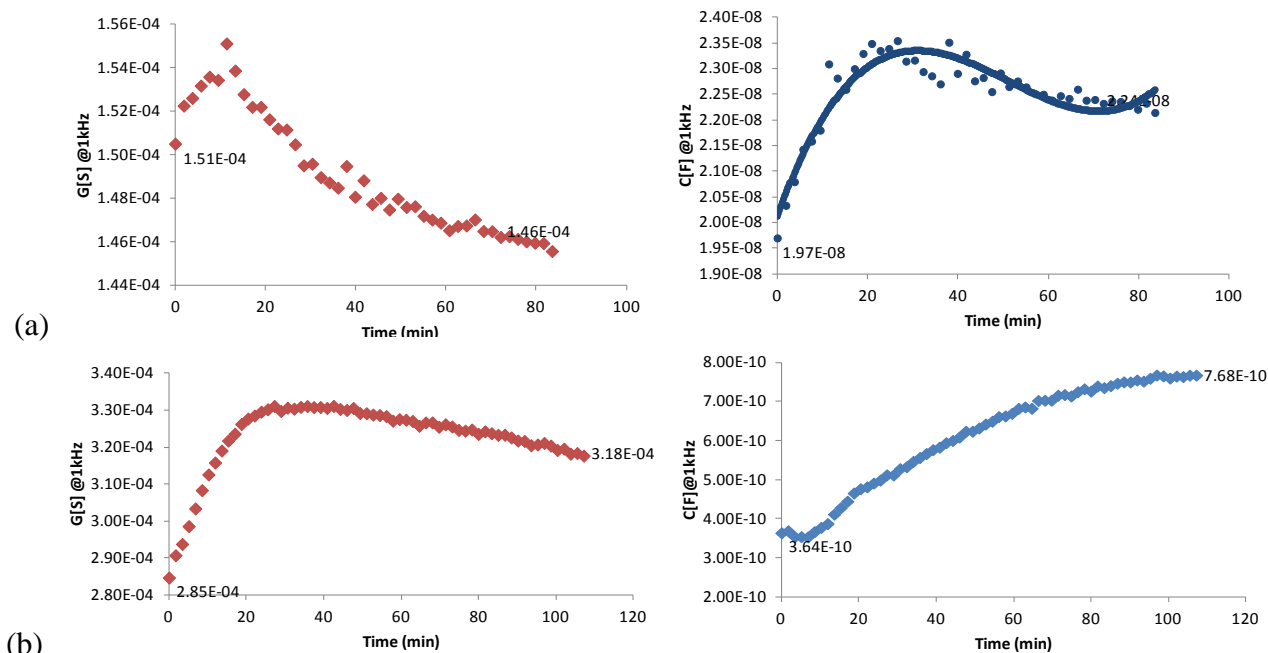


Figure 63 - Capacitance and conductance at 1 kHz during backwashing of hollow fibre membrane fouled with: (a) 1% and (b) 10% dunder feed. One of the fibres was fitted with a wire electrode.

Total percentage changes of capacitance and conductance during backwashing process of two membranes (fouled with 1% and 10% feed) are shown in Figure 64.

Capacitance increased over a wide range of frequency, from 10 Hz to 10 kHz. The maximum capacitance increase of ~12% (for membrane fouled with 1% feed) and ~110% (for membrane fouled with 10% feed) was recorded at 1 kHz. In overall, conductance declined about 15% during backwashing of membrane fouled with 1% feed while a slight ( $< 10\%$ ) conductance raise was recorded during backwashing of the membrane fouled with 10% feed. This can be due to release of higher concentration of solute accumulated on the surface of the membrane fouled with 10% feed.

Generally, it can be concluded that the capacitance increase at mid-frequency range (e.g. 1 kHz) is an indication of the foulant removal during backwashing process. This is in agreement with the results of fouling experiments that showed capacitance decline at mid-frequency range ( $\sim 1$  kHz) was a good indication for membrane fouling.

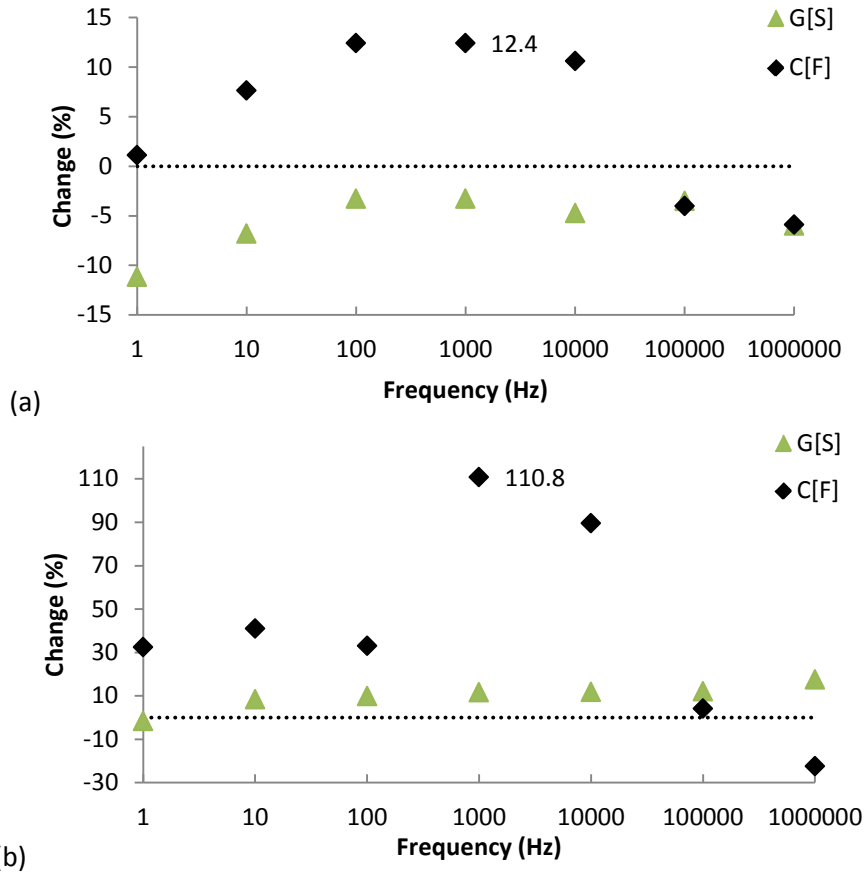


Figure 64 - Total percentage change of capacitance, conductance during backwashing of hollow fibre membrane fouled with 10% dunder feed. One of the fibres was fitted with a wire electrode.

Figure 65 compares the percentage of capacitance increase for two electrode configurations for membrane fouled with 1% and 10% feed. Using both modules the capacitance increase was significantly higher when the membrane fouled with 10% feed was backwashed.

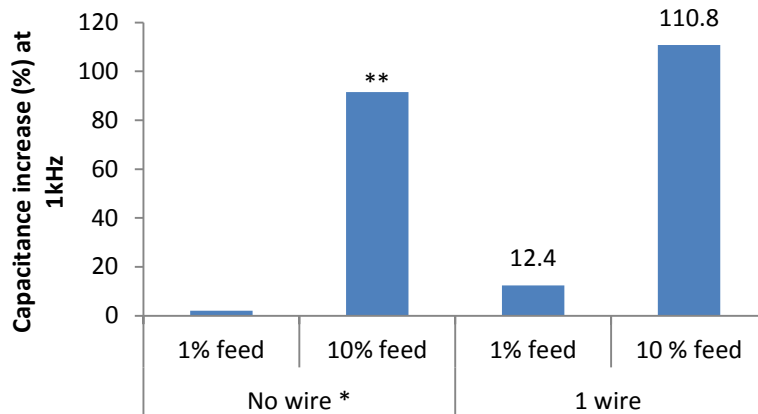


Figure 65 - Capacitance change during backwashing recorded using modules with different electrode configurations.\* Capacitance increase recorded at early stage of backwashing is considered for the configuration with no wire inside the fibres.\*\* In comparison with the values for 1 wire module, this value is an over estimation.

This is because the membrane fouling was more advanced when the membrane was fouled with 10 % feed. The flux declined about 15% and 50% respectively when 1% and 10% feed solutions were used for fouling.

The relatively low level of capacitance changes during backwashing of the membrane fouled with 1% feed could be due to partial removal of the loose foulant layer on the surface of membrane during handling and exchanging the content of MBR from feed to water.

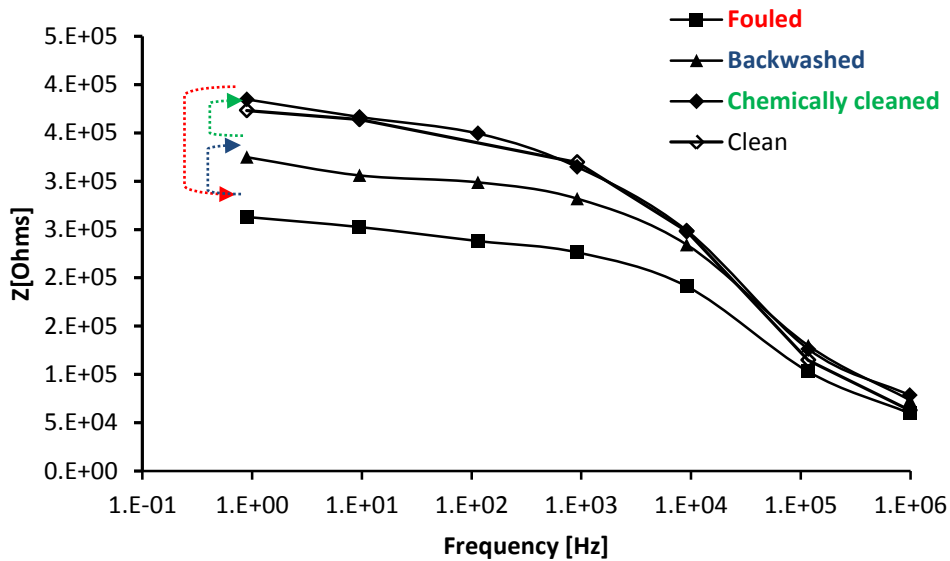
The values for the module with no wire are overestimated compared to the value for the other module, because instead of the overall change the increasing trend at the beginning of backwashing is considered in this estimation. Even with this unfair comparison, the values measured using the module fitted with a wire inside one of the fibres were greater than the values obtained using the module with no wire. These results are in agreement with the results of fouling experiments and once more show that fitting a wire electrode inside the fibres is required for monitoring fouling and backwashing of outside-in hollow fibre membranes.

### **3.4.3. Effect of electrode configuration on characterisation of fouled membranes**

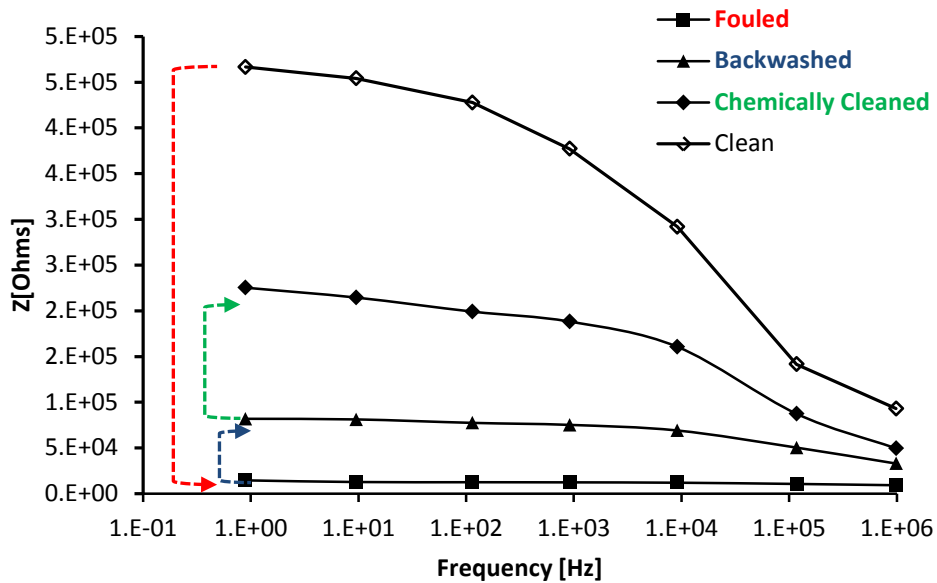
After backwashing process membranes were soaked in detergent solution for 3 hours and then gently washed using a soft brush. After careful rinsing with water, the detergent inside the membranes was removed by 1 hour filtration of water. The impedance of the chemically cleaned membrane was measured and compared with the impedance of the membrane after fouling and backwashing.

The impedance spectra measured using two electrode configurations are shown in Figure 66 and Figure 67. Figure 66 shows the impedance of membrane measured using the module with no wire fitted inside the membrane fibres. The data shown in Figure 66-a are collected when the membrane was fouled using 1% feed. This graph shows that the impedance declined significantly due to

fouling, but backwashing increased the impedance. Chemical cleaning was also effective in returning the impedance to the level similar to that of the clean membrane.



(a)

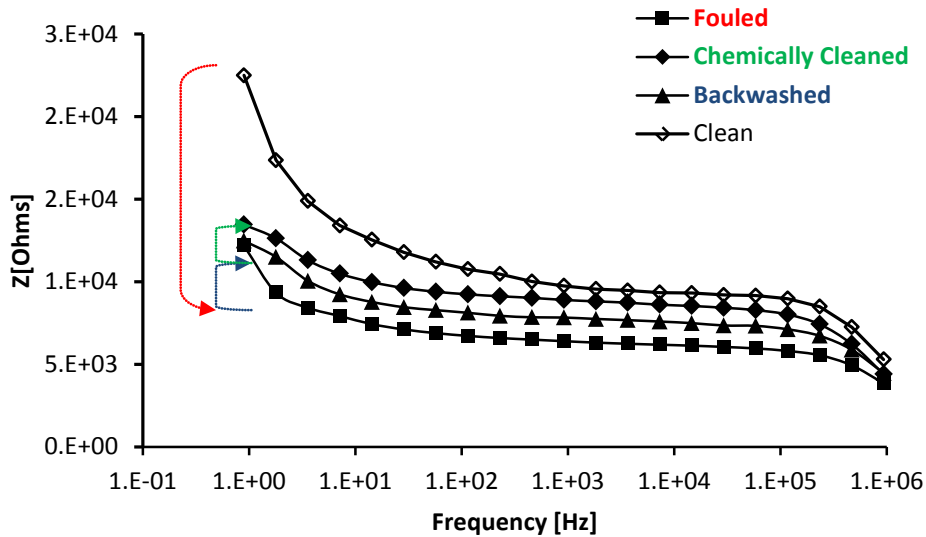


(b)

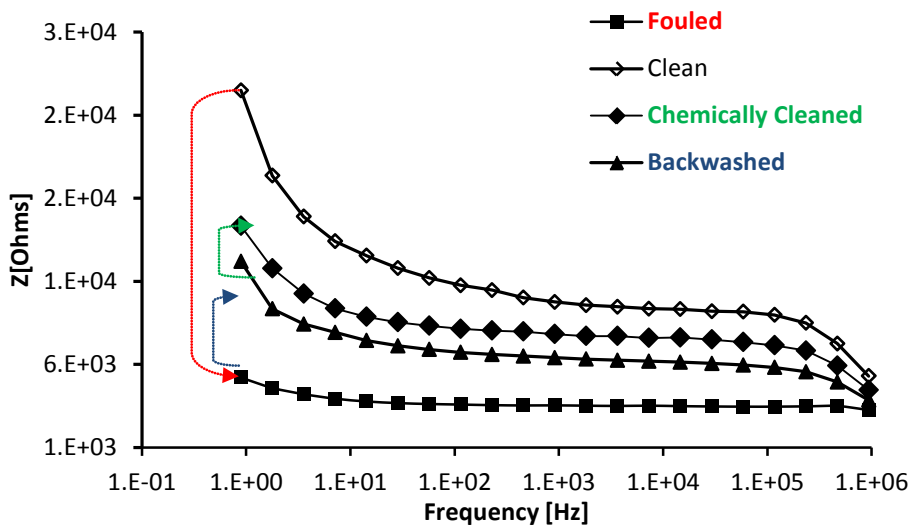
Figure 66 - Impedance of clean, fouled, backwashed and chemically cleaned hollow fibre membrane measured using the module with one common electrode on the permeate side (i.e. no wire): a) membrane fouled using 1% dunder feed, and b) membrane fouled using 10% dunder feed.

When the membrane was fouled with 10% feed, the impedance decline was more significant. Similar to the previous experiment, backwashing increased the impedance. However, chemical cleaning did not return the impedance spectra to that of the clean membrane. These results suggested that the fouling created using 1% feed was almost reversible.

However, filtration using 10% feed resulted in partially irreversible fouling. Irreversible fouling could be due to penetration of foulant material inside the membrane structure or formation of the fouling layer tightly attached to the surface of membrane during fouling experiment using 10% feed solution.



(a)



(b)

Figure 67 - Impedance of clean, fouled, backwashed and chemically cleaned hollow fibre membrane measured using the module with one wire electrode fitted in one of the fibres (i.e. one wire): a) membrane fouled using 1% dunder feed, and b) membrane fouled using 10% dunder feed.

The experiments were repeated using the membrane module with a wire electrode fitted inside one of the fibres. The shape of impedance spectra were different from those measured using the previous electrode configuration (see Figure 67). The impedance was in general at least one order of

magnitude higher compared to the values shown in Figure 66. The trend of changes detected using two electrode configurations was similar. In general, fouling reduced the impedance, but backwashing and cleaning increase the impedance of the system.

The results of electrical impedance measurements using this electrode configuration also showed that backwashing and chemical cleaning helped to reverse the effect of fouling. These results are in agreement with the water flux values measured at different stages of fouling and cleaning. Typical flux data presented in Figure 68 show that fouling with 10% feed resulted in greater flux decline. These results also show that although backwashing and chemical cleaning increased water flux, the water flux of chemically cleaned membrane was significantly lower than the flux of clean membrane, when the membrane was fouled with 10% feed solution. This result was expected and in agreement with the results of EIS measurements.

In the case of the membrane fouled with 1% feed solution, EIS measurements using the module with no wire inside the membrane fibres suggested that the chemical cleaning returned the membrane almost back to its clean state. However, using the module with a wire inside one of the fibres, the impedance spectra of clean and chemically cleaned membranes were noticeably different. The latter results are closer to the results of the water flux measurements. As shown in Figure 68, water flux of the cleaned membrane is 10% lower than the flux of clean membrane suggesting that the fouling was not reversed completely which also happens in actual practice.

This could be an indication of pore blocking that was not reversed by cleaning. The impedance decline at 1 kHz relative to the impedance of clean membrane is used for comparing two electrode configurations. The values are plotted in Figure 69. The impedance decline due to fouling measured using the module with 1 wire inside the membranes were slightly higher than the values recorded using the module with no wire inside the membranes.

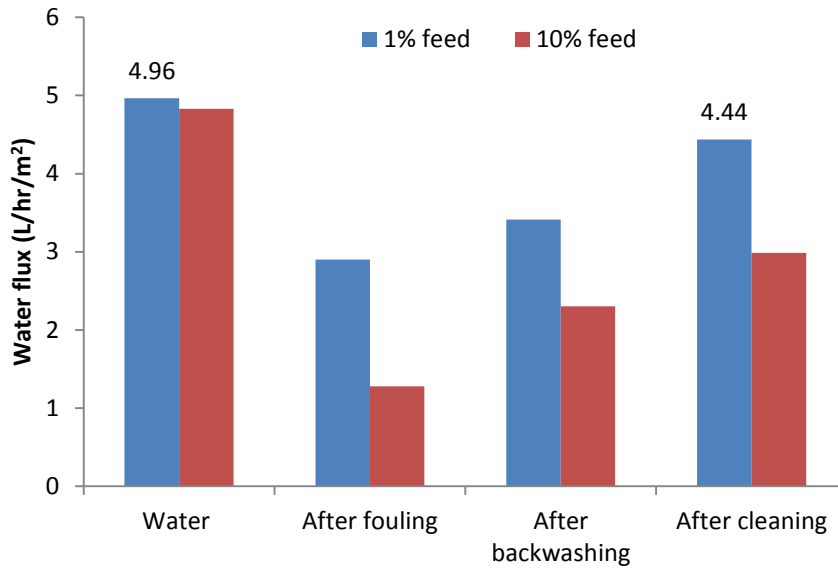


Figure 68 - Typical water flux data at different stages of fouling and cleaning process.

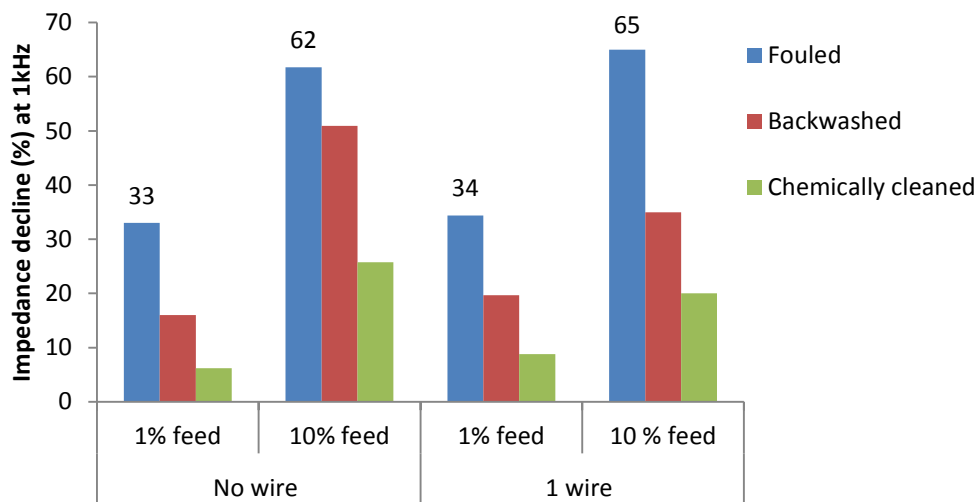


Figure 69 - Impedance decline relative to clean membrane measured using modules with different electrode configurations: after fouling, backwashing and cleaning processes.

Using both electrode configurations, the effects of fouling, backwashing and chemical cleaning were detected. Comparing the results with flux data, it was shown that better results were achieved using the configuration with a wire fitted in one of the membrane fibres.

These experiments show that EIS can be used for membrane autopsy and off-line monitoring of fouling and cleaning processes.

### 3.4.4. Separation performance of hollow fibre membranes

Using different characterisation methods, the dunder feed was characterised, and the results are presented in Table 1. Based on the specifications provided by the manufacturing company, this hollow fibre membranes are classified as ultrafiltration membranes. However, unlike flat membranes the molecular-cut-off (MWCO) of hollow fibre membranes is not usually reported.

The molecular weight or size distribution of particles in the feed was characterised using microfiltration membranes with known average pore size. 100 ml of 1% dunder feed solution was filtered using PES microfiltration membranes, and the permeate mass to estimate the flux was monitored by time. The data are shown in Figure 70. The linear trend of permeate weight using microfiltration membrane with 3 µm average pore size show that this membrane was not fouled. This indicates that the feed did not contain particles larger than 3 µm.

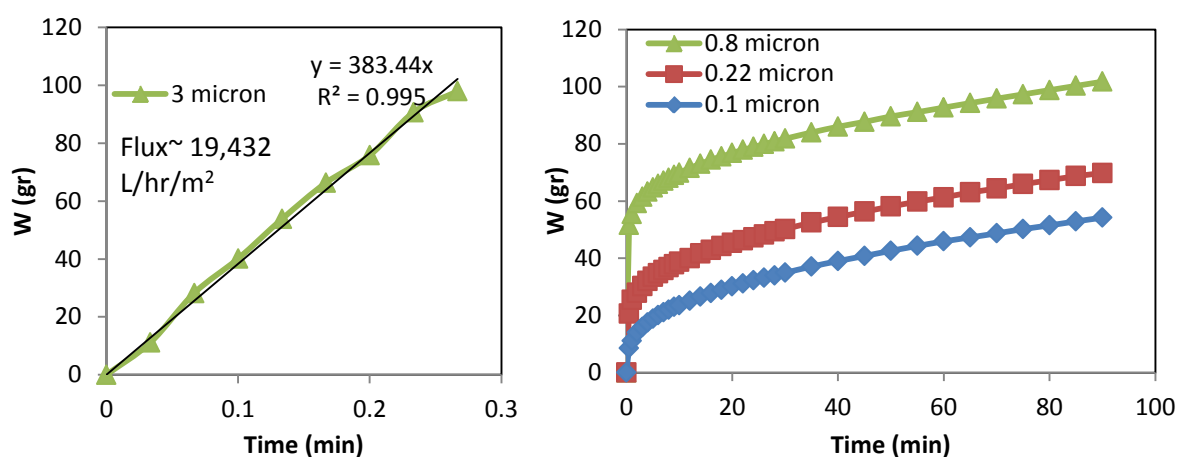


Figure 70 - Accumulated weight of the filtrate during filtration of 1% dunder feed at 100 kPa using flat PES microfiltration membranes with average pore size of 3, 0.8, 0.22 and 0.1 µm.

The slowing growth of permeate weight using other microfiltration membranes (i.e. with average 0.1, 0.22 and 0.8 µm pore size ) showed that these membranes were fouled or blocked. This feed was a mixture of minerals and organic matters. A simple blocking due to deposition of minerals can be removed by backwashing but organic foiling is less reversible in nature. These results cannot be conclusive in determining the type of fouling. Figure 71 shows that the flux decline was very quick partially due to the membrane compaction but mainly due to fouling.

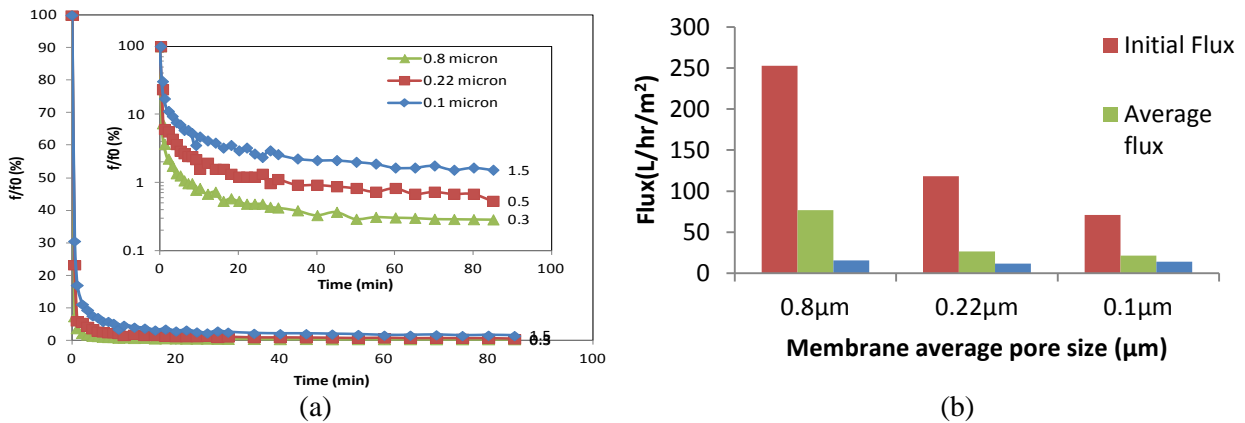


Figure 71 - Flux decline as a function of time (a) and initial, average and final flux of permeate (b) during filtration of 1% dunder feed at 100 kPa using flat PES microfiltration membranes with average pore size of 0.8, 0.22 and 0.1 μm.

The fouling of the membrane with smaller pore size was slightly slower due to lower initial and average flux. The initial, average and final flux values are shown in Figure 71.

The membranes were weighed before filtration of 100 ml of feed, and were weighed again after the fouled membranes were dried, and the solid content of the permeate was estimated. In case of the hollow fibre membranes, samples of feed and permeate were dried at 80 °C for 24 hours to measure their solid contents. The solid content of feed, and permeates of microfiltration membranes and the hollow fibre membranes are compared in Figure 72.

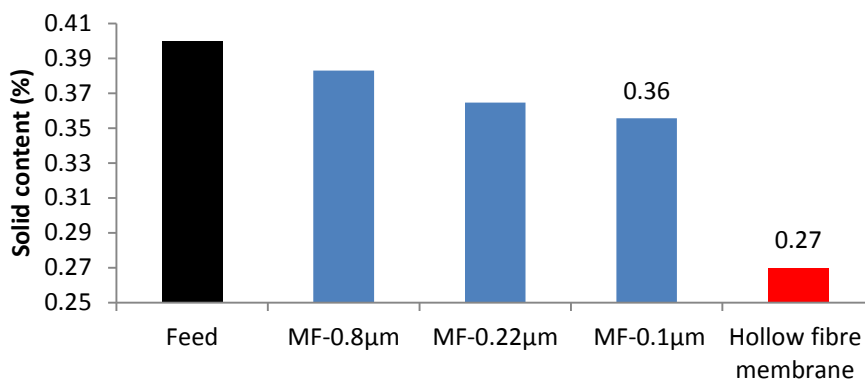


Figure 72 - Solid content of 1% dunder feed compared with the solid content of the permeates of flat microfiltration and hollow fibre membranes.

In spite of heavy fouling, the solid content only reduced by 10% using the microfiltration with smallest average pore size (i.e. 1 μm). This suggests that most of the particles in the feed were smaller than 1 μm. Using hollow fibre membranes, solid content was reduced about 40%. This

shows that the hollow fibre membranes can remove particles smaller than 1  $\mu\text{m}$  and hence are in ultrafiltration range.

Table 2 shows the characteristic properties of feed and permeate of hollow fibre membranes. Filtration using hollow fibre membranes reduced the organic content (i.e. COD) and colour by ~56% and 41%, respectively. Higher organic content decline (compared to that of solid content) is an indication that the feed contains a high concentration of salts that are not separated using hollow fibre membranes. This is also reflected in conductivity changes. As expected, filtration using hollow fibre did not reduce the conductivity. The slight conductivity increase is due to evaporation of permeate during ~20 hours filtration.

Table 2 -Characterisation of feed and permeate of hollow fibre membranes.

	COD (mg/L)	Colour (PtCo)	Conductivity $\sigma$ ( $\mu\text{S}/\text{cm}$ )	Solid Content (%)
Feed (1 % feed)	3025	1730	1260	0.40
Permeate	1324	1020	1400	0.24
Change (%)	-56	-41	11	-41

The permeate of the hollow fibre membranes was filtered using 1  $\mu\text{m}$  microfiltration and ultrafiltration membranes. The microfiltration membrane was not fouled, but slight fouling was detected using ultrafiltration membrane with 20 kDa molecular weight cut off as shown in Figure 73. This showed that MWCO of hollow fibre membrane was slightly higher than 20 kDa.

The permeate of hollow fibre membrane was also filtered using ultrafiltration membrane with 5 kDa molecular weight cut off. Solid content of feed, permeate of hollow fibre membrane and ultrafiltration membranes are compared in Figure 74. The hollow fibre membrane reduced the solid content of the feed by 39% and filtration of the permeate using 20 kDa and 5 kDa improved this value to ~45% and 55%, respectively. Similar results were obtained when the concentration of feed was increased 10 fold, to 10% dunder.

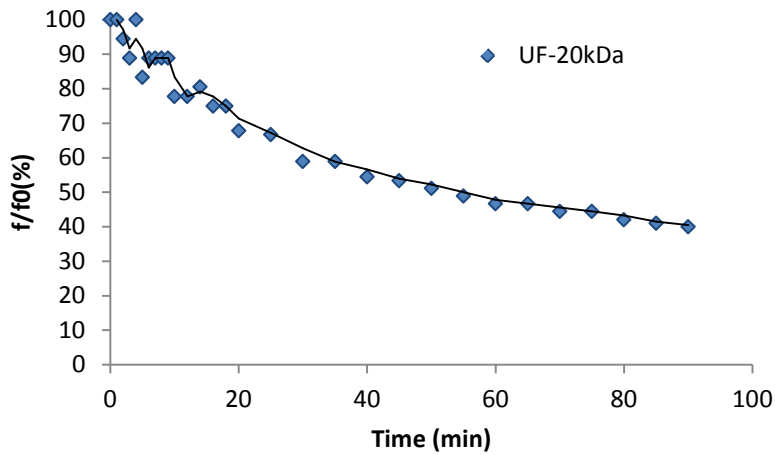


Figure 73 - Flux decline during filtration of the permeate of hollow fibre membrane using ultrafiltration membrane with 20 kDa molecular weight cut off.

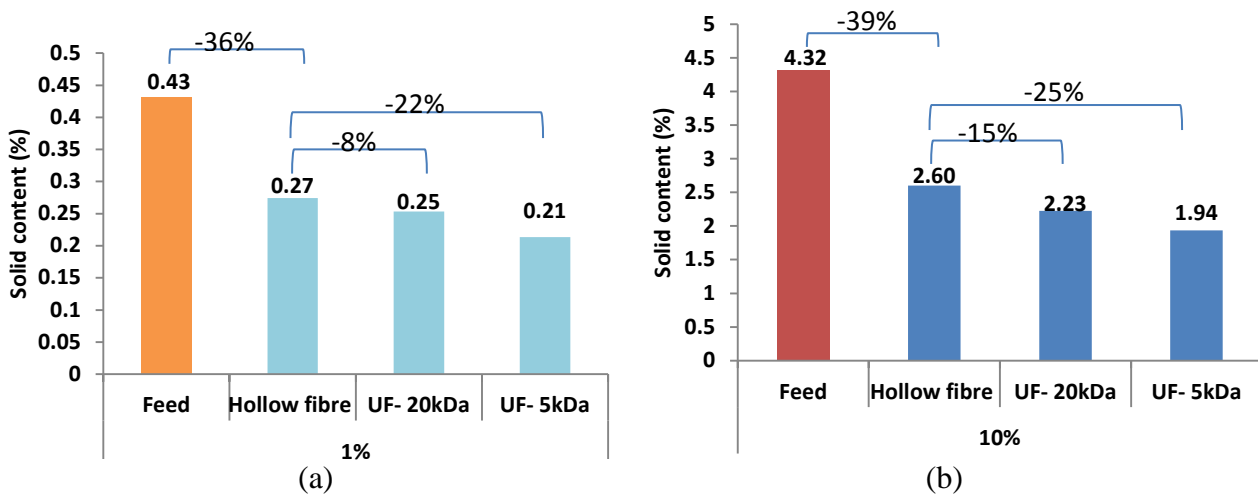


Figure 74 - Solid content of the feed, permeate hollow of fibre and ultrafiltration membranes: a) 1% and b) 10% dunder feed. The permeate of hollow fibre membrane was used as feed for ultrafiltration membranes.

These experiments show that hollow fibre membranes were able to remove the organic materials with molecular weight greater than 20 kDa. However, as expected the salts were not removed by these membranes. The organic removal can be improved further using ultrafiltration membranes with 5 kDa MWCO. The separation performance of these hollow fibre membranes was superior to the performance of flat microfiltration and ultrafiltration membranes. These results suggest that hollow fibre membranes can provide a solution for the problem of waste dunder.

### 3.5. Summary

Electrical impedance spectroscopy was capable of detecting the fouling of hollow fibre membranes during filtration of yeast by-product wastewater. Fitting at least one of the fibres with a wire electrode was necessary for accurate detection of fouling although without inserting a wire inside the fibres, fouling was detected. Using this configuration, relative capacitance decline at mid-frequency range (e.g. 1 kHz) was proportionate to the relative flux decline due to fouling. Accordingly, a significant increase in capacitance at 1 kHz was measured during backwashing. This confirmed that the electrical impedance of membrane was dominant at mid-frequency range, making this frequency suitable to monitor fouling and cleaning processes.

The hollow fibre membranes had significantly better separation performance in comparison with flat membranes. The molecular cut off (MWCO) of hollow fibres was about 20 k Dalton. Fouling of hollow fibre was significantly lower than the fouling rate of the flat membranes. These results suggested that with optimising the process and possibly adding another filtration process this ultrafiltration hollow fibre membranes can be used to separate the organic materials from minerals in dunder waste.

## 4. Conclusions

The experiments on model and industrial feeds showed that the electrical impedance spectroscopy (EIS) is capable of detecting the fouling of hollow fibre membranes. Experiments on flat, inside-out hollow fibre, and outside-in hollow fibre membranes using different feeds showed that capacitance decline at mid-frequency range (e.g. 1 kHz) can be used as an indication for membrane fouling.

The experiments on flat membranes showed that 3-terminal and 4-terminal electrode configurations were necessary for detection of membrane fouling. However, even 4-terminal configuration the most effective electrode configuration, relative capacitance decline was significantly lower than the flux decline.

The experiments on inside-out and outside-in hollow fibre membranes showed that using an appropriate electrode configuration, membrane fouling can be detected using 2-terminal EIS measurements. The best performance was achieved by increasing the surface area of the electrode on the permeate side probing the surface of membrane while using a relatively small electrode on the feed side. Therefore, inserting a wire inside the membrane fibre was unnecessary for inside-out membranes, but improved the performance of EIS in detecting the fouling of outside-in hollow fibre membranes. Experiments also showed that inserting electrode wires inside all fibres was not required.

Fitting a wire electrode inside one of the fibres of outside-in hollow fibre membrane was found to be required for detection of fouling in a larger membrane module used for filtration of dunder waste (industrial wastewater). These experiments also showed that aeration of membrane bioreactor did not affect the performance of EIS in detection of fouling. EIS was also shown to be effective in monitoring the backwashing process and off-line characterisation of membrane fouling.

Comparing the separation performance of outside-in hollow fibre membranes with that of flat membrane showed that hollow fibre membranes can be very effective in solving the problem of dunder waste by separating organic materials and valuable slats.

Experiments on hollow fibre membranes, both inside-out and outside-in, showed that using a suitable electrode configuration the relative capacitance decline measures at mid-frequency range (e.g. 1 kHz) was comparable and sometimes greater than the flux decline due to fouling. Similarly, a significant capacitance increase at same frequency range was measured by EIS. These results suggested that the performance of EIS on detection of fouling was better in case of hollow fibre membranes in comparison to flat membranes.

## 5. Future works

This research showed that electrical impedance spectroscopy has a great potential for monitoring the fouling of hollow fibre membranes. In spite of the initial doubts due to lack of information before starting this research, the outcome of the present study showed that the performance of EIS potentially is better in detecting the fouling of hollow fibre membranes in comparison with flat membranes.

Considering the expanding market of membrane bioreactors especially for municipal purposes, developing an electrical sensor to monitor fouling seems to be financially justified and profitable. However, this research was one of the first and more research and development works are required to develop a fouling sensor based on electrical impedance spectroscopy. These are the suggestion for a future work:

- 1) Using the prototype designed in this research as a canary module for monitoring the fouling of an industrial scale membrane bioreactor for long term;
- 2) Comparing the performance of 2-terminal configurations with that of 3-terminal configuration and designing a prototype for these measurements if the 3-terminal measurements yielded better results;
- 3) Systematic measurements for finding a relationship between the EIS results and mechanism of fouling;
- 4) Driving a fouling index extracted from EIS data and modifying the EIS control software for online plotting the fouling index (instead of capacitance and conductance data) as a function of time; and
- 5) Developing an alarm sensor for detecting the threshold of irreversible fouling and the need for backwashing.

## 6. Collaborations

The project was a collaborative research between the University of Technology Sydney (UTS) and INPAHZE. This project was funded by the Australian Water Recycling Centre of Excellence, through the Australian Government's National Urban Water and Desalination Plan.

Prof. Vigneswaran was the primary supervisor of the project. Prof. Hans Coster as the chief scientist of INPAHZE was the advisor. He also provided access to lab facilities as the director of Bio-engineering laboratory at the University of Sydney (USYD).

Followings were the contribution of the collaborators:

- UTS provided the laboratory access and working space for the fellow.
- USYD provided laboratory access and facilities for the project.
- INPAHZE provided an electrical impedance spectroscopy machine for the project.
- Fellow conducted the experiments and prepared the reports and presentations for the project meetings.
- Collaborators had regular meetings.

## 7. Progress and delays

Table 3 shows the timetable of the projects. It was planned to start the project from the beginning of July, but the project was somewhat delayed for administrative and legal reasons.

Table 3 -Timetable of the project.

No	Task	Jul 13	Aug	Sep	Oct	Nov	Dec	Jan	Feb	Mar	Apr 14
1	Designing and construction of a prototype chamber to fit the hollow fibre and the electrodes required for electrical measurements	<i>D</i>									
2	Testing the prototype setup to monitor the MF hollow fibre membranes during filtration of different feeds	<i>D</i>	<i>D</i>								
3	Preparation of Report 1		<i>D</i>	<i>D</i>	<i>D</i>						
4	Optimizing the prototype module.										
5	Testing the performance of the EIS system in detecting the fouling of comparable flat sheet MF membranes and comparing the results with the outcome of experiments on hollow fibres						<i>D</i>	<i>D</i>	<i>D</i>		
6	Preparation of final report										

In spite of the considerable delay at the beginning, the deadline for the first report was met successfully for the first report. However, the second phase of the project was slightly delayed due to limitations in access to laboratory facilities. The centre was notified of the possibility of delay when the electrical impedance spectroscopy, the most important instrument for the research, was broken. The project was extended officially, and the experiments were completed within the extended timeline.

## **8. Networking activities**

The research project has provided the opportunity for UTS and INPHAZE to start a collaboration discussion with BASF in Germany. The Inge inside-out membranes were provided by this company and were used in the research. Fellow has been in contact with the R&D group at BASF regarding the experiments on these membranes. The results of the experiments on these membranes will be shared with this collaborator to showcase the outcome of this research. The research team plans to continue this collaboration.

A collaborative network is also established with a research group at RWTH Aachen University in Germany. The collaborative work with this group has resulted in a specific prototype chamber for characterising the structure of hollow fibre membranes. The results will be published as a journal paper in a close future. The results of the first phase of the present study was shared and discussed with the researchers from Aachen University. The results of the final phase are planned to be shared during a Skype meeting.

### **8.1. Publicity and documents**

The outcome of the project will be presented in North American Membrane Society (NAMS 2014) conference that will be held in Huston, Texas in June 2014. The paper is accepted for oral presentation.

The outcome of this research will be published in high impact journals in the field of water and membrane research. This research is expected to generate 3 journal papers.

## 9. Signatures

### FIRST REPORT

**PROJECT TITLE:** Characterizing the Performance and Fouling of Hollow Fibre Membranes

**FUNDING LEVEL:** \$ 80,000

**PARTICIPANTS:**

**Australian Water Recycling Centre of Excellence (AWRCoE)**



**University of Technology Sydney (UTS)**



**INPHAZE Pty Ltd**



**SIGNATURES:**

Centre Fellow	Dr. Mariam Darestani		<i>T. Darestani</i> 26.9.13
Supervisor	Prof. Vigneswaran	UTS	<i>Vigneswaran</i>
Industry partner	Dr. Ditta Bartels	INPHAZE	<i>D. Bartels</i>
	Prof. Hans Coster		<i>Hans Coster</i>

## 10. References

1. Martinez-Sosa, D., et al., *Anaerobic submerged membrane bioreactor (AnSMBR) for municipal wastewater treatment under mesophilic and psychrophilic temperature conditions*. *Bioresource Technology*, 2011. **102**(22): p. 10377-10385.
2. Meng, F., et al., *Recent advances in membrane bioreactors (MBRs): membrane fouling and membrane material*. *Water Research*, 2009. **43**(6): p. 1489-1512.
3. Judd, S., *The status of membrane bioreactor technology*. *Trends in Biotechnology*, 2008. **26**(2): p. 109-116.
4. Daigger, G.T., et al., *Are membrane bioreactors ready for widespread application?* *Environmental Science & Technology*, 2005. **39**(19): p. 399A-406A.
5. Drews, A., *Membrane fouling in membrane bioreactors—characterisation, contradictions, cause and cures*. *Journal of Membrane Science*, 2010. **363**(1): p. 1-28.
6. Le-Clech, P., V. Chen, and T.A. Fane, *Fouling in membrane bioreactors used in wastewater treatment*. *Journal of Membrane Science*, 2006. **284**(1): p. 17-53.
7. Orazem, M.E. and B. Tribollet, *Electrochemical impedance spectroscopy*. The Electrochemical Society series 2008, Hoboken, N.J.: Wiley. xxxi, 523 p.
8. Sluyters-Rehbach, M., *Impedances of Electrochemical Systems - Terminology, Nomenclature and Representation .1. Cells with Metal-Electrodes and Liquid Solutions*. *Pure and Applied Chemistry*, 1994. **66**(9): p. 1831--1891.
9. Coster, H.G.L., T.C. Chilcott, and A.C.F. Coster, *Impedance spectroscopy of interfaces, membranes and ultrastructures*. *Bioelectrochemistry and Bioenergetics*, 1996. **40**(2): p. 79-98.
10. Decarolis, J., S. Hong, and J. Taylor, *Fouling behavior of a pilot scale inside-out hollow fiber UF membrane during dead-end filtration of tertiary wastewater*. *Journal of Membrane Science*, 2001. **191**(1): p. 165-178.
11. Wirth, D. and C. Cabassud, *Water desalination using membrane distillation: comparison between inside/out and outside/in permeation*. *Desalination*, 2002. **147**(1): p. 139-145.
12. Ghogomu, J., et al., *Hollow-fibre membrane module design: comparison of different curved geometries with Dean vortices*. *Journal of Membrane Science*, 2001. **181**(1): p. 71-80.
13. Sheehan, G. and P. Greenfield, *Utilisation, treatment and disposal of distillery wastewater*. *Water Research*, 1980. **14**(3): p. 257-277.
14. Matthew, P., *Development and practical application of an assessment procedure for land disposal of yeast waste (dunder) as a resource recovery scheme*. 2003.
15. Matthew, P., C.J. Birch, and P. Saffigna. *Assessment of waste for use on agricultural land*. in *4th International Crop Science Congress*. 2004. The Regional Institute Ltd.
16. Coster, H., et al., *Characterisation of ultrafiltration membranes by impedance spectroscopy. I. Determination of the separate electrical parameters and porosity of the skin and sublayers*. *Journal of Membrane Science*, 1992. **66**(1): p. 19-26.
17. Kavanagh, J., et al., *Fouling of reverse osmosis membranes using electrical impedance spectroscopy: Measurements and simulations*. *Desalination*, 2009. **236**(1): p. 187-193.
18. Coster, H.G., T.C. Chilcott, and A.C. Coster, *Impedance spectroscopy of interfaces, membranes and ultrastructures*. *Bioelectrochemistry and Bioenergetics*, 1996. **40**(2): p. 79-98.
19. James Watkins, E. and P.H. Pfromm, *Capacitance spectroscopy to characterize organic fouling of electro dialysis membranes*. *Journal of Membrane Science*, 1999. **162**(1): p. 213-218.
20. Benavente, J., et al., *Sulfonated poly (ether ether sulfones): characterization and study of dielectrical properties by impedance spectroscopy*. *Journal of Membrane Science*, 2000. **175**(1): p. 43-52.

21. Park, J.-S., et al., *Characterization of BSA-fouling of ion-exchange membrane systems using a subtraction technique for lumped data*. Journal of Membrane Science, 2005. **246**(2): p. 137-144.
22. Chen, J.C., Q. Li, and M. Elimelech, *In situ monitoring techniques for concentration polarization and fouling phenomena in membrane filtration*. Advances in Colloid and Interface Science, 2004. **107**(2): p. 83-108.
23. Chen, V., H. Li, and A. Fane, *Non-invasive observation of synthetic membrane processes—a review of methods*. Journal of Membrane Science, 2004. **241**(1): p. 23-44.
24. Antony, A., et al., *In situ structural and functional characterization of reverse osmosis membranes using electrical impedance spectroscopy*. Journal of Membrane Science, 2013. **425**: p. 89-97.
25. Długołęcki, P., et al., *On the resistances of membrane, diffusion boundary layer and double layer in ion exchange membrane transport*. Journal of Membrane Science, 2010. **349**(1): p. 369-379.
26. Gao, Y., et al., *Characterization of forward osmosis membranes by electrochemical impedance spectroscopy*. Desalination, 2013. **312**: p. 45-51.
27. Xu, Y., et al., *Electrochemical impedance spectroscopy analysis of sulfonated polyethersulfone nanofiltration membrane*. Desalination, 2011. **271**(1): p. 29-33.
28. Marx, G.H. and D.B. Kell, *Dielectric spectroscopy as a tool for the measurement of the formation of biofilms and of their removal by electrolytic cleaning pulses and biocides*. Biofouling, 1990. **2**(3): p. 211-227.
29. Chilcott, T., et al. *In situ characterization of fouling in reverse osmosis membranes using electrical impedance spectroscopy*. in *Journal of Physics: Conference Series*. 2013. IOP Publishing.
30. Gille, D. and W. Czolkoss, *Ultrafiltration with multi-bore membranes as seawater pre-treatment*. Desalination, 2005. **182**(1): p. 301-307.
31. Wang, P. and T.-S. Chung, *Design and fabrication of lotus-root-like multi-bore hollow fiber membrane for direct contact membrane distillation*. Journal of Membrane Science, 2012. **421**: p. 361-374.
32. De Bartolo, L., et al., *Human hepatocyte morphology and functions in a multibore fiber bioreactor*. Macromolecular Bioscience, 2007. **7**(5): p. 671-680.
33. Krüger, R., R. Winkler, and P. Berg. *Innovative ultrafiltration technology in a seawater desalination plant in the Mediterranean Sea*. in *IDA World Congress on Desalination and Water Reuse, Maspalomas, Gran Canaria, Spain*. 2007.
34. Mutamim, N.S.A., et al., *Application of membrane bioreactor technology in treating high strength industrial wastewater: a performance review*. Desalination, 2012. **305**: p. 1-11.
35. Smith, A.L., et al., *Perspectives on anaerobic membrane bioreactor treatment of domestic wastewater: a critical review*. Bioresource Technology, 2012. **122**: p. 149-159.
36. Ji, G.L., et al., *Structure formation and characterization of PVDF hollow fiber membrane prepared via TIPS with diluent mixture*. Journal of Membrane Science, 2008. **319**(1-2): p. 264-270.
37. Mishima, K., et al., *Solubility of polymer in the mixtures containing supercritical carbon dioxide and antisolvent*. Fluid Phase Equilibria, 1998. **144**(1-2): p. 299-305.
38. Macdonald, D.D., *Reflections on the history of electrochemical impedance spectroscopy*. Electrochimica Acta, 2006. **51**(8-9): p. 1376-1388.
39. Coster, H.G.L., et al., *Characterization of Ultrafiltration Membranes by Impedance Spectroscopy .1. Determination of the Separate Electrical Parameters and Porosity of the Skin and Sublayers*. Journal of Membrane Science, 1992. **66**(1): p. 19-26.
40. Coster, H.G.L., et al., *Electrical impedance spectroscopy characterisation of conducting membranes I. Theory*. Journal of Membrane Science, 2002. **195**(2): p. 153-167.

41. Coster, H.G.L., et al., *Electrical impedance spectroscopy characterisation of conducting membranes II. Experimental*. Journal of Membrane Science, 2002. **195**(2): p. 169-180.
42. Park, J.S., et al., *Characterization of BSA-fouling of ion-exchange membrane systems using a subtraction technique for lumped data*. Journal of Membrane Science, 2005. **246**(2): p. 137-144.
43. Nijmeijer, K., et al., *Transport limitations in ion exchange membranes at low salt concentrations*. Journal of Membrane Science, 2010. **346**(1): p. 163-171.
44. Kavanagh, J.M., et al., *Fouling of reverse osmosis membranes using electrical impedance spectroscopy: Measurements and simulations*. Desalination, 2009. **236**(1-3): p. 187-193.
45. Chen, V., H. Li, and A.G. Fane, *Non-invasive observation of synthetic membrane processes - a review of methods*. Journal of Membrane Science, 2004. **241**(1): p. 23-44.
46. Nguyen, P.H. and G. Paasch, *Transfer matrix method for the electrochemical impedance of inhomogeneous porous electrodes and membranes*. Journal of Electroanalytical Chemistry, 1999. **460**(1-2): p. 63-79.
47. Chen, J.C., Q.L. Li, and M. Elimelech, *In situ monitoring techniques for concentration polarization and fouling phenomena in membrane filtration*. Advances in Colloid and Interface Science, 2004. **107**(2-3): p. 83-108.
48. Chilcott, T.C., et al., *Ionic double layer of atomically flat gold formed on mica templates*. Electrochimica Acta, 2009. **54**(14): p. 3766-3774.
49. Gaedt, L., et al., *Electrical impedance spectroscopy characterisation of conducting membranes: II. Experimental*. Journal of Membrane Science, 2002. **195**(2): p. 169-180.
50. Macdonald, J.R. and E. Barsoukov, *Impedance spectroscopy: theory, experiment, and applications*. History, 2005. **1**: p. 8.
51. Darestani, M., H. Coster, and T. Chilcott, *Piezoelectric membranes for separation processes: Operating conditions and filtration performance*. Journal of Membrane Science, 2013. **435**: p. 226-232.
52. Sim, L., et al., *Detection of reverse osmosis membrane fouling with silica, bovine serum albumin and their mixture using *in-situ* electrical impedance spectroscopy*. Journal of Membrane Science, 2013. **443**: p. 45-53.